UTS UNIVERSITY OF TECHNOLOGY SYDNEY

Metal and protein correlation in the brain and eye in Alzheimer's disease

by Seyed Mostafa Hosseinpour Mashkani

Thesis submitted in fulfilment of the requirements for the degree of

Doctor of Philosophy

under the supervision of A/Prof. David Bishop, A/Prof. Mojtaba Golzan

University of Technology Sydney
Faculty of Science, School of Mathematical and Physical Sciences

February 2023

CERTIFICATE OF ORIGINAL AUTHORSHIP

I, *Seyed Mostafa Hosseinpour Mashkani,* declare that this thesis is submitted in fulfilment of the requirements for the award of *Doctor of Philosophy*, in the *School of Mathematics and Physical Science, Faculty of Science* at the University of Technology Sydney.

This thesis is wholly my own work unless otherwise referenced or acknowledged. In addition, I certify that all information sources and literature used are indicated in the thesis.

This document has not been submitted for qualifications at any other academic institution.

This research is supported by the Australian Government Research Training Program.

Signature: Production Note:
Signature removed prior to publication.

Date: 03/02/2023

Acknowledgments

Completing my PhD in nanobiotechnology is undoubtedly the biggest achievement in my whole life. PhD, Doctor of Philosophy, means the study of the fundamental nature of knowledge, reality, and existence. From my point of view, PhD, as the name implies, includes not only deep learning and deep passion for problem-solving but also how to engage with a multidisciplinary team (enhancing the spirit of collaboration), how to be patient and resilient during the ups and downs of life, and how to strengthen the spirit of persistence to achieve an ultimate goal. Every single moment I look back, I sincerely realise that I would not have completed my journey without all the people in my life, including my wife, my family, my supervisors, my colleagues, my friends, who have supported me in one way or another. I would like to thank everyone who paved the hard way of my PhD.

First of all, I would like to express thanks to my principal supervisor, **A/Prof. David bishop**, who helped me to finish my PhD journey. Under his supervision and leadership, I learned how strengthening my positive attitude towards life and being consistent and hardworking can affect reaching our ultimate goal. He taught me how to communicate with other people to expand the angles of the PhD project. I appreciate him teaching me how to become an independent researcher and an expert in my field.

I would like to express my gratitude to my co-supervisor, **A/Prof. Mojtaba Golzan**, the Deputy Head of School, Research Graduate School of Health, for introducing me to the world of neuroscience. Having not taken any biology classes prior to joining this project, Mojtaba supported me how to do handle my biological experiments. Under his supervision and leadership, I learned how to think critically and scientifically, how to design experiments,

how to be more organised, how to be more accurate during conducting experiments and analysing the data. I appreciate his effort and advice regarding my paper and my thesis.

I would like to express my gratitude to **A/Prof Olga Shimoni** for her efforts to provide lab facilities during my PhD. During the two years of my PhD, she spent significant time comforting me and inspiring me to keep a positive attitude towards the PhD. I appreciate her keeping her office door open to answer the student's questions.

I would like to express my warm thank to my colleagues, **Dr. Mika T Westerhausen and Dr. Behjat Sheikholeslamibourghanifarahani,** who gave me some valuable suggestions that how I could increase my knowledge in biology and bioanalytical chemistry.

Special thanks to **my parents** who have consistently supported me since my childhood. They tried their best to provide a supportive and safe environment so I could become who I am now. I will always owe them for their entire kindness and efforts.

I would like to sincerely acknowledge my heart and soul, my love, my wife, **Mahnaz Maddahfar**, who spent significant time teaching me how to be a better scientist, a better mentor, and a better person in general. I appreciate her because she believes in me more than I do myself. Without her, I would not have been able to pass through the difficult moments.

I would like to acknowledge the **International Research Training Program Scholarships (IRTP)**, for supporting my PhD journey. Thank you so much.

I would like to acknowledge the **Florey Institute of Neuroscience and Mental Health** and **Netherlands Brain Bank (NBB)** for providing me mice and human samples.

I like to acknowledge **Australian Nanotechnology Network** (ANN) for supporting me financially to attend conferences during my PhD journey.

Format of thesis

This is a thesis by a conventional with seven chapters.

Chapter 1 includes a comprehensive study of a PhD project called a literature review.

Chapter 2 includes Materials and methods.

Chapters 3-6 are experimental, results, and discussion sections.

Chapter 7 includes the conclusions, and future perspectives.

List of publications, conferences, and awards

[1] **Seyed Mostafa Hosseinpour Mashkani**, David Bishop, Newsha Raoufi-Rad, Paul A. Adlard, Olga Shimoni, S. Mojtaba Golzan*, Distribution of Copper, Iron, and Zinc in the Retina, Hippocampus, and Cortex of the Transgenic APP/PS1 Mouse Model of Alzheimer's Disease (Cells, 2023, 12, 1144). The published paper results from Chapter 3.2.1. https://doi.org/10.3390/cells12081144

[2] **Seyed Mostafa Hosseinpour Mashkani**, David Bishop*, MT Westerhausen, Paul A. Adlard, S. Mojtaba Golzan*, Age-dependent changes of retinal and brain transition metal levels and expressions of zinc regulatory proteins of the human and APP/PS1 mouse model of Alzheimer's Disease (submitted to Metallomics). The submitted paper results from Chapters 3.2.2, 4, and 5.

[3] Mahnaz Maddahfar, Shihui Wen, **Seyed Mostafa Hosseinpour Mashkani**, Lin Zhang, Olga Shimoni, Martina Stenzel, Jiajia Zhou, Barbara Fazekas de St Groth*, Dayong Jin*. Stable and high-efficient antibody-nanoparticles conjugation (Bioconjugate Chem, 2021, 32, 6, 1146-1155). https://doi.org/10.1021/acs.bioconjchem.1c00192

[4] Javad Safaei, **Seyed Mostafa Hosseinpour Mashkani**, Hao Tian, Caichao Ye*, Pan Xiong*, and Guoxiu Wang*, Self-Assembled $NbOPO_4$ Nanosheet/Reduced Graphene Oxide Heterostructure for Capacitive Desalination (ACS Appl. Nano Mater, 2021, 4, 11, 12629-12639). https://pubs.acs.org/doi/abs/10.1021/acsanm.1c03180

[5] Javad Safaei, Yifu Gao, **Mostafa Hosseinpour**, Xiuyun Zhang, Yi Sun, Xiao Tang, Zhijia Zhang, Shijian Wang, Xin Guo, Yao Wang, Zhen Chen, Dong Zhou*, Feiyu Kang*, Lei Jiang*, and Guoxiu Wang*, Vacancy Engineering for High-Efficiency Nanofluidic Osmotic

Energy Generation (J. Am. Chem. Soc, 2023, 145, 4, 2669-2678). https://pubs.acs.org/doi/10.1021/jacs.2c12936

Conferences:

[1] **Seyed Mostafa Hosseinpour Mashkani,** Olga Shimoni, David Bishop, Mojtaba Golzan, Visualising Alzheimer's disease using Upconversion Nanosensor, International Conference on Nanoscience and Nanotechnology (ICONN 2020) and International Conference on BioNano Innovation (ICBNI- Poster presentation). February 2020 at Brisbane, Australia.

[2] **Seyed Mostafa Hosseinpour Mashkani,** Olga Shimoni, David Bishop, Mojtaba Golzan, Early diagnosis of Alzheimer's disease, Alzheimer's Association International Conference® (AAIC®) Satellite Symposium, September, 2019.

List of Acronyms (in alphabetic order)

Age-related macular degeneration	AMD
Alzheimer's disease	AD
Amyloid-β	Aβ
Amyloid-beta precursor protein	APP
Bovine serum albumin	BSA
Central nervous system	CNS
Comma separate values file	CSV
Computed tomography	CT
Double-transgenic mouse models of Alzheimer's disease	APP/PS1
Ganglion cell layer	GCL
Glyceraldehyde 3-phosphate dehydrogenase	GAPDH
Hematoxylin and Eosin	H&E
Hippocampus	HPC
Immunofluorescence	IF
Inner nuclear layer	INL
Inner plexiform layer	IPL
Inner segment of photoreceptors	IS
Knockout	KO
Laser ablation-inductively coupled plasma-mass spectrometry	LA ICP-MS
Magnetic resonance imaging	MRI
Metallothioneins	MTs
Mild cognitive impairment	MCI

Monoclonal antibodies	mAbs
Neurofibrillary tangle	NFT
Optimal cutting temperature compound	OCT
Outer nuclear layer	ONL
Outer plexiform layer	OPL
Phosphate-buffered saline buffer	PBS
Phosphate-buffered saline with tween	PBST
Pigment epithelial cells	PE
Positron emission tomography	PET
Potential of hydrogen	pH
Quantum dots	QDs
Reactive oxygen species	ROS
Retinal pigment epithelium	RPE
Solution nebulisation-inductively coupled plasma-mass spectrometry	SN-ICP-MS
Standard error of the mean	SEM
Wild Type	WT
Zinc transporter 3	ZnT3
Zinc transporter 3	ZIP3
4', 6-Diamidino-2-Phenylindole	DAPI

Contents

List of Figures

List of Tables

Abstract

Alzheimer's disease (AD) is pathologically characterised by neurofibrillary tangles and amyloid-β oligomerisation, which may be instigated by transition metals dyshomeostasis (Zn, Cu, and Fe). AD diagnosis is intricate, with physicians using expensive and invasive methods, such as computed tomography (CT), magnetic resonance imaging (MRI), and positron emission tomography (PET). Hence, significant demand exists for new research to discover a non-invasive diagnostic technique for monitoring AD patients at an early stage. There is growing evidence that monitoring changes in the eye may reflect brain alterations in AD, making the eye a strategic roadmap for diagnosing AD early.

Hence, this thesis focused on the anatomical distributions and concentrations of transition metals and zinc transporter proteins (ZnT3 and ZIP3) in the brains and eyes of AD and healthy mice and human samples to investigate the correlation between pathological changes in the eye and brain in AD.

Inductively coupled plasma-mass spectrometry (ICP-MS) and laser ablation-ICP-MS (LA-ICP-MS) were used to investigate the age-related changes and anatomical distributions and concentrations of metal ions in the brain and eye of WT and APP/PS1 mice models. The abundance and expression of zinc transporters in the eye and brain of the mice models (WT and APP/PS1) were measured using immunofluorescence (IF) and Western blot.

Transition metals and zinc transporters results demonstrated that there was a significant difference between the metal concentrations and zinc transporters abundances in the WT and APP/PS1 mice models (higher transition metals and zinc transporters in the WT than APP/PS1).

These results were compared to data collected from human samples (brain and eye). While AD human samples possessed higher transition metal concentrations compared with healthy samples, our protein study revealed that the AD patients had lower zinc transporters abundance than healthy samples.

Finally, the use of quantum dot-labelled amyloid-beta as a multimodal imaging tag for high-resolution immunofluorescent imaging followed by quantitative LA-ICP-MS imaging of amyloid plaques in AD was determined to be unsuitable. A high Te background was observed in the human samples which prevented the co-localisation of IF images with the quantitative LA-ICP-MS data.

This thesis is the first to report on the distribution and concentration of transition metals and zinc transporter proteins in mice and human eye retinas of individuals with AD.

These findings provide invaluable insights into a better understanding of AD pathogenesis and introduce transition metals and proteins in the retina as potential biomarkers for early AD diagnosis and disease progression monitoring.

Chapter 1: Literature review

1: Literature review

1.1 Metals in biology

Metals play crucial roles in many cellular and subcellular functions, such as oxygen formation to hypoxia sensing, with transition metals such as Fe, Cu, Mn, Zn, Co, and Ni have dual roles due to their unique chemical and physical properties. Transition metals have multiple valence states under physiological conditions, facilitating their involvement in single electron transfer reactions, making them ideal for biological systems. For instance, over 300 protein families have been identified that can exploit zinc.[1] Dyshomeostasis of metals can cause cytotoxicity, which may result in several diseases ranging from hemochromatosis and anemias to neurodegenerative disorders, including Alzheimer's and Parkinson's.[2] Therefore, knowing chemical species, locations, and abundance of metals is the key to realising their role in biological systems[3] and characterised diseases such as age-related macular degeneration,[4] neurodegeneration, etc.

1.1.1 Sources of metals

The human body requires below 100 mg of trace elements to function daily, with their perturbation negatively impacting the human body and, in the worst cases, resulting in death as they directly impact metabolic and physiologic processes.[5] A broad and complex system inside the human body is responsible for managing and maintaining essential trace elements within a normal physiological range.

Essential micronutrients include almost 30 vitamins and minerals (Ca, P, Mg, Fe, Zn, Cu, and Mn), which the human body cannot naturally produce.[6] These micronutrients are

supplied from the diet and require transport via the blood. Uptake of transition metals from the diet includes three steps.[7]

1. Moving metal ions from the environment towards the cell.

2. Carrying them into the cell through the cell membrane.

3. Transporting metal ions to the place of utilisation within a cell or other cells within the organism.

The organism must absorb and concentrate environmental elements when their levels are too low. In contrast, when experiencing high concentrations of essential elements, organisms must reduce element uptake to evade toxic effects.

1.2 The role of metals in Alzheimer's disease

AD pathology is characterised by oxidative stress, neuroinflammation, calcium dysregulation, mitochondrial malformation and altered distribution, neurofibrillary tangle (NFT) formation, amyloid-β (Aβ) oligomerisation, synaptic toxicity, and metal dyshomeostasis.[8] Increased knowledge of the distribution and concentration of transition metals in different brain regions may be helpful for the early diagnosis of AD. Metals such as Zn, Cu, and Fe greatly influence the precipitation of amyloid beta (Aβ) and its related toxicity in AD.[9] However, agreement as to their location, concentration, and roles has not been achieved.

It is well known that in the central nervous system (CNS), the copper concentration decreases in the frontal, occipital, and parietal lobes in AD patients.[10] In AD patients' brains, copper levels also decrease in the amygdala and hippocampus.[11] Another study reported the frontal cortex of AD patients shows an increased tendency to bind exchangeable copper (loosely bound to proteins and enzymes, which can be readily exchanged with other molecules).[12] No

significant changes in the Cu levels in the cerebral spinal fluid (CSF) of AD and healthy controls were observed.[13, 14] There are many reports regarding the increased,[14, 15] decreased[16, 17] or unchanged[18, 19] Cu levels in the serum or plasma in AD subjects. Moreover, many studies also detected excess amounts of free Cu in the serum.[20-26] Several animal model studies have revealed that copper accumulation around plaques in the brain is associated with AD.[27, 28] Amyloid-beta precursor protein (APP) can reduce Cu^{2+} to Cu^{+} by its selective and high-affinity Cu binding site in the extracellular domain.[29-31] There are three selective high and low-affinity binding sites on the surface of Aβ (His6, His13, and His14) to bind with Cu, which mediates toxicity.[32] Cu^{2+} plays a vital role in creating β-sheet structures, which are believed to be an initial step of the toxic aggregation of the fibrillar form of Aβ. Consequently, the interaction of Aβ with Cu results in the fibril and free radical (oxidative stress) formation, which are two of the hallmarks of AD pathogenesis.[27, 33] Iron is critical for maintaining neuronal tissue and synthesising myelin and neurotransmitters.[34] However, accumulation of Fe results in increasing Aβ production and tau dysfunction and in neuronal cell death.[35] Some studies claimed that iron levels increased in AD subjects' globus pallidus and putamen.[36] [37-39] Alternatively, research based on meta-analysis showed that the Fe level was either reduced or unchanged in AD patients compared with healthy subjects.[40, 41] It was recently reported that APP could control the level of Fe in the brain by removing it from the cells, similar to the ceruloplasmin enzyme.[42] Interestingly, this phenomenon increased by 70 % in cortical tissue in AD samples.[43, 44] Conversely, iron increases APP processing, which results in the formation of senile plaques and oxidative stress and, consequently, oligomerisation and more Aβ generation.[45]

Finally, the disturbance of iron levels impacts neuronal populations within the hippocampus (HPC) via Fenton and Haber-Weiss reactions,[46] creating oxidative lipids that further increase neurotoxicity and AD pathogenesis.[47] Therefore, providing a metal-based map of AD and healthy subjects would be beneficial for recognising the higher-risk regions in AD brains.

Considerable research has shown that both high and low zinc concentrations might cause neuronal death through the mechanisms summarised in Fig. 1.1.[48, 49] According to some studies, zinc levels significantly increase in AD patients' hippocampus, amygdala, neuropil, and brain cortex.[11, 50, 51] In contrast, Schrag and his group reported, based on meta-analysis, that there are no significant changes in zinc levels in the AD neocortex.[52] A further three meta-analyses[40, 53, 54] were performed on the level of zinc in plasma and serum in AD patients and healthy controls with conflicting results. The Zn levels in some patients increased and in others decreased, while it did not change in others.

Zn can interact with proteins and enzymes which are involved in neurodegenerative disease.[55] Zn can also accept and donate electrons, leading to the formation of reactive oxygen species (ROS).[56, 57]

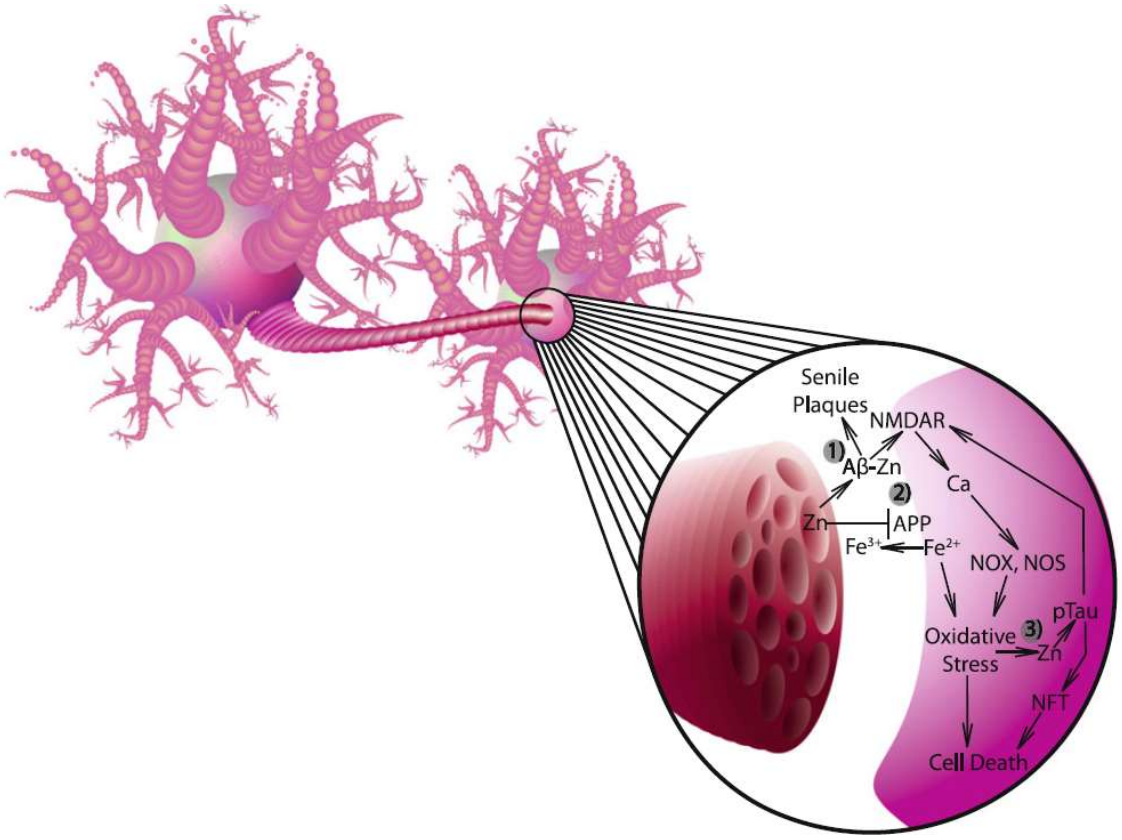

Fig.1.1 Different pathways of zinc concentrations contribute to AD progression.[49]

There is a clear correlation between Aβ toxicity and zinc concentration, with high Aβ toxicity occurring at high Zn concentration (~mM) while neuroprotection occurs at low zinc concentrations (<50 μM).[58-60] Additional evidence for the impact of Zn on the amyloid plaques is that using metal chelators to remove free Zn significantly enhances the solubilisation of Aβ deposits in both AD and controls.[61] Human/clinical evaluations, rat/mice models, and cell lines are the platforms for pharmacological studies of metal-chelating agents.[61] Moreover, Cuajungco and Lees[62, 63] proposed that releasing Zn after increasing its initial concentration in intracellular environments causes the precipitation of Aβ proteins and compromises the viability of neurons. A greater understanding of the roles of these transition

metals, and in particular Zn, will inform future diagnostic methods and therapeutic treatments.

1.3 Biological functions of Zinc

It is estimated that the total amount of zinc in the human body is 1.4-2.3 g,[64] with the highest Zn concentrations located in the retina (464 μg/g) and choroid complex (472 μg/g) compared to bone, muscle, liver, pancreas, and kidney tissue.[64, 65] The average total of Zn in the human brain is 150 mmol/L, about 10-fold serum zinc levels.[66] Zn absorption occurs in the small intestine while it is excreted in the skin, sweat, via the kidneys, urine, and via the large intestine/colon, in faeces.[67]

Zinc in mammalian biological systems exists in three forms depending on its molecular behaviour.[68] First, non-exchangeable and non-reactive immobile zinc is tightly bound to proteins, accounting for approximately 54 % of total zinc. Secondly, labile Zn loosely bound to a ligand accounts for 44.7 %, while the third, reactive or free zinc, exists at less than 1 %.

Free zinc ions (Zn^{2+}) are found in several locations in the central nervous system (CNS), including the retina,[64] hippocampus,[69] and other regions of the cerebral cortex.[70] Zn is involved in numerous biological functions divided into three main roles: catalytic, regulatory, and structural.[71] Approximately 10 % of human proteins have a zinc cofactor, and their function highly depends on the Zn concentration.[72]

Zn is an essential nutrient for the immune system since it is necessary to form antibodies, white blood cells, thyroid gland, and hormone function.[73-75] Zinc is also required for the catalytic activity of more than 200 enzymes,[76, 77] wound healing,[77] immune function,[77,

[78] protein and DNA synthesis, and cell division.[79] Furthermore, Zn is needed for the sense of taste and smell[80, 81] and the growing process during pregnancy till adolescence.[82-85]

Zinc is necessary to produce neurotransmitters in the brain. Zinc deficiency in the brain results in behavioural changes and brain functions by activating the hypothalamic-pituitary-adrenal axis, the excitability of glutamatergic neurons, impairment of CaMKII, CREB, and BDNF, and alterations in GPR39 Zn^{2+} sensing receptor.[86]

Zn is an essential metal for vision and eye health. It helps convert vitamin A, involved in visual phototransduction, where it serves as the crucial part of photopigment, into the form that enables low-light vision in the eyes.[87, 88] . Additionally, Zn is necessary for releasing vitamin A from the liver.[89, 90] Zn has the highest volume (464 μg/g) in the retina, controls communication between retinal cells and governs channels that enable ions to flow in and out of cells.[65, 91] Transporting nutrients into the retina via pigment epithelium is only possible in the presence of zinc-dependent proteins.[92] Akagi et al. reported that while Zn is present in various parts of the retina, including pigment epithelial cells (PE), the inner segment of photoreceptors (IS), the outer nuclear layer (ONL), the inner nuclear layer (INL), the outer plexiform layer (OPL) and the inner plexiform layer (IPL), and the ganglion cell layer (GCL), PE and IS have the highest Zn concentrations.[93] They also report that Zn is involved in neural processes in the OPL and IPL, while in the Golgi apparatus, it is assumed to catalyse metalloenzyme reactions in the retinal pigment epithelium (RPE), IS, INL, and GCL. Zn initiates biochemical reactions in the nerve cells in the eye and controls neurotransmitters that move between retinal nerve cells.[94]

Zinc levels during pregnancy (1.1 to 2.0 mg/day) are essential for developing the typical palate, lip, brain, eyes, heart, bones, lungs, and urogenital system in infants.[95] Its

antioxidant properties are assumed to act against accelerated aging, which hastens the recovery process after an injury.[83] There is also some evidence that the combination of Zn with antioxidant vitamins results in the slowing progression of age-related macular degeneration, which changes eyesight with aging.[96] Even at low levels, Zinc is an efficient antimicrobial agent. For instance, zinc supplementation can help treat acute gastroenteritis in children.[97] [98, 99] Zinc can be used as a communication signal by the salivary gland, prostate, immune system, and intestine with other cells.[100] Zinc plays a fundamental role in synaptic plasticity, which is essential in memory storage.[101-103] Carbonic anhydrase and carboxypeptidase are two examples of more than 200 enzymatic reactions containing Zn, which are necessary for regulating carbon dioxide and protein digestion.[104] An overabundance of zinc suppresses copper absorption, causes the malfunction of antibiotics, and creates an upset stomach.[5, 105, 106]

1.4 Consequences of zinc deficiency and overload

Zinc is an essential trace metal playing vital roles in numerous biological functions. At the same time, high Zn concentration results in toxicity, as shown in Fig.1.2.[107] The signs of acute Zn toxicity include nausea, vomiting, stomachache, diarrhoea, and headaches.[108, 109] Chronic zinc toxicity from exposure to high levels of zinc (>40 mg/day)[110] may lead to low levels of high-density lipoprotein or good cholesterol, reducing immune system function and copper shortage.[111, 112] In enterocytes lining the intestines, zinc regulates the expression of metallothioneins (MTs),[113] which act as intracellular ligands and stop the absorption of metals into the bloodstream, preventing metal toxicity.[114-116]

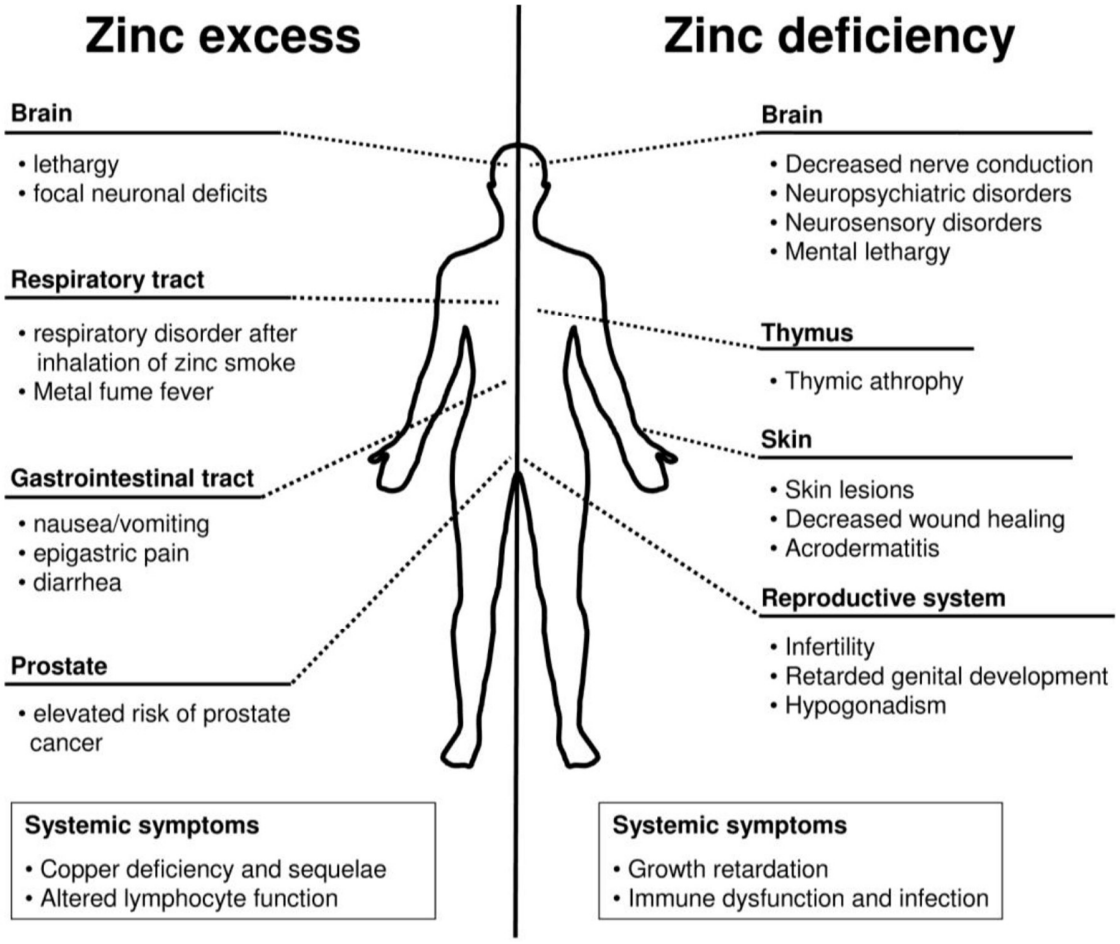

Fig.1.2. Comparison of the impact of zinc excess versus deficiency.[107]

Exposing cortical cell culture to 300-600 μM of Zn for 15 minutes causes extensive neuronal death.[117] Since high amounts of free Zn, stored in neurons' terminals, can be released by depolarisation,[118] Zn may have an influential role in neuronal injury. Moreover, depolarisation of the membrane resulting in brain injury increases the Zn capability to act as a neurotoxin.[119-122] Zn is a crucial part of the excitotoxic cascade after ischemia, seizures, and head trauma.[122-124]

The first study by Tonder and colleagues in 1990 showed that Zn accumulation might play a role in the selective degeneration of dentate hilar neurons after cerebral ischemia.[125]

Meanwhile, in dying or dead neurons, Zn accumulation occurs in the hippocampal hilar region and other damaged areas of the brain, including hippocampal CA1, neocortex, thalamus, and striatum.[126]

1.5 Zinc homeostasis in the brain

Understanding the mechanisms related to metal sensing and regulation is vital to comprehending their biological roles. Zinc homeostasis in the brain is very complicated, depending on its life cycle, including acquisition, distribution, and usage. Changing the homeostasis of zinc in the brain contributes to neurological diseases such as Alzheimer's disease, Parkinson's disease, and amyotrophic lateral sclerosis.[48, 62] Intracellular zinc homeostasis is achieved by metallothioneins (MTs)[127] and effluxing of Zn^{2+} into extracellular space by vesicles,[128, 129] Zn^{2+} transporters, and Zn^{2+} permeable ion channels, as shown in Fig. 1.3.

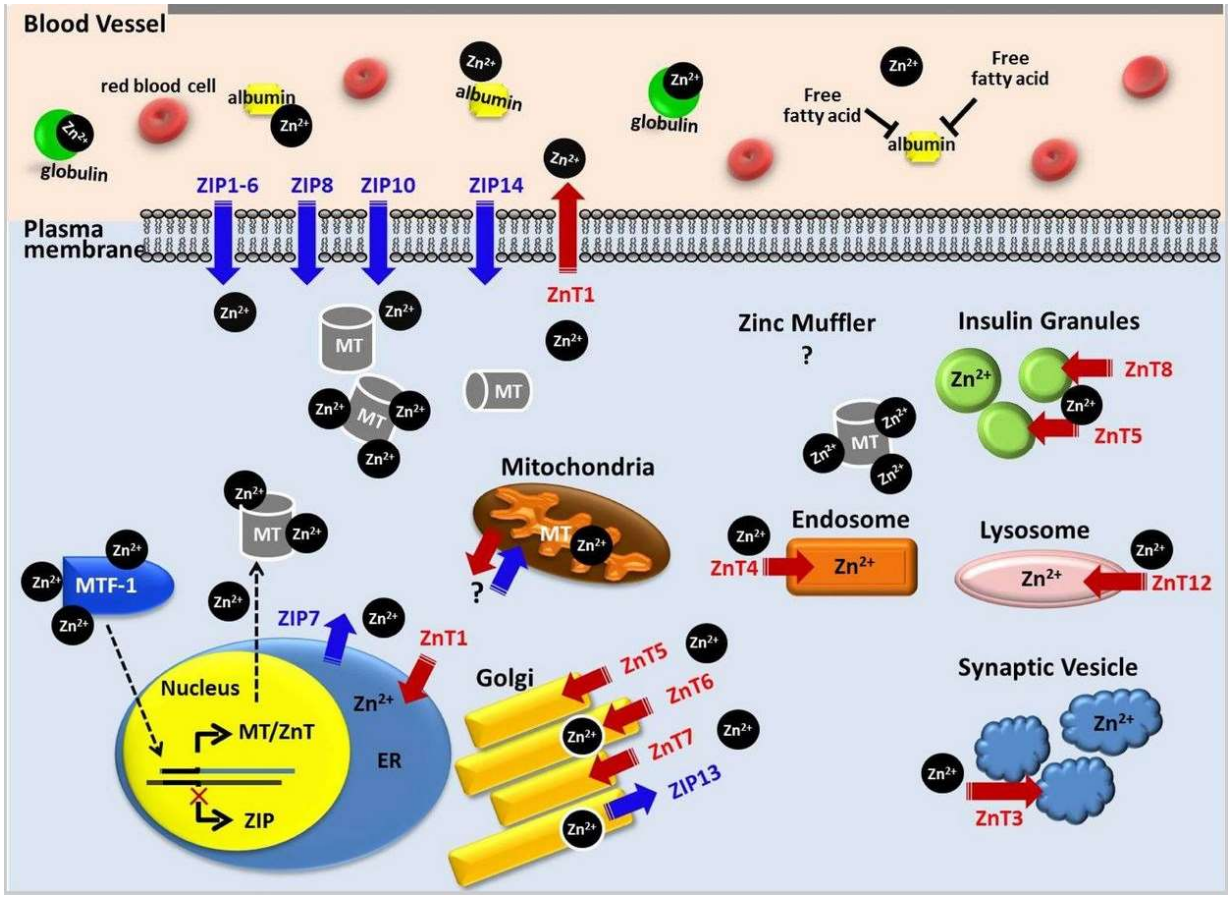

Fig.1.3 Schematic illustration of the molecular mechanisms involved in intracellular Zn^{2+} homeostasis.[130]

1.5.1 Metallothioneins (MTs)

The MTs (MT-I, MT-II, and MT-III) family is involved in intracellular zinc homeostasis and can bind up to seven zinc ions.[131-134] Metals such as zinc and copper stimulate MT-I and MT-II in astrocytes.[131] MT-III is a vital regulator of neuromodulatory zinc in the brain and is highly expressed in zinc-containing glutamatergic neurons.[135-137] Previous investigations on MT-III in Alzheimer's disease have reported contradictory findings. Some studies show MT-III malfunction in AD.[138, 139] In contrast, others indicate normal MT-III function in AD.[140, 141] In mammals, the metal-responsive transcription factor-

1 (MTF-1) regulates zinc levels by activating the expression of genes that maintain several copies of the metal-responsive element in their promoters.[142]

1.5.2 Zinc transporters

Zinc transporter proteins in the cell membranes are responsible for trafficking Zn into the cells and then carrying it into and out of intracellular organelles.[143-145] Zinc transporters include at least six different transporter groups. Three are involved in transporting Zn in bacteria but not in eukaryotes: the ABC transporters, the RND transporters, and the CorA proteins.[145, 146]

Some of the E1-E2 ATPases proteins, which act as the ion and lipid pumps in eukaryotes, have a role as the Zn transporter.[147] These Zn transporters are mainly from two groups of proteins: ZRT or IRT-like proteins (ZIP, SLC39A) and cation diffusion facilitators (CDF/ZnT, SLC30A)[148-151 152] which have an opposite function of maintaining cellular Zn homeostasis and was produced genetically in 1996 based on a mouse genomic ʎ library screening.[63] Until now, at least 14 ZIPs and 10 ZnTs have been reported. Figure.1.4 shows the subcellular localisation of ZnT and ZIP transporters and zinc transport direction.[153]

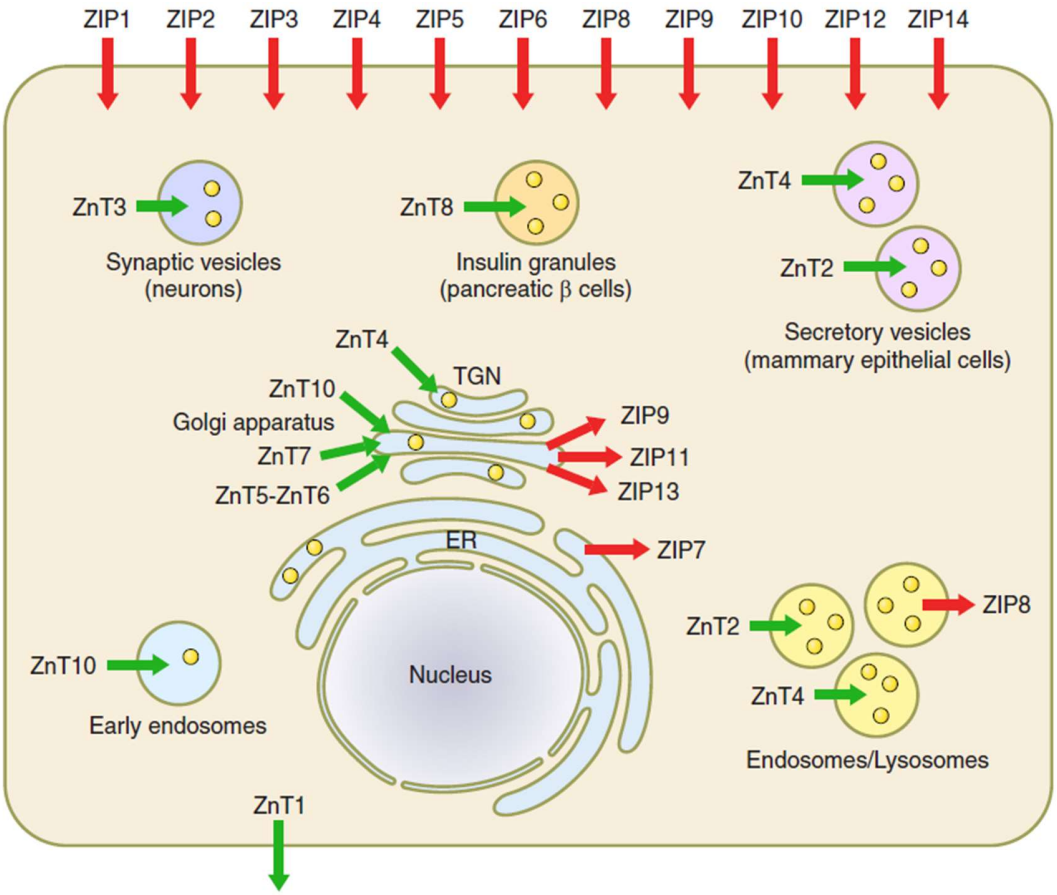

Fig.1.4 Subcellular localisation of ZnT and ZIP transporter proteins, and zinc transport direction.[153]

1.5.2.1 SLC30A (ZnT3) family of transporters

The SLC30 proteins, mammalian transporters, are part of a vast family of cation diffusion facilitator transporters which comprise Zn transporters with similar topology among bacteria, fungi, nematodes, insects, plants, and mammals.[154] In addition to Zn, ZnT transporters can also transport other cations, such as Fe, Mn, and Cd.[155]

The ZnT3 protein is localised on the membrane of intracellular organelles.[156] It adjusts the level of Zn by secreting cytoplasmic zinc into various compartments, storing or delivering it to the proteins that require zinc for their activities (Fig. 1.5).

Cole et al.[156] developed ZnT3 knockout mice and proved that these mice do not have histochemically detectable zinc, inferring that the ZnT3 protein serves as a zinc transporter. According to the zinc transporter function in yeast, the ZnT3 protein works via an electrogenic antiport, exchanging one hydrogen ion for one zinc ion.[157, 158]

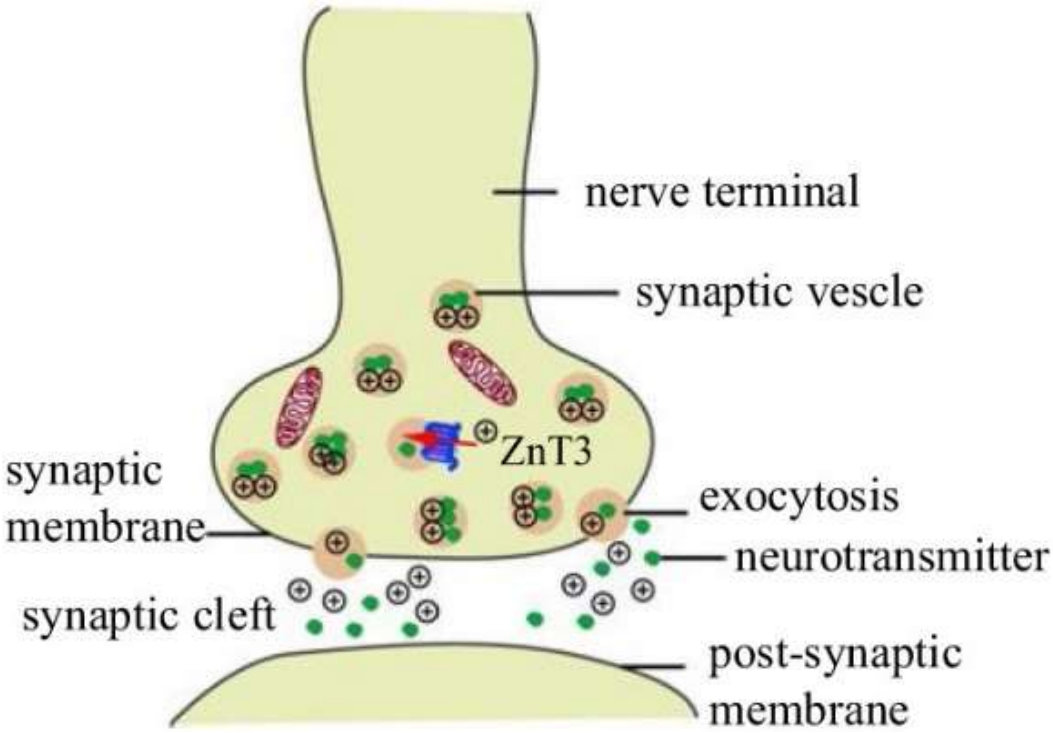

Fig. 1.5. Cellular localisation of ZnT3 transporters in an axon terminal.[159]

The position of ZnT3 in the brain has been shown by electron microscopy to be at the membranes of glutamatergic and tyrosine hydroxylase-positive synaptic vesicles in the zinc-enriched terminals in neural tissue.[160, 161] Epithelial cells of the choroid plexus,[162] the

Bergmann glial cells in the cerebellar cortex,[163] and the postganglionic neurons of mouse superior cervical ganglia[161] are additional locations of ZnT3 expression.

During ageing, the human brain, in the cerebral cortex, will face decreasing expression levels of ZnT3.[58] This downward expression is more evident in AD [58] or Parkinson's disease.[164] In agreement with decreasing the ZnT3 expression in AD or Parkinson's disease, aged ZnT3-KO mice show deficiencies in learning and memory.[58, 165, 166] The ZnT3 expression levels may affect Zn concentration and nutrients, so that omega-3 acid decreases the ZnT3 gene expression in the human neuroblastoma cell line M17.[167]

1.5.2.2 SLC39A (ZIP3) family of transporters

ZIP superfamily transporters (ZIP1-14) are found in all organisms from bacteria to mammals. They transport metals, including Zn, Fe, Mn, and possibly others, by transporting them into the cytoplasm across cellular membranes by influx or efflux from the extracellular space or intracellular, respectively (Fig. 1.6).[168] Three members of the ZIP superfamily (ZIP1-3) have been identified in mice and humans. The ZIP3 protein is localised on the plasma membrane and lysosomes.[168]

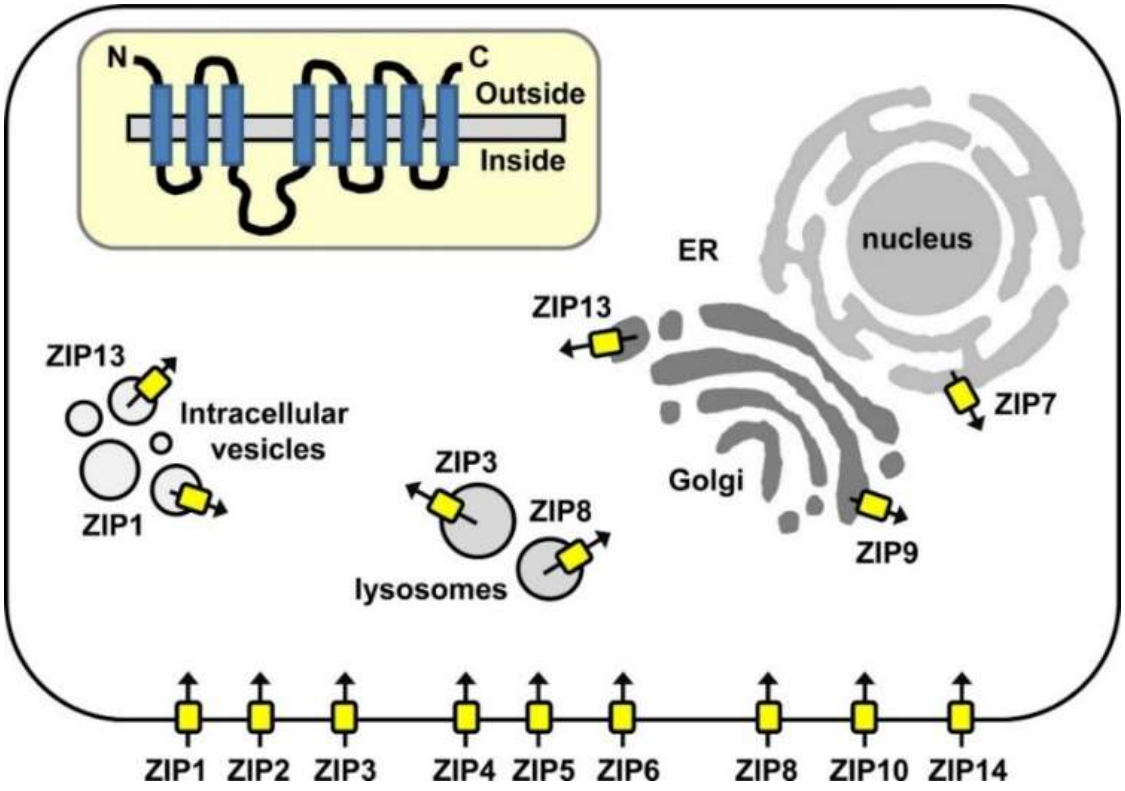

Fig.1.6 Subcellular localisation of human ZIP transporter proteins.[168]

The mouse ZIP3 gene (SLC39A3) encodes an eight-transmembrane-domain protein responsible for Zn uptake by mammary epithelial cells and is controlled by prolactin.[168] Mice with ZIP3 knockdown show a decreased Zn^{2+} uptake due to ZIP3 malfunction in importing Zn^{2+}.[169-172] Shannon L. Kelleher proposes that in ZIP3-null mice, [173] while ZIP3 protein is not necessary for adjusting the level of Zn, it is vital when dietary Zn becomes limited. In another study, Jodi Dufner-Beattie et al. found that while Zn seems to be the favoured metal for ZIP3, the Zn uptake process by ZIP3 was suppressed by all metals (Cu, Cd, Mn, Co, Ag, Mg, and Ni except Fe), inferring that ZIP3 transports other metals.[174]

1.6 Zinc in the eye

Galin's research on ocular tissues in 1962[65] revealed that the retina and choroid have the highest zinc concentration. In contrast, the cornea, iris, and sclera have the lowest amount, as shown in Table. 1.1.

Table.1.1 Total zinc concentration in tissues

Ocular tissues	Parts Per Million	Reference
Cornea	25-35	64
Iris	17-26	64
Ciliary Body	189-288	64
Retina	385-571	64
Choroid	419-562	64
Optic Nerve	67-161	64
Sclera	47-52	64
Lens	17-29	64
Bone	218	64
Muscle	197	64
Liver	179	64
Pancreas	115	64
Kidney	194	64

Most of the intracellular Zn in the eye is bound to zinc-binding proteins.[175-177] [93] However, a considerable amount of Zn is exchangeable because of its dynamic nature and participation in different biological processes[178, 179], as shown in Fig. 1.7.

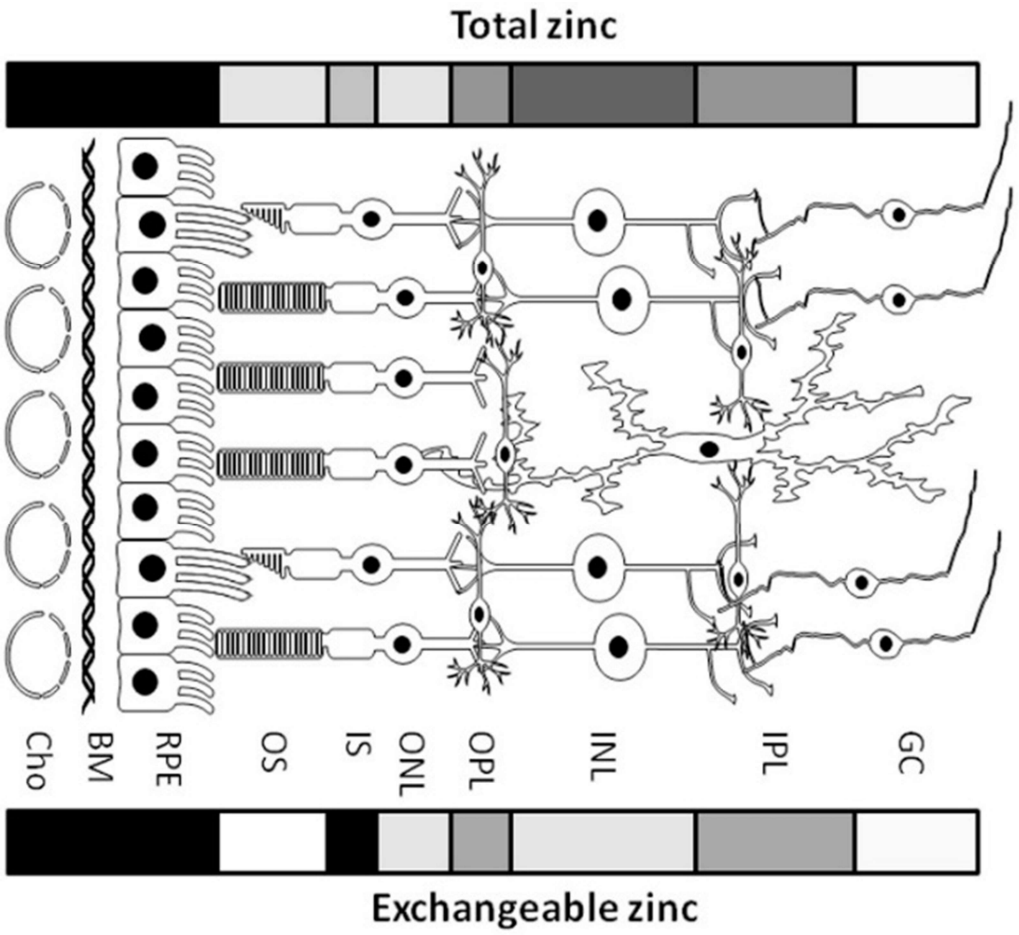

Fig.1.7 The cellular organisation of the retina. The shaded bar on the bottom[176, 180, 181] and top shows exchangeable zinc and total zinc level in the different layers.[182-185] (Note: Darker shading indicates higher zinc concentration)

1.6.1 Zinc in retinal cellular function

A functional retina is necessary for vision. Zinc is fundamental to retinal operation since many enzymes essential for retinal function are zinc-binding proteins (Fig. 1.8).[87] Zn participates in retinal functions via interaction with taurine and vitamin A, modifies plasma membranes in the photoreceptors, regulates the light-rhodopsin reaction within the

photoreceptor, modulates synaptic transmission, and acts as an antioxidant in both the retinal pigment epithelium and retina.[186]

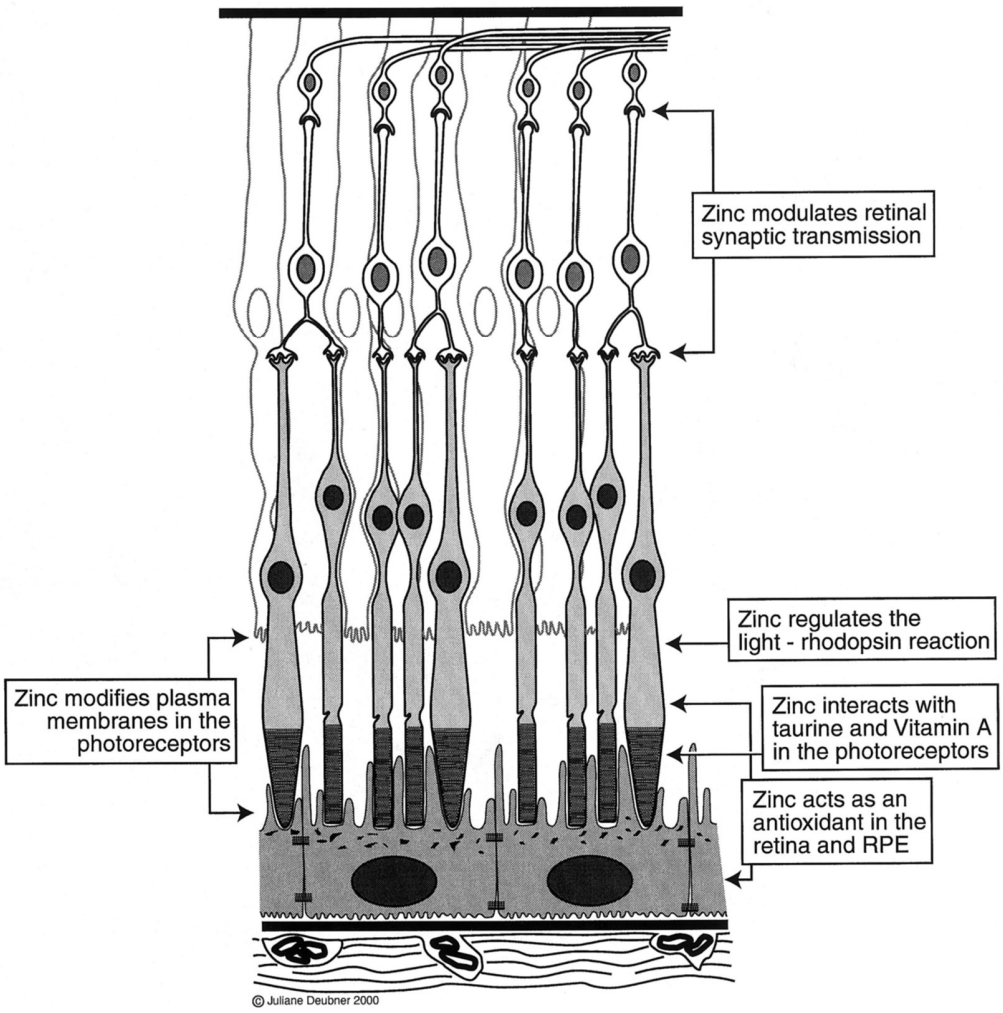

Fig. 1.8. Functions of zinc in the retina and retinal pigment epithelium.[87]

Protein aggregation found in sub-RPE deposits between the RPE cell and Bruch's membrane may indicate the malfunction of several zinc-dependent proteins.[187] While low concentrations of Zn have been reported to be neuroprotective, high concentrations have adverse outcomes.[188]

The activity of phagocytosis enzymes in photoreceptor outer segments is highly dependent on the Zn level. For instance, Wyszynski and colleagues reported that the function of α-mannosidase enzyme found in RPE cell lysosomes which degrade the outer photoreceptor segment, relies on zinc concentration.[189] Still, many ocular functions and degenerative eye diseases related to Zn concentrations need further investigation.

1.7 Alzheimer's Retinopathy: Observing Disease in the Eye

Recently, investigating Alzheimer's disease and other dementias has evolved to consider the eye-brain connection due to difficulty accessing the brain structure.[190, 191] The brain-eye tissue relationship has become an area of high interest among ophthalmologists and neurologists. Studies on the brain and eye demonstrate that diseases and conditions of the brain impact the eye, mainly because the optic nerve and retina of the eye are brain tissue that exists outside the brain.[192] Alzheimer's disease and dementia from brain cell damage appear to impact the retina.[193]

The retina's primary role is to convert light signals into decodable neuronal impulses for transmission to the brain, enabling visual perception. The retina consists of two main structural components, light-sensitive neurosensory retina and retinal pigment epithelium (Fig. 1.9).[194]

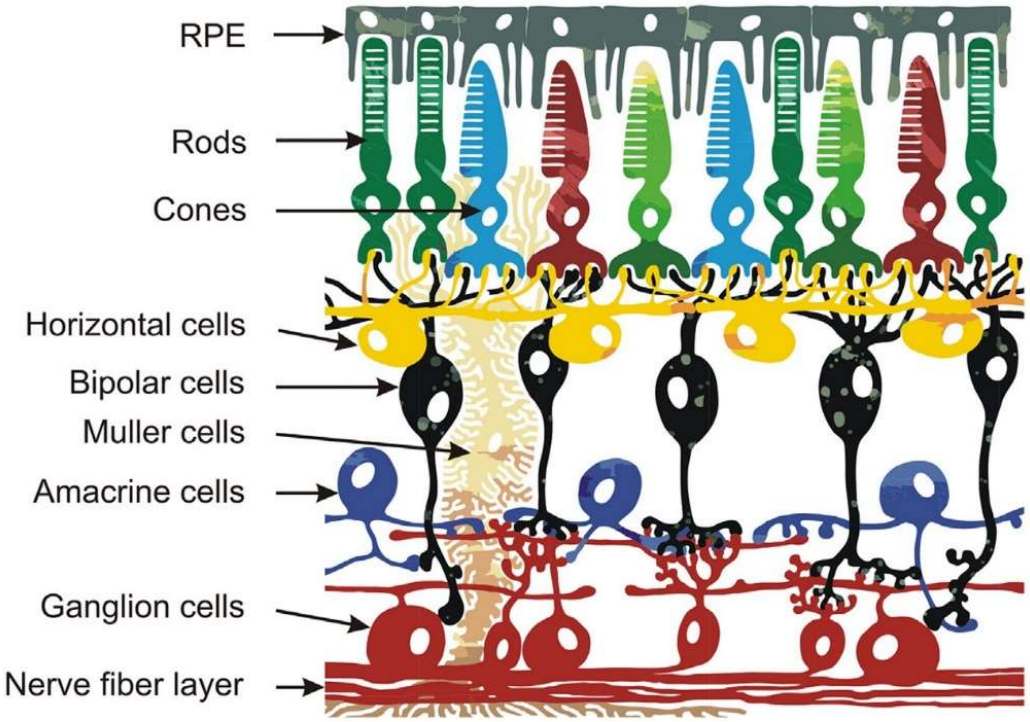

Fig.1.9 Schematic representation of the retina.[194]

The neuroretina is part of the brain's central nervous system (CNS) that is not protected by bone and is easily accessible for non-invasive high-resolution imaging.[195] Many structural and functional characteristics of the retina are identical to the brain, including the blood barrier and populations of neurons and glial cells responsible for secreting proteins related to the amyloid, such as beta-secretase 1 (BACE1), gamma-secretase, apolipoprotein E, and clusterin.[196-203] Their microvasculature is also morphologically and physiologically alike. The retina is physically connected to the brain via the optic nerve axons, with efflux and the influx of the as-synthesised amyloid beta-protein precursor from retinal ganglion cells.[196, 204]

Studies have revealed that patients with cognitive decline, mild cognitive impairment (MCI), and AD frequently suffer from visual impairments, abnormal electroretinogram patterns, and circadian rhythm disturbances, which could be attributed to retinal damage.[205-210] Additionally, a growing body of evidence demonstrates the presence of neural degeneration[191, 211] and Aβ in the retinal tissue of AD patients.[191, 207, 212] Fig.1.10 illustrates the retinal pathology in AD patients.[195]

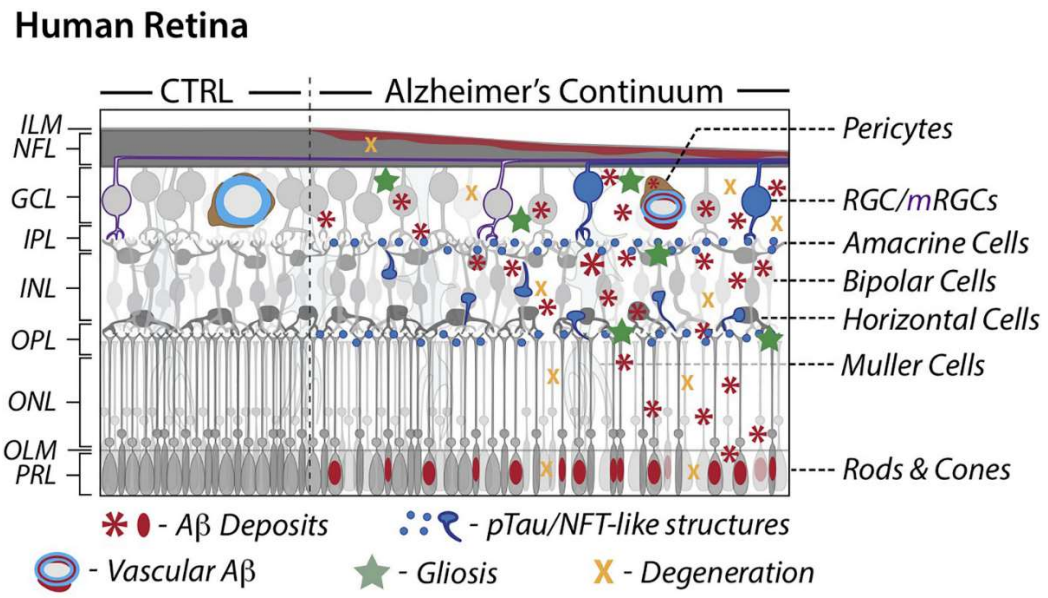

Fig.1.10 Schematic illustration of retinal pathology in AD patients.[195]

Although surveying changes related to AD in the retina are a beneficial strategy for its early diagnosis, obtaining high-quality images for analysis can be restricted by, for example, pupil size, formation of senile cataracts, and media opacities. While the retina may be modified by other diseases, such as diabetes and age-related degenerative conditions, the anterior eye is more accessible for imaging and less affected by the factors listed above.[213]

Overall, the potential for non-invasive retinal imaging, the close relationship between the retina and brain and their anatomical sub-structures, represents a new and unique window towards more comprehensive studies of neurodegenerative diseases such as Alzheimer's and Parkinson's.

1.8 In situ imaging of metals in tissues

Identifying and quantifying trace metals in their native physiological environment is necessary to understand their role in neurodegenerative processes better. Early histochemical methods, such as Turnbull's blue, dithizone, and rhodanine, were developed for the microscopic identification of Fe, Zn, and Cu in tissues, facilitating the representation of transition metals.[214, 215] A wide variety of highly sensitive instruments and microanalytical techniques have since been developed for the in situ analysis of transition metals. Table 1.2 shows some of the currently available microanalytical methods for the in situ detection of trace metals in cells and tissues.[216-218]

Depending on the task, each of these microanalytical technique (Table.1.2) has advantages and disadvantages. For instance, MRI and PET suffer from common drawbacks, including high costs, low spatial resolution, limited accessibility, poor sensitivity and specificity,[219] and the absence of standardisation and scalability. Fluorescence microscopy-based methods are highly sensitive in live cell and tissue studies. However, they have some limitations such as scattering, narrow penetration depth, photobleaching, phototoxicity, lack of external calibration standards, and inaccurate data interpretation resulting from interfering probes and dyes with the lipid vesicles, etc.[220] Synchrotron and focused ion-beam-based microscopes offer the best combination of sensitivity and spatial resolution; however, due to their ionizing high-energy excitation beam are not ideal for studying live organisms.[218]

Metal concentrations of anatomical regions have been measured through various analytical techniques, such as flame-induced atomic absorption spectrometry, electrothermal atomic absorption spectrometry, and optical emission spectrometry with excitation in inductively coupled plasma.[221] However, these techniques result in losing spatial information, which is vital when disease states being assessed involve small, well-defined regions or specific cell types. Laser ablation-inductively coupled plasma-mass spectrometry (LA-ICP-MS) has received much attention for visualising metals in biological systems due to its advantages, such as higher sensitivity, lower matrix effect and less sample preparation.[222]

Table.1.2 Microanalytical techniques for in situ imaging of trace metals in biology.

Analytical method	Detection limit	Spatial resolution (µm)	Analytical depth (µm)	Quantification	Ref
Electron Probe X-ray Microanalysis	100 (µXAS) µg/g	0.03	0.1-1	Semi-quantitative	210
Proton Beam Microprobe (PIXE, RBS, & STIM)	1-10 µg/g	0.2-2	10-100	Quantitative (PIXE-RBS)	210
X-ray Microprobe (SXRF, µXAS, µXANES)	0.1-1 (SXRF) 100 (µXAS)	0.03-0.2	> 100	Quantitative	210
Laser Ablation-Inductively coupled plasma - mass spectrometry (LA-ICP-MS)	0.01 µg/g	15-50	200	quantitative	210
Positron Emission Tomography (PET)	high pM	1000-2000	no limit	Semi-quantitative	211
Magnetic Resonance Imaging (MRI)	mM – low µM	25-100	no limit	Semi-quantitative	211
Optical Fluorescence Microscopy	pM to nM	2000-3000 (in vivo) 0.2-0.5 (in vitro)	< 1 cm	Semi-quantitative	211
Visible Light Microscopy	Low-µM	0.2-0.5	0.01-1	Semi-Quantitative	212

1.9 Aims of this thesis

This thesis aims to investigate the concentrations of transition metals (Cu, Zn, and Fe) and zinc transporter proteins (ZnT3 and ZIP3) in the brain and eye of mice and human

samples (AD and healthy) to explore their role in AD, defining any correlations between the eye and brain tissues that occur in AD.

This aim will be addressed by the specific objectives:

I. Visualising anatomical distributions and concentrations of transition metals (Zn, Fe, and Cu) in the cross-sectional slices of the brain and eye of mouse model (WT and APP/PS1, 9-month) by laser ablation-inductively coupled plasma-mass spectrometry (LA-ICP-MS).

II. Investigate the age-related changes in transition metal concentrations in the eye and brain of mice models (WT and APP/PS1, 9-and 18-month old) by solution nebulisation-inductively coupled plasma-mass spectrometry (SN-ICP-MS).

III. Assess the abundance and expression of ZnT3 and ZIP3 in the eye and brain of mice models (WT and APP/PS1, 9-and 18-month old) by immunofluorescent imaging and Western blot, respectively.

IV. Examine the role of ZnT3 as the Zn transporter in the eye and brain of the mice model (knockout and WT, 3, 11, and 14 months) using SN-ICP-MS.

V. Study the concentrations of transition metals and zinc transporters proteins in the human brain and eye (9 cases with AD and 6 controls) by LA-ICP-MS and immunofluorescence.

VI. Identify the amyloid plaques in the mice and human samples (control and AD, eye and brain) using Quantum dot labelled amyloid-beta.

Chapter 2: Materials and Methods

2. Materials and Methods

All experiments were conducted within the Graduate School of Health (GSH) at the University of Technology Sydney (UTS).

2.1 Sample preparation

2.1.1 Mice sample preparation

APP/PS1, a double transgenic mouse expressing a chimeric mouse/human amyloid precursor protein (Mo/HuAPP695swe) and a mutant human presenilin 1 (PS1-dE9), and age-matched C57BL6 littermate WT were received from the University of Melbourne (Florey Institute, 19-060-FINMH). A previous study conducted by our group investigated the behavioural phenotype of APP/PS1 and WT mice. Their findings showed a non-significant decline in the displacement index (novel object recognition) in APP/PS1 mice, along with a non-significant increase in the displacement index among WT mice from 6 to 12 months. [223] Upon removing brains and eyes, they were placed in the solution consisting of paraformaldehyde (4 % w/v) and phosphate-buffered saline buffer (PBS) (0.1 M, pH 7.4) and stored at 4 ℃ overnight. Then, they were transferred into a 30 % sucrose solution (PBS) for three days to cryoprotect the tissue. Next, the sucrose solution was removed, and the left sagittal side of the brain was placed with the tweezers in the side of the embedding mould. Specifically, the brain's flat side was oriented so that it lay flat against the inner surface of the embedding mould. This ensured proper contact and alignment of the brain with the embedding mould for further processing. It is worth noting that the whole eye sample was placed in the middle part of the

embedding mould. Afterward, embedding mould was filled with optimal cutting temperature compound (OCT) while bubbles were removed with tweezers and kept at -80 ℃.

2.1.2 Human sample preparation

The human eyes and brains were collected from the Netherlands Brain Bank and processed under the same protocol. We received human eye and brain tissues embedded in paraffin blocks, not as sections. All ethical requirements in relation to tissues obtained from the Netherland Brain Bank (NBB) were covered by NBB's ethical guidelines and processes. A biosafety approval was sought and obtained from UTS prior to commencement of experiments: "(2016-05-R-G) Implications of retinal neurodegeneration in Alzheimer's Disease. Fig.2.1 represents the Paraffin-embedding process for human tissues.[224]

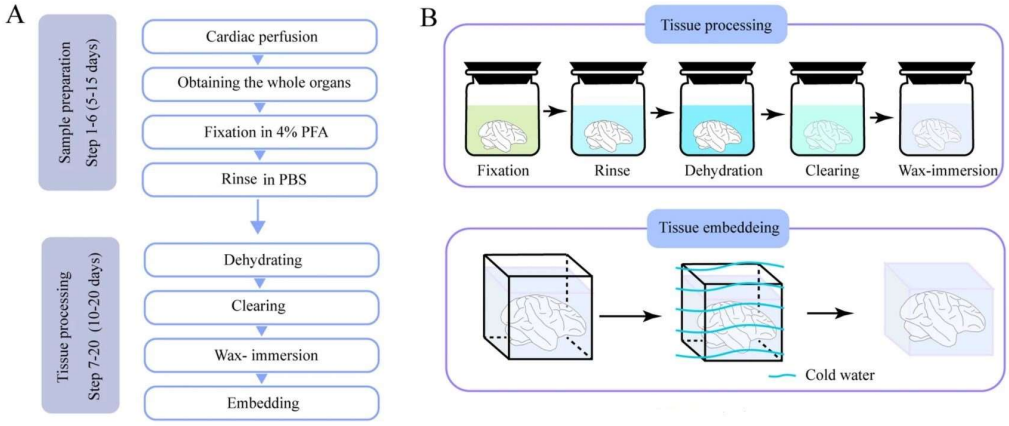

Fig.2.1 Schematic diagram for the entire experimental procedure. (A) Flowchart for the all steps of the protocol. (B) Schematic diagram illustrating the procedure for embedding brain tissue.[224]

2.2 Instrumentation

2.2.1 Cryosectioning

All frozen tissue sectioning was performed using Leica CM1950 (Leica biosystem).[225] The specimen and blade holder temperature were set to -20 ℃ to keep the

structure of embedded OCT samples during the sectioning. The thickness of each slice was set to 10 μm. Each specimen is positioned and sectioned at the same angle to the blade to achieve consistency in the sectioning process. A few initial slices are cut from the sample to remove excess OCT to section from the fresh sample. Four and three slices of eye and brain samples were placed on the surface of microscope slides, respectively. Finally, all sectioned slides were stored at -80 ℃.

2.2.2 Microtome paraffin sectioning

All paraffin tissue sectioning was performed using MICROM HM 325 (Thermo Scientific Microtome).[226]

1: Cooling paraffin-embedded tissue blocks with ice before sectioning. It helps to have thinner sections; the small amount of moisture penetrating the block makes cutting easier.

2: Fill a water bath with ultrapure water and heat to 40-45 ℃.

3: Place the blade in the microtome holder, ensure it is secure and set the clearance angle. The clearance angle prevents contact between the knife facet and the face of the block.

4: Insert the paraffin block and orientate so the blade will cut straight across the block.

5: Embellish the block by cutting a few thin sections (30-50 μm) to cut a representative section.

6: Cut sections at a thickness of 10 μm, then pick up the sections and float them on the water's surface in the water bath, so they flatten out.

7: Use microscope slides to pick the sections out of the water bath and allow sections to dry overnight.

2.2.3 Laser ablation-inductively coupled plasma-mass spectrometry (LA-ICP-MS)

LA-ICP-MS was applied to measure the concentration of Zn, Fe, and Cu and their distribution in the WT and APP/PS1 mice model (9 month) and human samples.[227] This research was carried out on a Teledyne Cetac LSX-213 G2+ laser hyphenated to an Agilent Technologies 7700 ICP-MS, with argon used as the carrier gas. LA-ICP-MS conditions were optimized on NIST 612 Trace Element in Glass CRM. The human samples were ablated under 50 μm spot size and a scan speed of 200 μm/s at a frequency of 20 Hz. The mice samples were ablated under 50 μm spot size and a scan speed of 100 μm/s at a frequency of 20 Hz. Quantification was performed via external, matrix-matched six-point calibration standards containing differing concentrations of Zn, Fe, Cu, and Mn in gelatine as per the method by Westerhausen et al.[228] The data were collated into a single image file using in-house developed software and quantified and visualized using ImageJ.

2.2.4 Solution nebulisation-inductively coupled plasma-mass spectrometry (SN-ICP-MS)

Solution nebulisation-inductively coupled plasma-mass spectrometry (SN-ICP-MS) was used to analyze digested ZnT3-knockout, WT, and APP/PS1 mice models and digested standards. SN-ICP-MS was performed using 7700x series ICP-MS (Agilent Technologies, Waldbronn, Germany), which is equipped with a micromist^{TM} concentric nebuliser (Glass Expansion, West Melbourne, Australia) and a Scott type double pass spray chamber. All experiments used 99.9995 % ultra-high purity liquid argon (Argon 5.0, Coregas Pty Ltd, Yennora, NSW, Australia). Solution-based samples were transferred to the ICP-MS using a 1.02 mm internal diameter Tygon tubing and a three channels peristaltic pump. The solutions were pumped at a continuous flow rate of 1.0 mL/min. Then, they were delivered to the

plasma of the ICP via a Micromist nebulizer and Scott type double pass spray chamber. It is worth mentioning that a 100 ppb Rhodium solution in 1 % HNO_3 was used as an internal standard and introduced into the analyte flow via a T connector post-pump.

2.2.5 Microscopy

Zeiss Axioscan slide-scanning microscope, high-throughput, was used for fluorescence imaging. It has two light sources, including the super-fast 7 wavelengths LED light source Zeiss Colibri 7 and the white light LED light source X-Cite Xylis, allowing the selection of the appropriate wavelengths. It is equipped with Peltier-cooled cameras from the Zeiss Axiocam portfolio to support brightfield and fluorescence applications with state-of-the-art imaging performance.

2. 3 Immunofluorescence and Hematoxylin and Eosin (H&E)

2.3.1 Materials

1: Phosphate-buffered saline (PBS) (137 mM NaCl, 2.7 mM KCl, 10 mM Na_2HPO_4, 1.76 mM KH_2PO_4, pH 7.4) was purchased from Sigma Aldrich (P4417-50TAB).

2: Rehydration reagents: xylene (534056-4L) and Ethanol (95 %, 64-17-5) were purchased from Sigma Aldrich.

3: Heat-induced epitope retrieval reagent: Sodium citrate buffer was purchased from Sigma Aldrich (pH 5.5, P4922).

4: Endogenous peroxidase blocking solution: 3 % H_2O_2 was purchased from Sigma Aldrich (88597).

5: Blocking reagent: Bovine Serum Albumin was purchased from Sigma Aldrich (A3059).

6: Primary antibody: Anti-ZIP3 antibody (GenTex, GTX85133) and Anti-ZnT3 antibody (Merck, SAB2105534).

7: Secondary antibody: Anti-Goat IgG (whole molecule)-Cy3 antibody produced in rabbit) was purchased from Sigma Aldrich (C2821-1ML).

8: Thioflavin S was purchased from Sigma Aldrich (T1892-25G).

9: Triton™ X-100 was purchased from Sigma Aldrich (X100-1L).

Before tissue staining, all counterstains, primary and secondary antibody concentrations, fixation, blocking, and washing steps should be optimized.

2.3.2 Immunofluorescence staining protocol of mice frozen tissue

First, the eye/brain tissues were permeabilized with Triton X-100 (1 %, 0.1 M PBS) and incubated at room temperature for 30 min, followed by washes with phosphate-buffered saline (PBS, 0.1M) (3 x 5 minutes). Next, tissues were blocked with PBS-BSA (5 %, 0.1 M) for 2 h at room temperature. Tissues were incubated with primary antibody dilution (1/1000) (Anti-ZIP3 antibody or Anti-ZnT3 antibody) in PBS-BSA (0.1 M, 1 %) overnight at 4 ℃ in a sealed and moist environment. The following day, the primary antibody solution was removed and washed with Triton X-100 (0.1 %, 0.1 M PBS) (5 x 4 minutes). Next, tissues were incubated with the secondary antibody dilution (1/1000) (Anti-Goat IgG (whole molecule)-Cy3 antibody produced in rabbit) in PBS-BSA (0.1 M, 1 %) at room temperature for 2 h. After incubation, the tissue was washed with PBST (0.1 %) (5 x 4 minutes) and incubated with Thioflavin S 1 % (brain) or 2 % (eye) for 1 min. Then, the tissue was washed thrice with 80 % ethanol, 95 % ethanol, and milli-Q water. One drop of 4', 6-Diamidino-2-Phenylindole (DAPI) was added to the surface of the tissue, covered with a coverslip, and air-dried (4 ℃, 12 h). Eventually, the coverslip was sealed with nail polish and imaged by fluorescence microscopy (Zeiss Axioscan slide-scanning microscope).[229]

2.3.3 Immunofluorescence staining protocol of paraffin embedded tissue

1: Human Paraffin-embedded eyes and brains are cut (10 um) and mounted on Superfrost plus slides. Slides are placed in plastic vertical slide holders and heated for 60 minutes at 50-60 °C in a dry oven to facilitate tissue attachment and soften the paraffin.

2: Remove paraffin and rehydrate tissues using the following slide wash/incubation sequences: xylene (2 x 2 minutes), 100 % ethanol (2 x 2 minutes), 90 % ethanol (2 x 2 minutes), 70 % ethanol (2 x 2 minutes), ddH_2O (1 x 2 minutes).

3: Wash slides with PBST (0.5 % Triton X100) (3 x 5 minutes).

4: Antigen retrieval was performed by submerging slides in excess antigen retrieval buffer and boiling them in a microwave using a microwave-safe container for 10 minutes. Then, allow slides to cool to room temperature (about 40 minutes).

5: Wash slides with PBST (0.5 % triton) (3 x 5 min).

6: Peroxidase blocking: To block endogenous horseradish peroxidase activity, slides are incubated in 0.3 % (v/v) hydrogen peroxide solution for 10 min at room temperature.

7: Wash with PBST (0.5 % triton) (3 x 5 min).

The rest of the procedure is the same as frozen tissue (see section 2.3.2 for details).[230]

2.3.4 Hematoxylin and Eosin (H&E)

Paraffin slides were placed in a slide holder and washed with Xylene (3 x 3 min), 100 % ethanol (3 x 3 min), 90 % ethanol (1 x 3 min), 70 % ethanol (1 x 3 min), and deionized water (1 x 3 min). Afterward, for hematoxylin staining, slides were incubated with Hematoxylin (1 x 3 min), followed by washing with tap water (1 x 3 min). Then, slides were dipped in acid ethanol (8-12 times), followed by washing with tap water (1 x 3 min). In the following, for eosin staining and dehydration, slides were incubated with eosin (1 x 30 sec)

and washed with 95 % ethanol (3 x 5), 100 % ethanol (3 x 5), and Xylene (3 x 5). Finally, slides were covered by glass coverslips and dried overnight in the hood.[231]

2.4 Western blot

APP/PS1 and normal-aged mice (9-and-18-month) brains were dissected on ice and processed immediately. Briefly, hippocampus tissues were homogenized in ice-cold radioimmunoprecipitation assay buffer [50 mM, Tris-Cl, pH 7.5, 150 mM NaCl, 1 % NP-40, 0.5 % sodium deoxycholate, and 1 % sodium dodecyl sulfate], supplemented with a protease inhibitor cocktail (Sigma-Aldrich P8340) and phosphatase inhibitors (50 mM NaF, 1 mM Na_3VO_4, and 30 mM Na_4P_{207}) (Sigma Aldrich P0001), using an ultrasonic probe. Then, the above-mixture protein solutions were centrifuged at 12000 G at 4 ℃ for 30 min. Afterward, the supernatants were collected, and total protein concentrations were determined using the BCA Protein Assay Kit (Pierce Biotechnology, Rockford, IL, USA). Hippocampal samples (40 µg) were separated by 12 % sodium dodecyl sulfate-polyacrylamide gel electrophoresis (140 V, 45 min) and transferred to a nitrocellulose membrane by iBlot®2 Dry Blotting System. Then, the nitrocellulose membrane was blocked by the blocking buffer, followed by incubation with primary antibodies overnight at 4 ℃. The dilutions of primary antibodies were 1:1000 for ZnT3 and ZIP3 and 1:10000 for glyceraldehyde 3-phosphate dehydrogenase (GAPDH). The following day, the membrane was washed with tris-buffered saline solution with the 0.1 % Tween 20 (TBST) and incubated with 20 mL buffer (10 mL blocking buffer + 10 mL TBST) containing 1.5 µL of secondary goat Ab (925-32211) for 1.5 h at room temperature. Then, gently shake with 10 mL of TBST, TBS, and water for 5 min. Finally, read with Odyssey® Dlx Imaging System.[232]

2.5 Data processing

The ICP-MS provides the data of each raster line in a numbered folder containing a correspondingly numbered comma separated values file (CSV), including the time-resolved elemental data. The structure of the CSV is in the form of the first column time in seconds. Each consecutive column is the signal of one of the measured elements in counts per second, starting from the lowest mass and ending with the highest mass. With the help of ImaJar (MassIamger Version 3.62b), developed by Robin Schmid, University of Munster, each CSV file was separated into individual elements followed merged into a single element image (Fig.2.2). The hippocampus and cortex regions of the brain were demarcated based on The Allen Mouse Brain Atlas.[233] The retina was demarcated using published papers that present Hematoxylin and eosin (H&E) images of retina structure. [234-236]

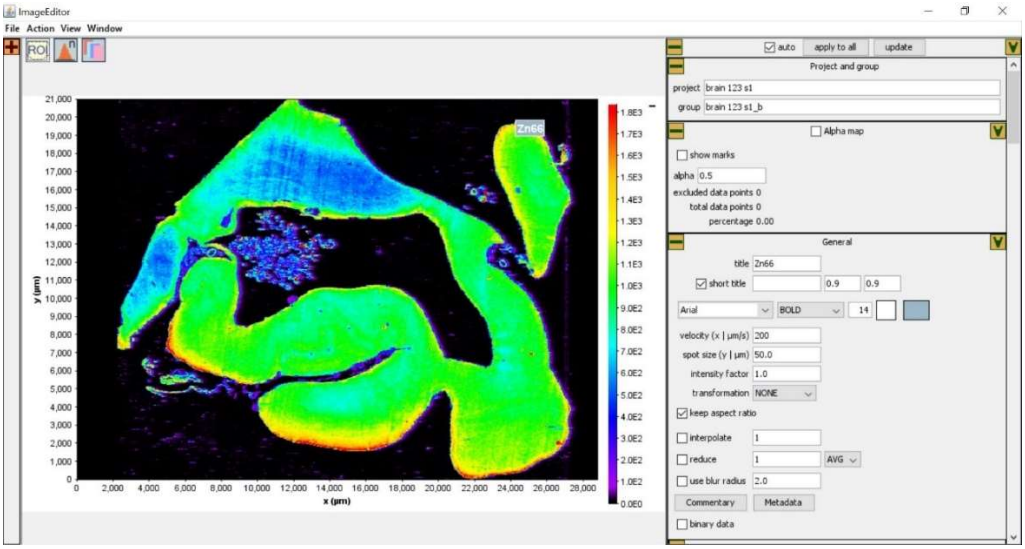

Fig.2.2 Graphic user interface for ImaJar software.

Chapter 3: Transition metals in Mice

3. Evaluation of Fe, Cu, and Zn in the eye and brain (WT and APP/PS1 mice models)

3.1 Introduction

The distribution and homeostasis of metal ions such as iron (Fe), copper (Cu), zinc (Zn), and calcium (Ca), which are crucial for maintaining normal physiological functions in the AD brain, have been discussed for almost six decades.[237]

The brain concentrations of Mn, Fe, Cu, and Zn range from 1.3-2.72, 21-120, 5.0-10.6, and 33-47 ng/g, respectively.[238] The deposition of Aβ within the neocortex, followed by oxidative stress and neuronal demise, is the hallmark of AD. There are many reports regarding the metallochemistry of Aβ, in which Fe, Zn, and Cu bind to Aβ and precipitate it into aggregates.[237, 239-241] On the one hand, low physiological concentrations of Zn^{2+} result in Aβ precipitation.[52] In addition, Cu^{2+} and Fe^{3+} have a higher impact on Aβ aggregation under mildly acidic conditions (e.g., pH 6.8-7.0) as compared to the Zn ion.[242] On the other hand, the high concentrations of Fe, Zn, and Cu in amyloid plaques suggest that oxidative stress generated from their dyshomeostasis and metal-protein interactions may be the mechanism underlying the aggregation and toxicity of senile plaques, which eventually results in AD.[44, 50, 243] Evidence suggests that removing (chelating) Fe, Cu, and Zn from amyloid plaques can reduce their toxicity and consequently, increase their solubility, which further demonstrates the impacts of Fe, Cu, and Zn in AD.[50, 244, 245]

There are several controversial reports regarding possible associations between age-related macular degeneration (AMD) and AD; these studies are based on mental state examination or word fluency scores.[246-249] Depleting intracellular Zn in the eye's retinal cells causes the caspase-dependent death of photoreceptors and other retinal neurons. As a result,

this Zn deficiency leads to the pathogenesis of AMD.[250] Furthermore, Age-Related Eye Disease Studies (AREDS) and several other research groups argue that dietary supplementation with Zn is an efficient strategy against AMD.[251-253]

Here, laser ablation-inductively coupled plasma-mass spectrometry (LA-ICP-MS) and solution nebulisation-inductively coupled plasma-mass spectrometry (SN-ICP-MS) were applied to study the transition metals (Cu, Fe, and Zn) anatomical distribution in cross-sectional slices and assess age-related changes in their concentrations in both the brain and the eye mouse model (WT and APP/PS1, 9-and 18-month old), respectively.

To the best of the author's knowledge, this is the first report investigating the concentrations and distributions of transition metals (Cu, Fe, and Zn) in the eye's retina AD mouse model.

3.2 Results

3.2.1. Visual distribution of transition metals in the brain and the eye of APP/PS1 and WT mice.

The first aim was to visualize the anatomical distributions of metal ions in the cross-sectional brain and eye slices obtained from 9-month old APP/PS1 and WT mice. LA-ICP-MS was used (see Section 2.2.3 for details) to produce a calibrated representative image of each metal's distribution (i.e., Cu, Fe, Zn). Image analysis was then performed to objectively quantify the concentrations of transition metals in the various regions of interest (i.e., hippocampus, cortex, retina). While the one-way ANOVA test and t-tests could be used to compare the concentrations of transition metals between the WT and APP/PS1 groups, we used t-tests to compare the metal levels between two groups (WT vs. APP/PS1) separately for each region of interest (retina, hippocampus, and cortex). We are more interested in

pairwise comparisons between individual groups. The metal levels in the hippocampus are significantly higher than in the retina, which could lead to a significant overall difference when we compare all three regions together using one-way ANOVA. As a result, it might not provide us with detailed information about which specific groups are driving the difference.

Copper (Cu)

The anatomical distributions of Cu in the brain and eye are shown in Fig. 3.1 (A and B, respectively). Visual assessment of the calibrated quantitative images demonstrated greater Cu enrichment in the hippocampus and cortex of WT mice compared with APP/PS1 mice (Fig.3.1 A). A similar pattern was also observed in the eye, with the retina of WT mice harbouring higher concentrations of Cu compared to the APP/PS1 mice (Fig.3.1 B). The image analysis results were consistent with the visual assessment, with higher concentrations of Cu observed in the brain and retina of WT mice compared with APP/PS1 mice (Fig.3.2). We excluded the ciliary body region in our image processing, and we believe that the area with high copper expression is part of the retina. Furthermore, we looked at the correlation between the retina and the brain- not the front of the eye. More specifically, retinal Cu concentrations (µg/g) were significantly higher in WT mice compared with APP/PS1 mice (18.2 ± 0.9 *vs* 16.2 ± 1.2, $p<0.001$). In the hippocampus and cortex, Cu levels (µg/g) were also significantly higher in WT mice compared with APP/PS1 mice (20.3 ± 1.4 *vs* 19 ± 0.5, $p<0.05$ for the hippocampus; 14.4 ± 1.2 *vs* 13 ± 1.5 $p<0.05$ for the cortex).

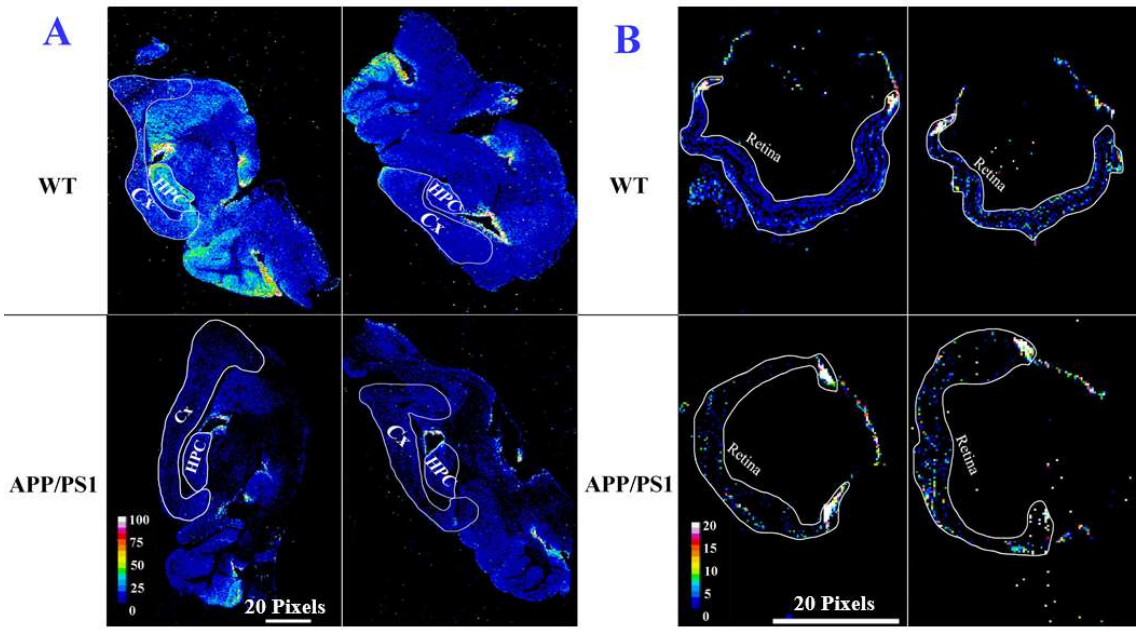

Fig.3.1 Spatial distribution of Cu in the brain (A) and eye (B). In each panel: sample map of 63Cu in sagittal brain/eye sections of 9-month-old WT (upper row) and APP/PS1 (lower row) mice. The scale represents calibrated Cu in ppm. HPC, hippocampus; CX, cortex. Side by side images of the brain and retina belong to two different animals

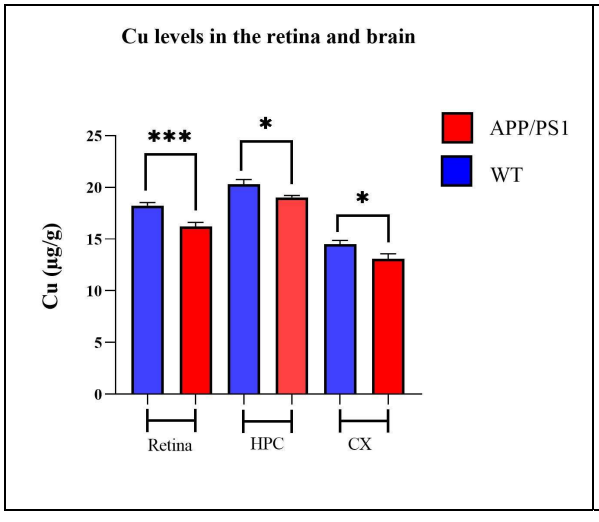

Fig.3.2. Metal quantification analysis. Cu levels in the retina, hippocampus, and cortex of 9-month old APP/PS1 and WT mice (n=10 mice in each group). Error bars represent Standard Error of the Mean (SEM). (*$p < 0.05$, ***$p < 0.001$, Student's t-test, unpaired). HPC, hippocampus; CX, cortex

- ***Iron (Fe)***

The spatial distributions of Fe in the brain and eye sections of a representative WT and APP/PS1 mouse is shown in Fig. 3.3 (A and B). Visual assessment of the brain calibrated quantitative images shows that the hippocampus and cortex of WT mice possess higher concentrations of Fe compared with APP/PS1 mice (Fig.3.3 A). The retina of WT mice displayed a similar pattern (higher Fe content) relative to the age-matched APP/PS1 mice (Fig.3.3 B). The image analysis also confirmed these observations: the brain and the retina of WT mice had higher Fe concentrations than APP/PS1 mice (Fig.3.4). In the retina and hippocampus, Fe concentrations (µg/g) were significantly higher in WT mice compared with APP/PS1 mice (82.5 ± 6.3 *vs* 73.1 ± 5.5, $p<0.01$ for retina, 53.5 ± 3.6 *vs* 37.3 ± 5.7, $p<0.0001$ for hippocampus). In the cortex, while Fe concentration (µg/g) in the WT mice was 1.13 times higher than that of APP/PS1 mice, the difference was not statistically significant (40.4 ± 5.3 *vs* 36.4 ± 6.3, p: 0.18).

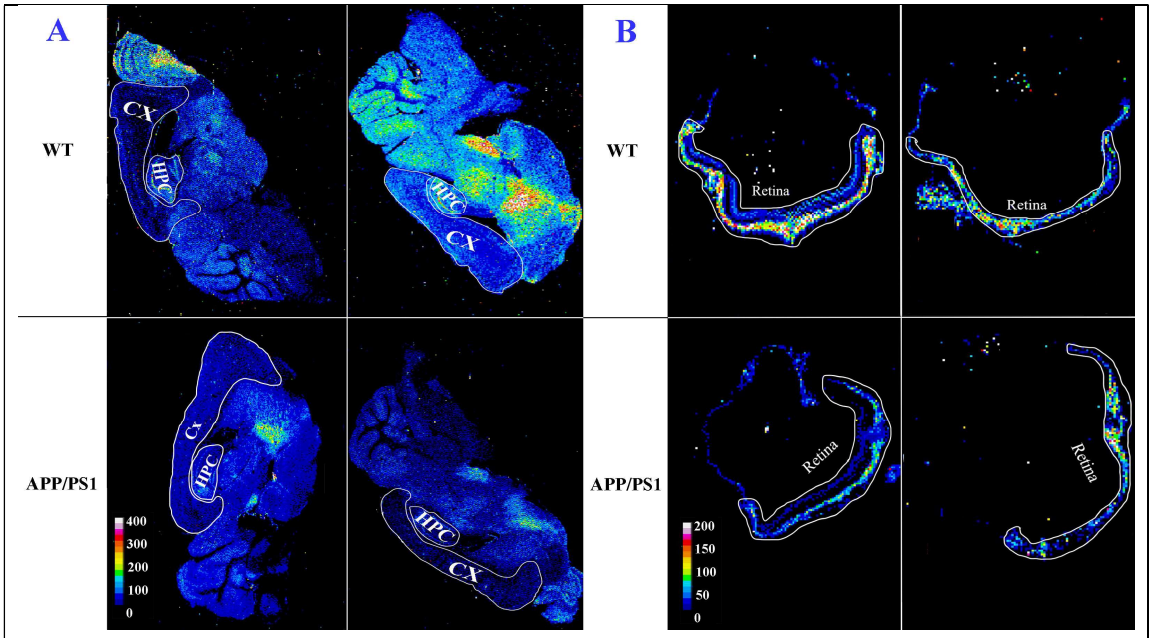

Fig.3.3 Spatial distribution of Fe in the brain (A) and eye (B). In each panel: sample map of 56Fe in sagittal brain/eye sections of 9-month-old WT (upper row) and APP/PS1 (lower row) mice. The scale represents calibrated Fe in ppm. HPC, hippocampus; CX, cortex. Side by side images of the brain and retina belong to two different animals.

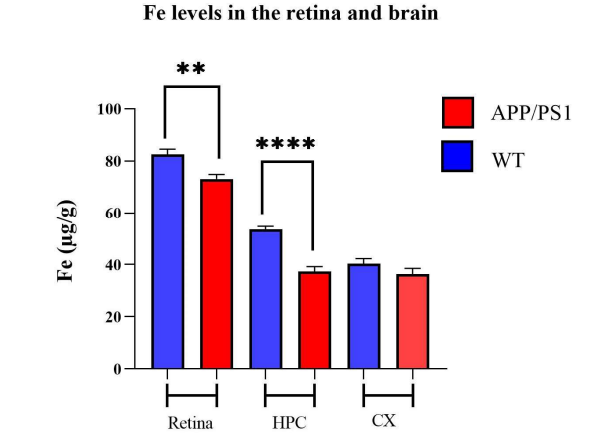

Fig.3.4. Metal quantification analysis. Fe levels in the retina, hippocampus, and cortex of 9-month old APP/PS1 and WT mice (n=10 mice in each group). Error bars represent Standard Error of the Mean (SEM) (**p < 0.01, ****p< 0.0001, Student's t-test, unpaired). HPC, hippocampus; CX, cortex.

- ***Zinc (Zn)***

The quantitative images of Zn distribution in the eyes and brains are shown in Fig. 3.5 (A and B). Surveying the calibrated quantitative images, illustrate higher Zn concentration

in the hippocampus and cortex of WT mice compared with in APP/PS1 mice (Fig.3.5 A). Similarly, the retina of WT mice also displayed the same trend harbouring higher zinc than the APP/PS1 mice (Fig.3.5 B). The image analysis demonstrated higher concentrations of zinc in the brain (HPC and cortex) and retina of WT mice compared with APP/PS1 mice (Fig.3.6). In summary, Zn concentrations (µg/g) were significantly higher in WT mice compared with APP/PS1 mice (59.8 ± 6 *vs* 52.3 ± 2.2, $p<0.01$ for the retina; 52.5 ± 8 *vs* 43.3 ± 2.7, $p<0.01$ for the hippocampus; 20.4 ± 0.9 *vs* 17.5 ± 1, $p<0.0001$ for the cortex).

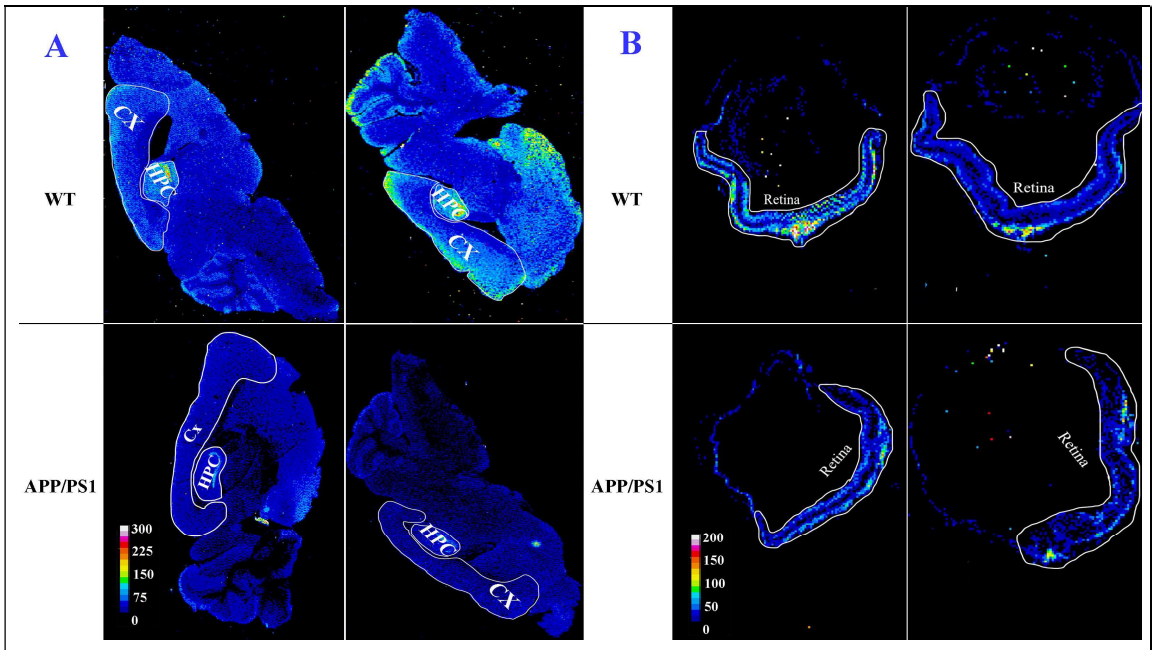

Fig.3.5 Spatial distribution of Zn in the brain (A) and eye (B). In each panel: sample map of 66Zn in sagittal brain/eye sections of 9-month-old WT (upper row) and APP/PS1 (lower row) mice. The scale represents calibrated Zn in ppm. HPC, hippocampus; CX, cortex. Side by side images of the brain and retina belong to two different animals.

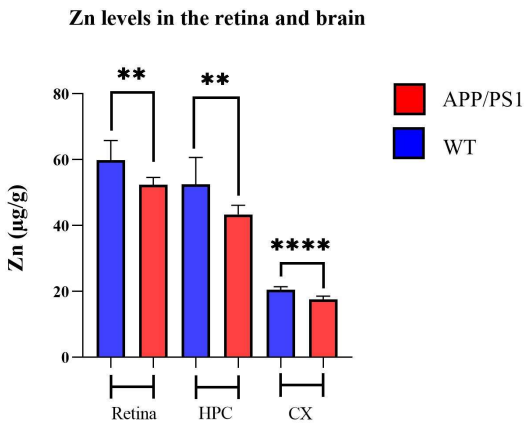

Fig.3.6. Metal quantification analysis. Zn levels in the retina, hippocampus, and cortex of 9-month old APP/PS1 and WT mice (n=10 mice in each group). Error bars represent Standard Error of the Mean (SEM) (**p < 0.01, ****p< 0.0001, Student's t-test, unpaired). HPC, hippocampus; and CX, cortex.

3.2.2. Age-associated changes in the transition metal concentrations of the brains and the eyes of APP/PS1 and WT mice.

To investigate age-related changes in transition metal concentrations, in both the brain and the eye, SN-ICP-MS was employed (see section 2.2.4 for details). The total concentration of each metal in the hippocampus, cortex and retina (per dry tissue weight) of 9- and 18-month old APP/PS1 and WT mice was measured. APP/PS1, a double transgenic mouse expressing a chimeric mouse/human amyloid precursor protein (Mo/HuAPP695swe) and a mutant human presenilin 1 (PS1-dE9) and age-matched C57BL6 littermate WT mice were used in our experiments. We chose to examine animals at 9 and 18 months of age, as this reflects a deposition in the hippocampus, cognitive impairment, and also impaired long-term potentiation (LTP) in the CA1 region of the hippocampus.[254] In addition to a comparison of the absolute concentrations between the two strains, a comparative analysis was performed by normalising the metal concentration in the retina of each animal to its corresponding concentration in the hippocampus. This was performed to ensure an accurate

and consistent interpretation of the transition metal concentrations in the retina and to remove any unknown biological bias (e.g., gender).

- ***Copper (Cu)***

The Cu concentrations in the retina, hippocampus, and cortex of 9- and 18-month old mice (APP/PS1 and WT) are summarised in Fig.3.7. The overall trend of higher Cu concentrations in the WT mice compared to the APP/PS1 mice (observed also on LA-ICP-MS images) was extended from 9 to 18 months of age. In both animal groups, retinal Cu concentrations (ng) were significantly higher at 18 months compared to 9 months of age (8871 ± 4134 *vs* 28871 ± 5071, $p<0.0001$ for APP/PS1, 21903 ± 6513 *vs* 32149 ± 7959, $p<0.05$ for WT). Comparison of the retinal Cu concentrations (ng/g) between the APP/PS1 and WT mice revealed a significant difference only at 9 months of age (21903 ± 6513 *vs* 9585 ± 3348, $p<0.01$).

Assessment of the normalised retinal Cu concentrations showed a 1.14 and 1.1 increase in WT (0.5 ± 0.8 *vs* 0.6 ± 0.3, p: 0.98) and APP/PS1 (0.6 ± 0.6 *vs* 0.6 ± 0.2, p: 0.99) mice from 9 to 18 months of age, respectively. In the brain, a 1.33-fold increase in the hippocampus Cu concentration (ng/g) of WT mice was observed from 9 to 18 months of age (33690 ± 25638 *vs* 45049 ± 14385, p: 0.39). The only statistically significant change in the brain was observed between the hippocampus Cu levels (ng/g) of 9- and 18-months old APP/PS1 mice (13389 ± 8023 *vs* 40470 ± 7275, $p<0.01$). Levels of total Cu (ng/g) in the hippocampus and retina of 9- and 18-month-old APP/PS1 and WT mice are as follows: retina of 9 months-old WT (21903 ± 6513) and APP/PS1 (8871 ± 4134), retina of 18 months-old WT (32149 ± 7959) and APP/PS1 (28871 ± 5071), hippocampus of 9 months-old WT (33690 ± 25638) and APP/PS1 (13389 ± 8023), and hippocampus of 18 months-old WT (45049 ± 14385) and

APP/PS1 (40470 ± 7275). Furthermore, the levels of total Cu (ng/g) in the normalised retinal are as follows: retina of 9 months-old WT (0.5 ± 0.8) and APP/PS1 (0.6 ± 0.6), retina of 18 months-old WT (0.6 ± 0.3) and APP/PS1 (0.6 ± 0.2). In the cortex, the Cu concentration (ng/g) of WT mice 9 months of age is 1.33-fold higher than 18-month WT (36565 ± 29319 *vs* 27396 ± 6559, p: 0.55). Further, there was a 1.21-fold increase in the Cu concentrations (ng/g) of APP/PS1 mice from 9 to 18 months of age (19452 ± 3454 *vs* 23553 ± 7601, p: 0.93).

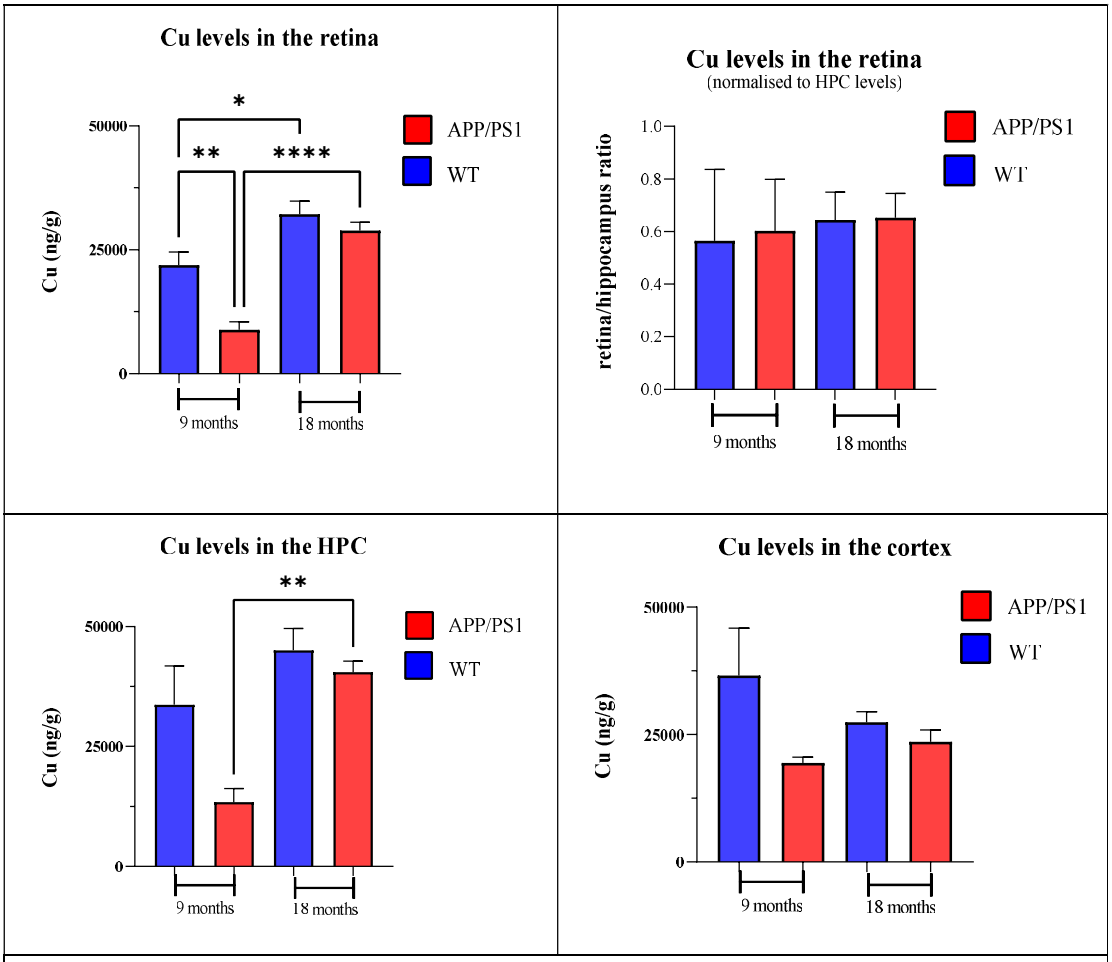

Fig. 3.7. Copper levels in the brain and retina of 9- and 18-month old APP/PS1 and WT mice. *Upper left)* Cu levels in the retina, *Upper right)* Cu levels in the retina, normalized to hippocampus levels, *Lower left)* Cu levels in the hippocampus, *Lower right)* Cu levels in the cortex. n=10 mice in each group. Error bars represent the Standard Error of the Mean (SEM) (*p < 0.05, **p < 0.01, ****p < 0.0001, Student's t-test, unpaired). HPC, hippocampus; CX, cortex.

- ***Iron (Fe)***

The iron concentrations in the retina, hippocampus, and cortex of 9- and 18-months old APP/PS1 and WT mice are shown in Fig.3.8. The higher Fe concentration in the WT compared to the APP/PS1 mice was quite evident at both 9 to 18 months of age. Nevertheless, overall, the Fe levels appeared to decline with ageing. In the eye, the retinal Fe levels (ng/g) were higher at 9 months of age compared with 18 months of age (317173 ± 64669 *vs* 64821 ± 22674, $p<0.01$ for APP/PS1, 372418 ± 275448 *vs* 189435 ± 57588 $p<0.05$ for WT). The normalised retinal Fe levels (ng/g) showed a 1.16 increase and 1.76 decrease in WT (3.3 ± 2.1 *vs* 3.9 ± 1.3, p: 0.93) and APP/PS1 (4.8 ± 3 *vs* 2.7 ± 0.7, p: 0.12) mice from 9 to 18 months of age, respectively. Comparing hippocampus Fe levels (ng/g) of APP/PS1 with WT mice revealed a significant difference at 9 months of age (101734 ± 58281 *vs* 50405 ± 9580, $P<0.01$). The hippocampus Fe levels (ng/g) were significantly higher in the 9 months-old WT mice compared with 18 months-old (101734 ± 58281 *vs* 50593 ± 12567, $p<0.01$). Similarly, the Fe levels (ng/g) in the cortex were significantly higher in the 9 months-old WT and APP/PS1 mice compared with 18 months-old (65828 ± 14723 *vs* 45528 ± 10853, $p<0.05$ for WT, 61330 ± 15166 *vs* 40695 ± 16743, $p<0.05$ for APP/PS1).

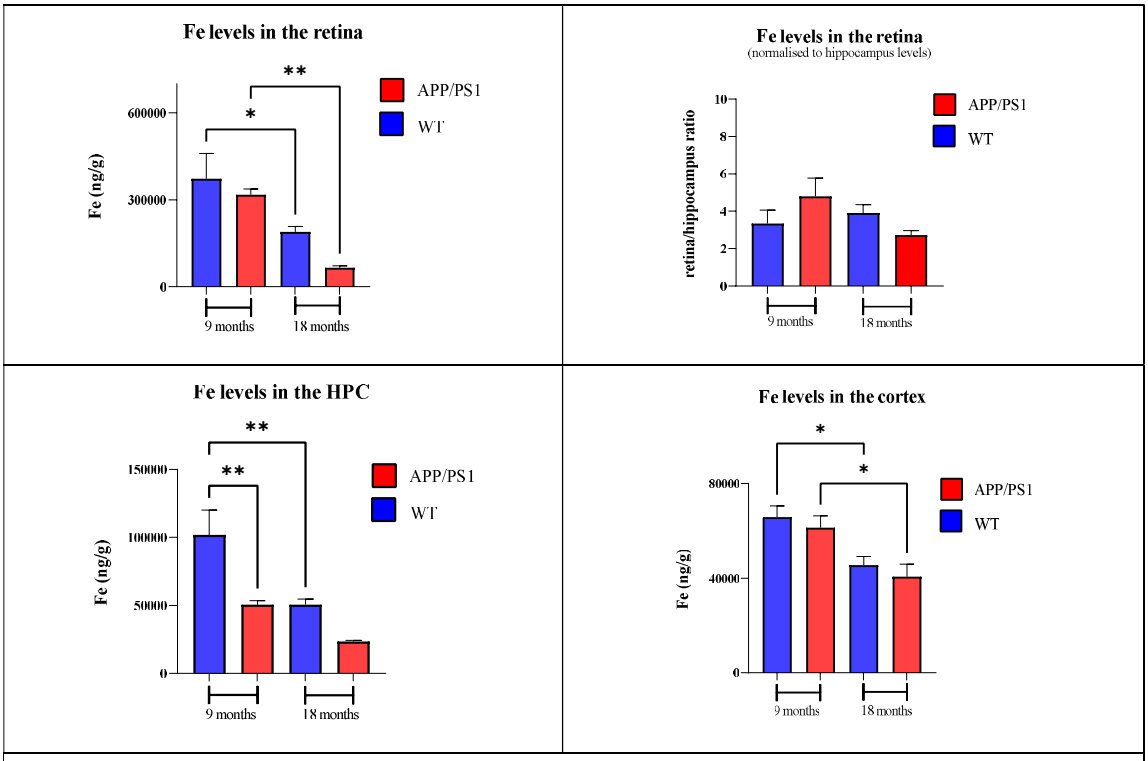

Fig. 3.8. Iron levels in the brain and retina of 9- and 18-month old APP/PS1 and WT mice. *Upper left)* Fe levels in the retina, *Upper right)* Fe levels in the retina, normalized to hippocampus levels, *Lower left)* Fe levels in the hippocampus, *Lower right)* Fe levels in the cortex. n=10 mice in each group. Error bars represent Standard Error of the Mean (SEM) (*p < 0.05, **p < 0.01, ***p < 0.001, ****p < 0.0001, Student's t-test, unpaired). HPC, hippocampus; CX, cortex.

- ***Zinc (Zn)***

Zinc concentrations in the retina, hippocampus, and cortex of 9- and 18-month-old APP/PS1 and WT mice are presented in Fig.3.9. Similar to Cu and Fe, WT mice possess higher Zn levels than APP/PS1 mice at both 9 to 18 months of age. Comparing eye Zn levels (ng/g) of APP/PS1 with WT mice revealed significant differences at 9 and 18 months of age (254879 ± 65664+ *vs* 155452 ± 63148, P<0.05 for 9 month, 221208 ± 112841 *vs* 124765 ± 23418, P<0.05 for 18 month). Assessment of the normalised retinal Zn levels (ng/g) revealed that 18-month old WT and APP/PS1 mice hold 1.2 and 1.65-fold higher Zn level (ng/g) than 9 months old (2 ± 0.7 *vs* 2.4± 1.4, p: 0.76 for WT, 1.3± 0.9 *vs* 2.2± 0.5, p: 0.17 for APP/PS1).

Comparing hippocampus Zn levels (ng/g) of APP/PS1 with WT mice revealed significant differences at 9 and 18 months of age (129776 ± 26015 *vs* 90260 ± 32474, $P<0.05$ for 9 month, 95707 ± 31509 *vs* 57336 ± 13008, $P<0.05$ for 18 month). The hippocampus Zn levels (ng/g) were significantly higher in the 9-month old WT and APP/PS1 mice compared with 18-month old (129776 ± 26015 *vs* 95707 ± 31509, $p<0.05$ for WT, 90260 ± 32474 *vs* 57336 ± 13008, $p<0.05$ for APP/PS1). In the cortex, we observed a decline in Zn levels from 9 to 18 WT, mice display 1.26-fold higher Zn level than older mice. Furthermore, a significant difference was observed between Zn levels (ng/g) of 18-month old WT and APP/PS1 mice (63050 ± 7659 *vs* 96328 ± 11446, $p<0.001$).

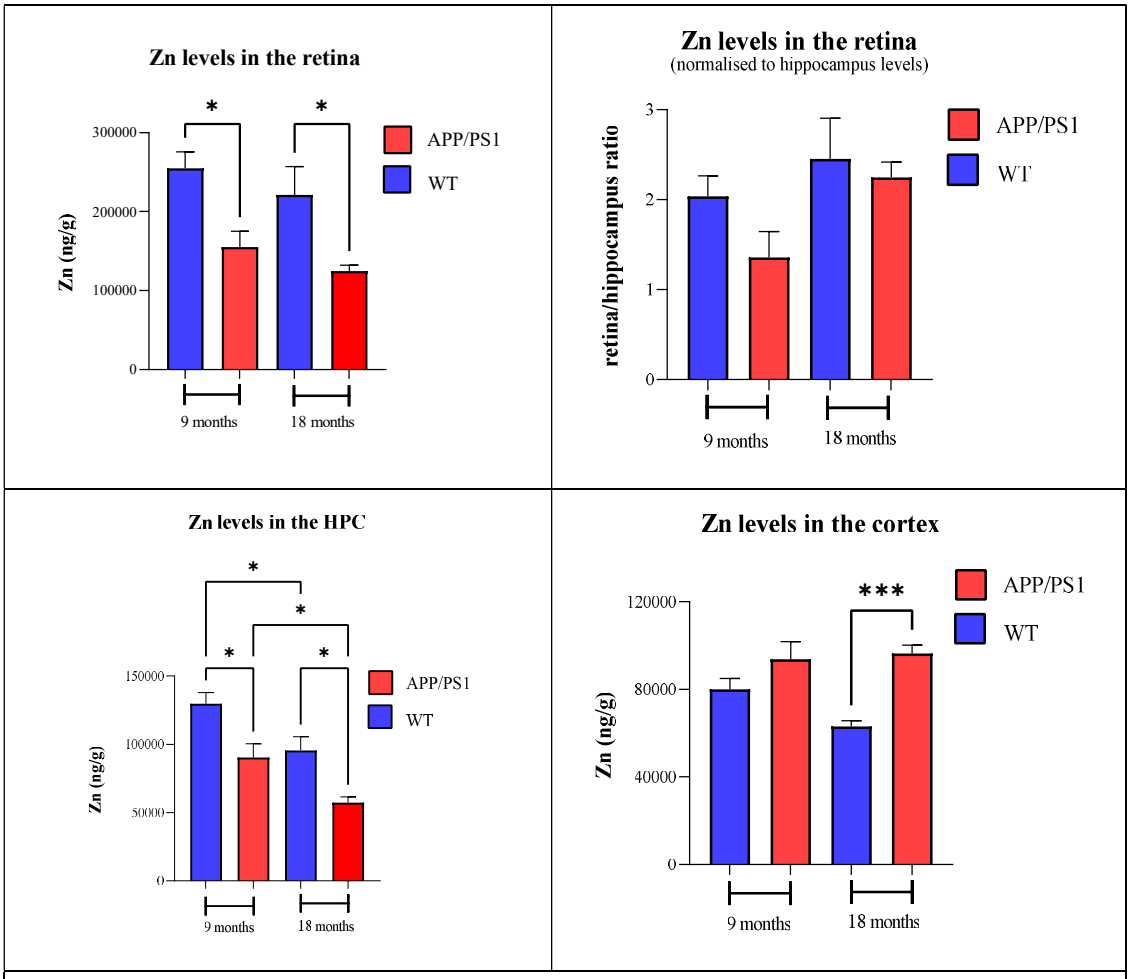

Fig. 3.9. Zinc levels in the brain and retina of 9- and 18- month's old APP/PS1 and WT mice. Upper left) Zn levels in the retina, Upper right) Zn levels in the retina, normalized to hippocampus levels, Lower left) Zn levels in the hippocampus, Lower right) Zn levels in the cortex. n=10 mice in each group. Error bars represent Standard Error of the Mean (SEM) (*p < 0.05, ***p < 0.001, Student's t-test, unpaired). HPC, hippocampus; and CX, cortex.

3.3 Discussion

In this chapter, we applied LA-ICP-MS to study the anatomical distribution of Cu, Fe, and Zn in cross-sectional slices obtained from the brain and the eye of APP/PS1 and WT mice (9 months). Calibrated image-based intensity analysis was also employed to quantify

transition metals levels in each of these organs. Furthermore, we used SN-ICP-MS to examine age-related changes in transition metal concentrations in both the brain and the eye.

Our findings showed that WT samples possess higher Cu, Fe, and Zn (except the cortex) than APP/PS1 mice at both 9 and 18 months of age. Moreover, whilst we observed an age-associated increase in Cu, the concentration of Fe and Zn declined over the same time period (i.e., 9 to 18 months of age). Collectively, our findings support the notion that metal dyshomeostasis plays a critical role in the AD pathology.[255, 256]

Previous studies that have investigated Cu concentration in AD and WT samples have reported contradictory findings with some studies showing Cu deficiency in AD,[52, 257-259] while others have reported higher Cu content in AD.[260] Our results have been consistent with the former with lower cerebral and retinal Cu volumes observed in the APP/PS1, compared with WT mice.

Cu ions,[261] through reduction from Cu^{2+} to Cu^{1+}, play a protective role against free radicals, an underlying cause for mitochondrial oxidative damage. Lower Cu content leads to higher levels of free radicals, as observed in amyloid plaques,[262] a hallmark pathology of AD.

Investigating age-dependent Cu levels showed an increase in Cu content, in both animal strains, from 9 to 18 months of age; however, Cu levels remained lower in APP/PS1 mice compared with WT mice at each time point. This is consistent with a previous study which showed an age associated rise in the Cu volume of the hippocampus.[263] A likelihood explanation for this phenomenon is the rising expression of Cu transporters or intracellular binding proteins, which leads to an increase in Cu uptake or Cu intracellular binding.

Alternatively, a decrease in cellular Cu efflux can also lead to an increase of intracellular Cu content.[263]

High levels of Fe have been reported in the cortical, hippocampal, and cerebellar neurons during the early stage of AD.[44, 264-266] Our results are in-line with previous studies with both cerebral and retinal WT samples depicting higher Fe volume than APP/PS1.[33] High levels of the carboxyl-terminal fragment of APP in the AD mouse brain, can lead to a reduction in Fe levels.[33] In addition, the lower level of iron regulatory proteins, including hepcidin, iron-homeostatic peptide, and ferroportin in AD, result in lower Fe levels.[267]

While we observed an age-associated decrease in Fe levels, 9-month old retina and hippocampus possess higher Fe levels than 18-month old in both the WT and APP/PS1 mice. This is in contrast to previous studies that have reported an age-dependent increase in Fe content.[268, 269] This inconsistent finding could be due to age-associated overexpression of Aβ42 and lower expression of iron regulatory proteins in AD, leading to decreased Fe content.[33] An age-dependent increase in brain hepcidin levels, which leads to a reduction in ferroportin-1 (FPN1) levels and subsequent iron accumulation, could be a possible reason for the lower iron concentrations observed in WT mice samples. [270] Published studies have reported conflicting findings with regard to the concentrations of Zn in AD and WT samples, with some studies showing Zn deficiency in AD[271, 272] whilst others have reported higher Zn volumes in AD.[11, 273] Our results have been compatible with the former, with lower cerebral and retinal Zn volumes observed in the APP/PS1, compared with WT mice. Lower Zn level in AD could be due to low-level expression of ZnT3, or Zn sequestration in senile plaques leading to a smaller pool of synaptic zinc.[49] A significant decline in Zn content was observed from 9 to 18 months of age in both animal strains. This is consistent with a similar study,[91]

which demonstrated that an age-dependent increase in the Metallothionein-3 (MT3),[274, 275] a predominant zinc-binding protein in the brain,[276] may lead to a reduction in the Zn volume.[277]

Despite the current study being the first to visualise and objectively quantify transition metal levels in the eye and brain of APP/PS1 of WT mice, our study has several limitations which should be noted. First, analysis of metal ion concentrations in eye and brain tissues has various challenges. There is always the possibility of contamination during the multiple steps of sample preparation which could hugely impact the metal concentration. Second, since samples are cut at an angle to the blade, it is possible that images are not truly representative, and thus, the quantified metal levels may not mirror the actual physiological metal content.[278] Third, transgenic animal models are artificially modified at a genetic level; hence, they may not represent the complex multifactorial origin of the most common form of AD, the sporadic variant.[279] AD progression in TG animal models happens in a very different time window than in AD patients.[280] Nevertheless, given that we had a control group in our study, the limitations described above should not alter the overall findings of our study.

3.4 Conclusion

This chapter demonstrated age-associated changes in the transition metal levels of the brain and eye mouse model (WT and APP/PS1, 9-18-month) through the solution nebulisation-inductively coupled plasma-mass spectrometry (SN-ICP-MS). In addition, eye and brain cross-sectional images of mouse model (WT and APP/PS1, 9-18-month) obtained from laser ablation-inductively coupled plasma-mass spectrometry (LA-ICP-MS) provided us with an anatomical distribution of metal ions. Our findings showed that WT samples portray higher Cu, Fe, and Zn (except the cortex) than APP/PS1 mice over the same age progression (i.e., 9 to 18 months of age). Moreover, whilst we observed an age-associated

increase in Cu, the concentration of Fe and Zn declined over the same time period (i.e., 9 to 18 months).

Zn is known to impact the concentration of Cu and Fe in AD.[281] Further, zinc therapy has been shown to have potential beneficial effects in preliminary AD clinical trials,[282, 283] which makes it more desirable for further AD research. In addition, compared with other transitional metals (Cu and Fe), Zn extensively is participated in cell signaling, particularly because it can act as a neurotransmitter.[284] Furthermore, zinc is critical in the retina's functioning and antioxidant defense mechanisms.[184] Additionally, among the three transition metals examined in the current study, Zn (130000 ng/g) was found to be the most abundant metal in the brain (compared to Cu (45000 ng/g) and Fe (100000 ng/g). Based on these findings, the next aim is to explore the potential roles of ZnT3 and ZIP3, as two main Zn transporters, in the eyes and brains of model mice (WT and APP/PS1, 9 to 18 month of age).

Chapter 4: Zinc transporter proteins in Mice

4. Evaluation of Zinc transporter proteins (ZnT3 & ZIP3) in the eye and brain (WT and APP/PS1 mice models)

4.1 Introduction

Zinc is a metal required for normal cell function and a structural element in proteins.[285] Monitoring in vivo and in vitro research on neurodegenerative diseases has highlighted that the level of zinc ions is critical to initiating or suppressing the Aβ aggregation in AD processes. The free zinc ion can be adjusted by metallothionein, superoxide dismutase, or other Zn-binding proteins. Mobilizing zinc across biological membranes is vital to keep cellular and subcellular Zn balance. Zn^{2+}, due to its hydrophilic nature, cannot pass through membranes via passive diffusion; hence, it needs active transport proteins.[161]

Two Zn transporter groups responsible for modulating the zinc concentration in the cytoplasm are ZnT (SLC30) and ZIP (SLC39) proteins.[286] These transporter proteins demonstrate tissue-specific expression, are located on plasma and vesicular membranes and have unique behaviour towards dietary zinc, hormones, and cytokines.[287]

ZIP transporter proteins increase Zn concentration in the cytoplasm by transporting zinc from intracellular organelles or the extracellular space to the cytoplasmic environment.[287] Jeffrey L. Noebels and colleagues examined the role of ZIP1 and ZIP3 on neurodegeneration, observing reduced neurodegeneration in the CA1 pyramidal cell in the ZIP1 and ZIP3 knock-out mice, validating the role of ZIP1 and ZIP3 as Zn transporter proteins.[288] Kar Wah Leung and colleagues reported the expression of ZIP3 transporter in a human RPE cell line.[289]

ZnT proteins, abundant in the hippocampus and cortex, modulate the cytoplasmic Zn concentration by increasing cellular zinc efflux or suppressing zinc in subcellular compartments.[159] Within the ZnT family, ZnT3 is in charge of adjusting the zinc ions concentration within synaptic vesicles. Consequently, ZnT3 malfunction causes vesicular zinc dyshomeostasis, which is associated with neurodegenerative diseases, including Parkinson's disease,[290] Alzheimer's disease,[229] and amyotrophic lateral sclerosis.[291]

In the eye, ZnT3 is present in several retinal layers, including the outer plexiform, inner nuclear, inner plexiform, and ganglion cell layers.[292, 293, 294]

Zinc levels in the ZnT3 knock-out mice are almost untraceable in brain synaptic vesicles, confirming the transporter role of ZnT3.[159, 295, 296] ZnT3 knock-out mice (developed by Cole et al.) demonstrated a lack of histochemically detectable zinc in either their mossy-fiber pathway or other zinc-secreting routes.[159] In 2008, Frederickson and colleagues reported that Zn levels in the hippocampal mossy fibres of ZnT3 knock-out mice were 2- to 3-fold lower than in age-matched wild-type (WT) mice, which further supports the role of ZnT3 protein as the brain zinc transporter protein.[297] Zn^{2+} has a critical role in learning and memory due to its function as a neuronal messenger and modulator of synaptic transmission and plasticity.[298, 299] Therefore, ZnT3 knock-out (KO) mice fail to express a cognitive phenotype.

In the current study, the abundance of zinc transporters (ZnT3-ZIP3) in the eye and brain of mice model (WT and APP/PS1, 9-18 months) is measured using immunofluorescence and Western blot. Furthermore, to validate the role of ZnT3 as a Zn transporter protein, zinc concentrations in the eye and brain of mice model subjects (knock-out and WT, 3, 11, and 14 months) are measured using solution nebulisation-inductively

coupled plasma-mass spectrometry (SN-ICP-MS) analysis. This study is potentially the first investigation of the distribution and concentration of the zinc transporter proteins (ZnT3 and ZIP3) in the eye and retina of mice model subjects with Alzheimer's disease.

4.2 Results

4.2.1 Evaluation of Zinc transporter proteins (ZnT3 & ZIP3) in the brain and eye tissues (WT and APP/PS1 mice models)

- ***ZnT3***

The abundance levels of the ZnT3 transporter in the retina and hippocampus for 9- and 18-month old APP/PS1 and WT mice are shown in Figs. 4.1. Visual assessment of immunofluorescence images of ZnT3 of 9 and 18-month old APP/PS1 and WT demonstrates high protein levels of ZnT3 in the hippocampus and retina of the WT samples compared with the APP/PS1. Figs. 4.2 show high-resolution micrographs of ZnT3 retinal staining for 9- and 18-month-old APP/PS1 and WT mice to distinguish genuine staining from potential background artifacts. As evidenced by Figs. 4.2, the staining is localized in various retinal layers (OS, IS, ONL, OPL, INL, IPL, and GCL), confirming the specificity and relevance of the staining procedure. Levels of ZnT3 in the hippocampus and retina for 9- and 18-month old APP/PS1 and WT mice are summarised in Fig. 4.3. Results from the intensity-based analysis (Fig.4.3) were in accordance with the visual assessment (Fig.4.1) with higher levels of ZnT3 abundance in the WT samples (brain and retina) compared with APP/PS1 mice samples. Retinal ZnT3 levels in WT mice are significantly higher at 9- and 18-month old of age compared with APP/PS1 mice (1.4 ± 0.1 vs 1.1 ± 0.09, $p<0.05$ for 9-month old, 1 ± 0.3 vs 0.7 ± 0.1, $p<0.05$ for 18-month old). Comparing the two timepoints, ZnT3 levels are significantly higher in the 9-month old WT and APP/PS1 mice compared with the 18-month

old mice (1.4 ± 0.1 vs 1 ± 0.3, $p<0.01$ for WT, 1.1 ± 0.09 vs 0.7 ± 0.1, $p<0.0001$ for APP/PS1). In the hippocampus, ZnT3 levels in WT mice were significantly higher at both 9 and 18 months of age compared with APP/PS1 mice (1.8 ± 0.3 vs 1.3 ± 0.1, $p<0.001$ for 9-month old mice, 1 ± 0.3 vs 0.7 ± 0.1, $p<0.05$ for 18-month old). The inter-age comparison reveals significantly higher levels of ZnT3 in both strains at 9-month of age compared with 18-month (1.8 ± 0.3 vs 1 ± 0.3, $p<0.0001$ for WT, 1.3 ± 0.1 vs 0.7 ± 0.1, $p<0.0001$ for APP/PS1).

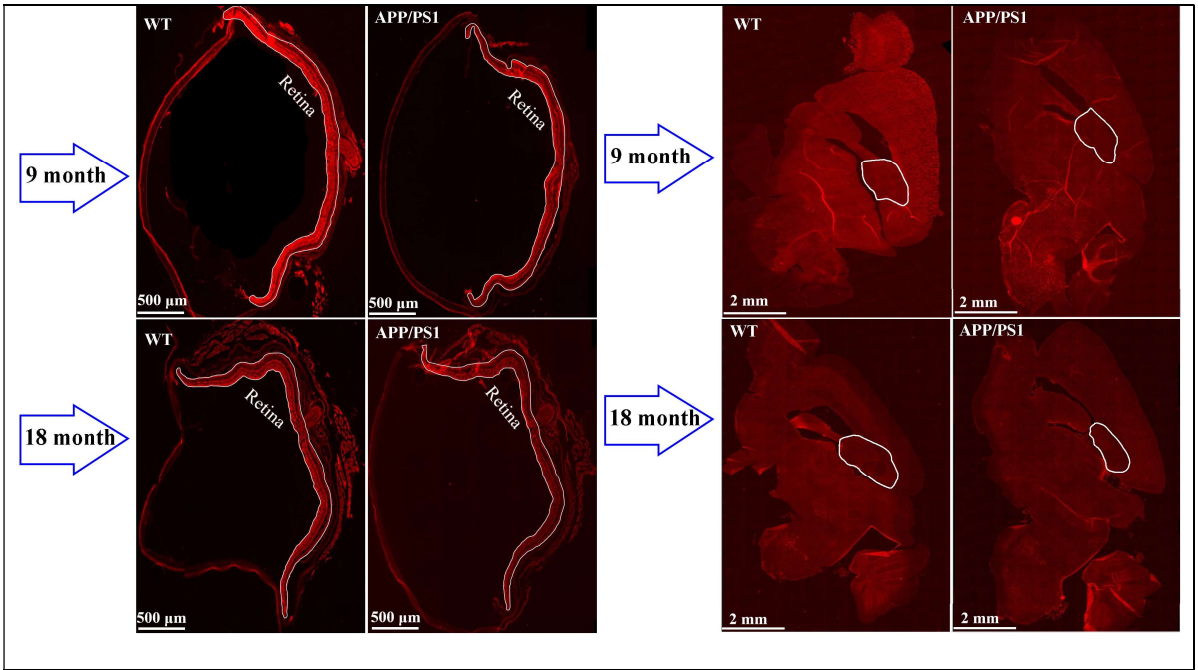

Fig.4.1 Representative immunofluorescence images for ZnT3 in the eye (Scale bar: 500 µm) and hippocampus (Scale bar: 2 mm). In each panel: abundance of ZnT3 transporter of 9-month old (*upper row*) and 18-month old (*lower row*).

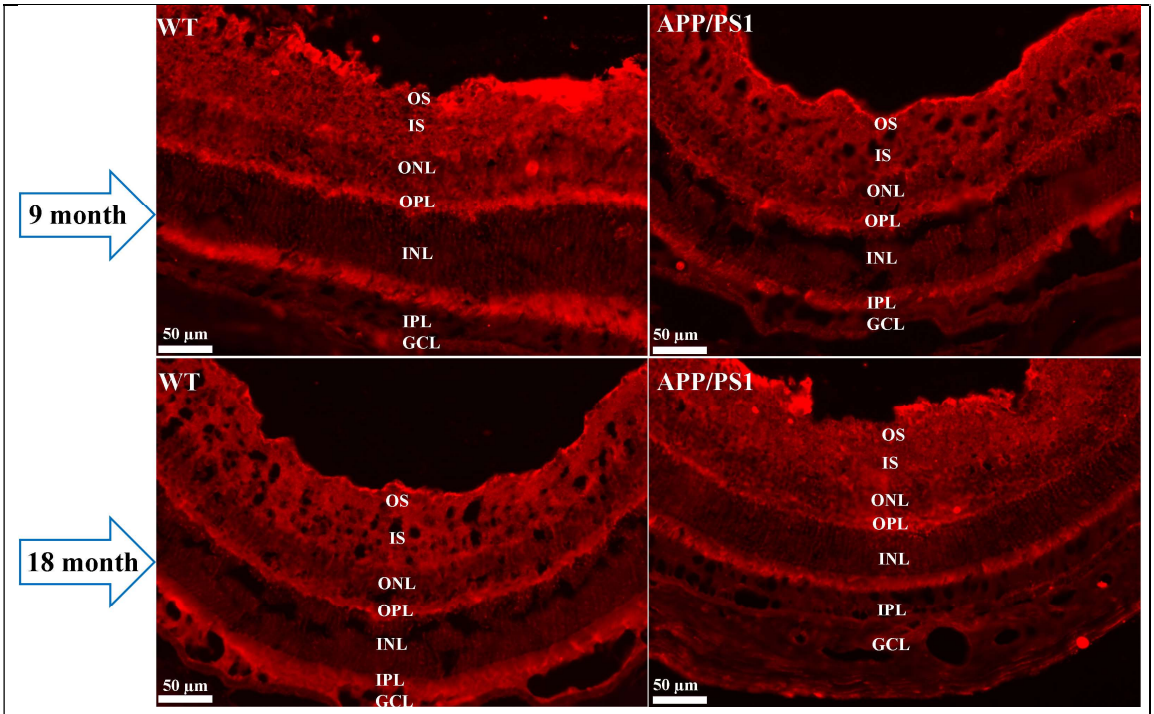

Fig. 4.2 Representative high-resolution immunofluorescence images of ZnT3 in the eye (Scale bar: 50 µm). In each panel: Abundance of ZnT3 transporter of 9-month old (upper row) and 18-month old mice (lower row).

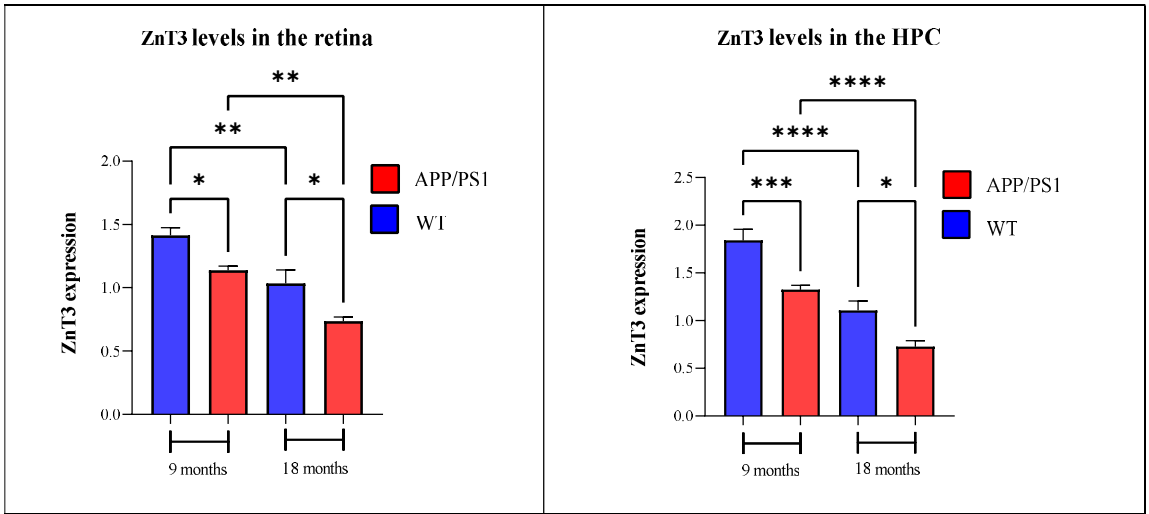

Fig. 4.3. ZnT3 levels in the retina and brain of 9- and 18- month APP/PS1 and WT mice. *left)* ZnT3 levels in the retina, *right)* ZnT3 levels in the HPC (n=10 mice in each group). Error bars represent Standard Error of the Mean (SEM) (****p< 0.0001, ***p< 0.001, and **p < 0.01, *p < 0.05, Student's t-test, unpaired). HPC, hippocampus.

- ***ZIP3***

ZIP3 abundance levels in the retina and hippocampus for 9- and 18-month old APP/PS1 and WT mice are demonstrated in Figs. 4.4. The surveying of immunofluorescence images of ZIP3 of 9 and 18-month old APP/PS1 and WT illustrates that the HPC and retina of the WT samples have higher levels of ZIP3 than the APP/PS1.

Fig. 4.5 presents ZIP3 expression levels in the hippocampus and retina for 9- and 18-month old APP/PS1 and WT mice. The intensity-based analysis results (Fig.4.5) are consistent with the visual assessment (Fig.4.4), with higher levels of ZIP3 expression in the brain and the retina of WT samples compared with APP/PS1 mice samples. Retinal ZIP3 levels were significantly higher only in 18-month old WT compared with APP/PS1 mice (1 ± 0.2 vs 0.5 ± 0.09, $p<0.0001$). Additionally, ZIP3 levels were significantly higher in the 9-month old WT and APP/PS1 mice compared with 18-month old (2.4 ± 0.2 vs 1 ± 0.2, $p<0.0001$ for WT, 2.1 ± 0.2 vs 0.5 ± 0.09, $p<0.0001$ for APP/PS1). In the hippocampus, and similar to the retina, ZIP3 levels were significantly higher only in 18-month old WT mice compared with APP/PS1 mice (1.9 ± 0.3 vs 1.5 ± 0.1, $p<0.05$). Comparing the two time points, 9-month old WT and APP/PS1 mice expressed significantly higher ZIP3 levels compared with the 18-month old (2.3 ± 0.3 vs 1.9 ± 0.3, $p<0.01$ for WT, 2.1 ± 0.2 vs 1.5 ± 0.1, $p<0.001$ for APP/PS1).

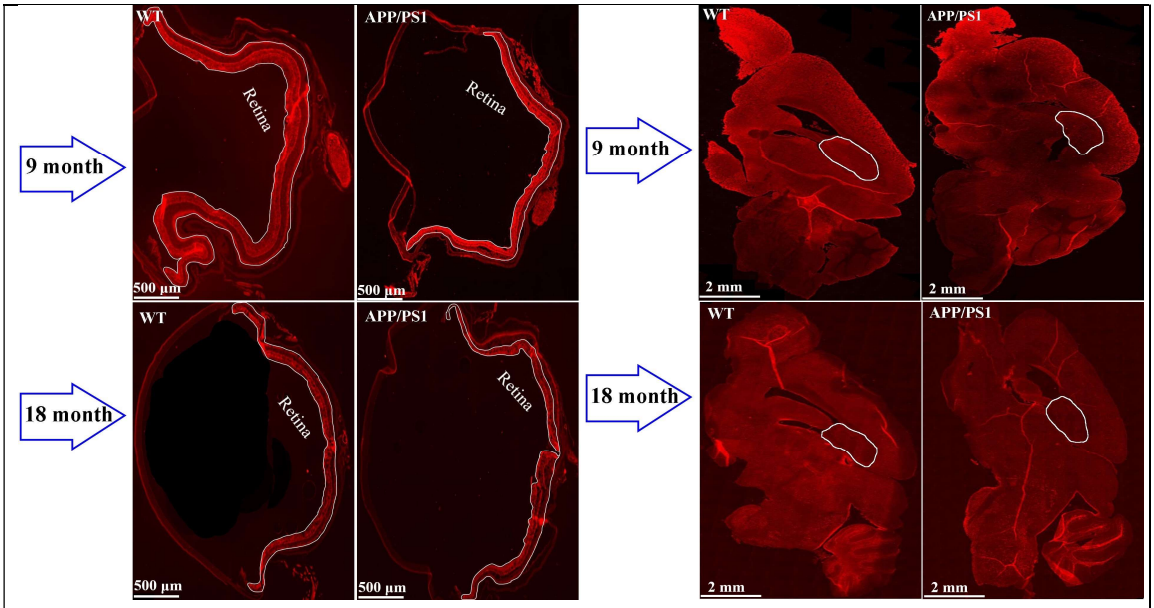

Fig. 4.4 Representative immunofluorescence images of ZIP3 in the eye (Scale bar: 500 µm) and hippocampus (Scale bar: 2 mm). In each panel: Abundance of ZIP3 transporter of 9-month old (*upper row*) and 18-month old mice (*lower row*).

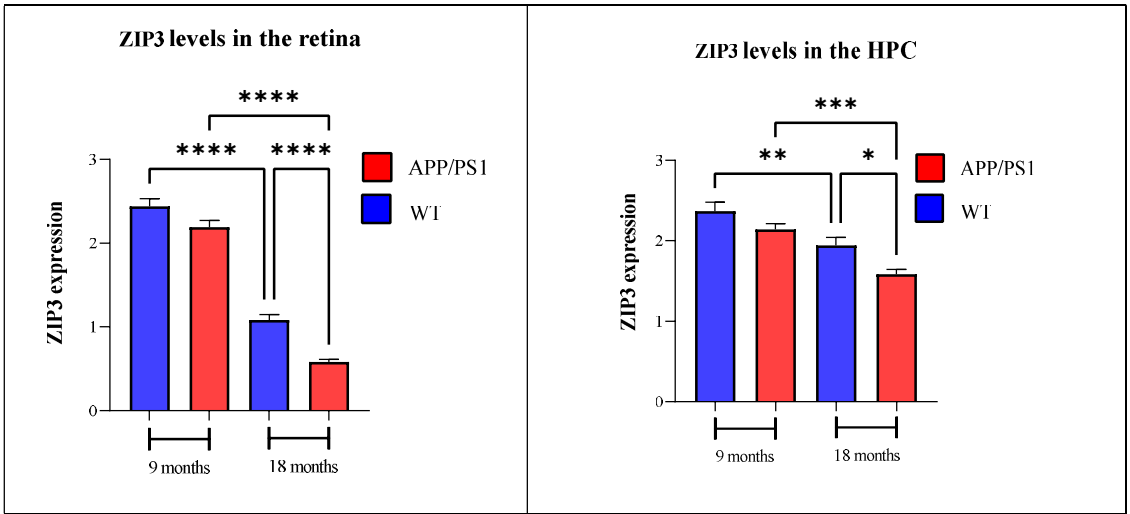

Fig.4.5. ZIP3 levels in the retina and brain of 9- and 18- month old APP/PS1 and WT mice. *left)* ZIP3 levels in the retina, *right)* ZIP3 levels in the HPC (n=10 mice in each group). Error bars represent Standard Error of the Mean (SEM) (****p< 0.0001, ***p< 0.001, and **p < 0.01, *p < 0.05, Student's t-test, unpaired). HPC, hippocampus.

4.2.2 Quantifying Zinc transporter protein levels (ZnT3 & ZIP3) in the hippocampus (WT and APP/PS1 mice models) using immunoblot

To further evaluate our immunofluorescence findings, immunoblotting was used to assess ZnT3 and ZIP3 levels.

- ***ZnT3***

Quantified ZnT3 levels (normalised to GAPDH) for 9- and 18-month old APP/PS1 and WT mice are shown in Figs. 4.6A and B. The ZnT3 expression in WT mice is significantly higher than in APP/PS1 mice at both 9-and 18-month of age (1.1 ± 0.1 vs 0.8 ± 0.1, $p<0.001$ for 9-month old, 0.8 ± 0.2 vs 0.5 ± 0.1, $p<0.01$ for 18-month old). There is a significant decline in ZnT3 expression between 9 to 18 months of age in both animal groups (1.1 ± 0.1 vs 0.8 ± 0.2, $p<0.01$ for WT, 0.8 ± 0.1 vs 0.5 ± 0.1, $p<0.01$ for APP/PS1).

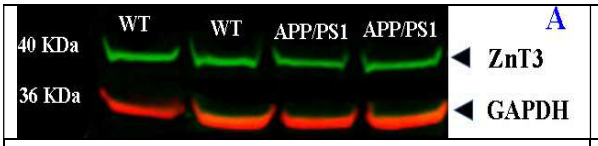

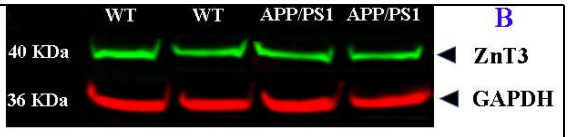

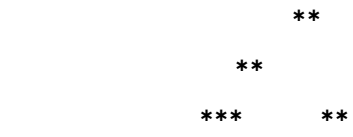

Fig.4.6. Representative Western blot image of Glyceraldehyde 3-Phosphate Dehydrogenase (red, 36 kDa) and ZnT3 protein (green, 40 kDa) for 9- and 18-month old APP/PS1 and WT mice, respectively (A-B) and integrated density value analysis of ZnT3 bands for 9- and 18-month old APP/PS1 and WT mice (n=10 mice in each group) (C). Error bars represent Standard Error of the Mean (SEM) (**p < 0.01, ***p< 0.001, Student's t-test, unpaired). HPC, hippocampus.

ZIP3 expression for 9- and 18-month-old APP/PS1 and WT mice are shown in Figs. 4.7A and B, respectively. At both ages, WT mice show higher ZIP3 expression than APP/PS1 mice (1.9 ± 0.6 vs 1 ± 0.6, $p<0.01$ for 9-month old, 1.3 ± 0.3 vs 0.5 ± 0.1, $p<0.01$ for 18-month old). An inter-age comparison shows a significant decline in ZIP3 levels between 9 to 18 months of age in WT mice only (1.9 ± 0.6 vs 1.3 ± 0.3, $p<0.05$ for WT, 1 ± 0.6 vs 0.5 ± 0.1, $p=0.09$ for APP/PS1).

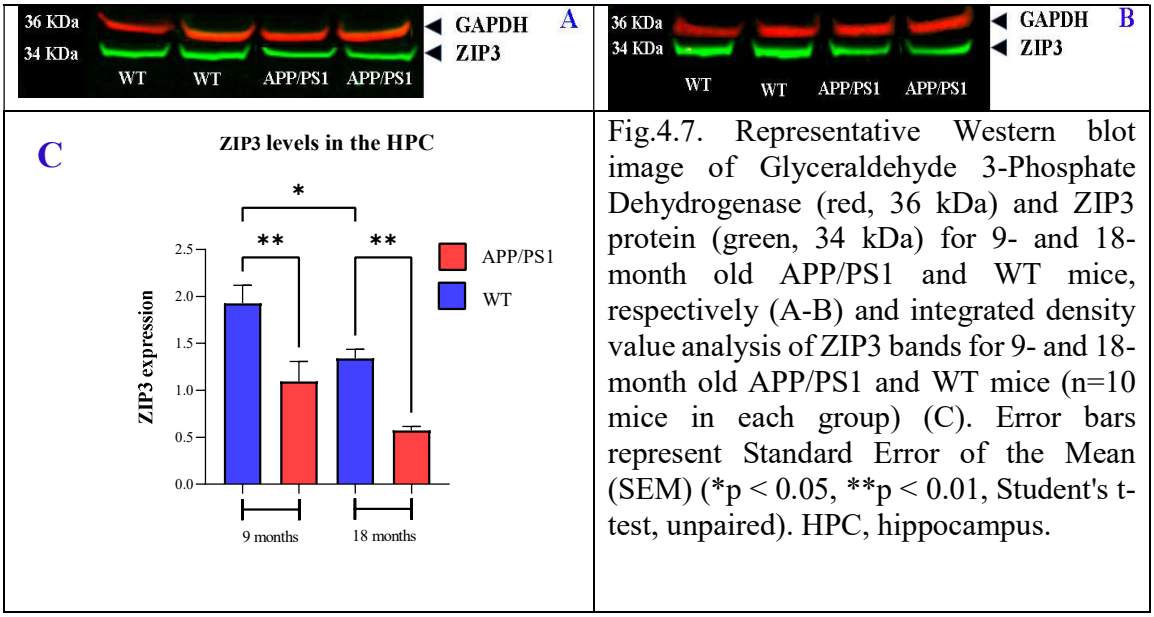

Fig.4.7. Representative Western blot image of Glyceraldehyde 3-Phosphate Dehydrogenase (red, 36 kDa) and ZIP3 protein (green, 34 kDa) for 9- and 18-month old APP/PS1 and WT mice, respectively (A-B) and integrated density value analysis of ZIP3 bands for 9- and 18-month old APP/PS1 and WT mice (n=10 mice in each group) (C). Error bars represent Standard Error of the Mean (SEM) (*$p < 0.05$, **$p < 0.01$, Student's t-test, unpaired). HPC, hippocampus.

4.2.3 Age-associated changes in the Zn levels of the KO and WT mice (3-11-and 14-month)

Variations in the abundance of ZnT3 were then analysed to assess if ZnT3 levels impact the histochemical reactive zinc or total elemental zinc in the brain and the retina. The total Zn concentrations (ng/g) in the hippocampus and the retina (per dry tissue weight) of 3, 11- and 14-month old ZnT3 knockout and WT mice were measured using SN-ICP-MS and are summarised in Fig.4.8. For this study, we selected 3, 11, and 14-month-old ZnT3 KO mice due to the significant phenotypic contrast between ZnT3 KO mice and APP/PS1 mice. ZnT3

KO mice exhibit age-dependent deficits in learning and memory that are manifested at older age (>6 months) but not at 3 months of age. These deficits are associated with significant alterations in key hippocampal proteins involved in learning and memory. A previous study from our collaborator, found that cortical ZnT3 levels fall with age in wild-type mice and particularly in Alzheimer's disease (AD) (-36%; $p < 0.0001$). Thus, age-dependent loss of transsynaptic Zn^{2+} movement leads to cognitive loss, and since extracellular beta-amyloid is aggregated by and traps this pool of Zn^{2+}, the genetic ablation of ZnT3 may represent a phenocopy for the synaptic and memory deficits of AD.[58] The overall trend of higher Zn concentrations in the WT mice compared to ZnT3 KO mice was extended from 3 to 14 months of age in both the retina and hippocampus. In the eye, retinal Zn concentrations in the WT mice were significantly higher compared with ZnT3 KO mice (33621 ± 12705 *vs* 21843 ± 3967, $p<0.05$ for 3-month old, 35542 ± 4818 *vs* 22834 ± 10391 $p<0.01$ for 11-month old, 30944 ± 2238 *vs* 15219 ± 3167 $p<0.$ 0.001 for 14-month old). The same trend was also observed in the brain, with higher hippocampus Zn concentrations in WT than in ZnT3 KO mice (64908 ± 8080 *vs* 49778 ± 2854, $p<0.0001$ for 3-month old, 65806 ± 22814 *vs* 41323 ± 2379 $p<0.01$ for 11-month old, 63394 ± 4677 *vs* 49690± 16693 $p<0.05$ for 14-month old).

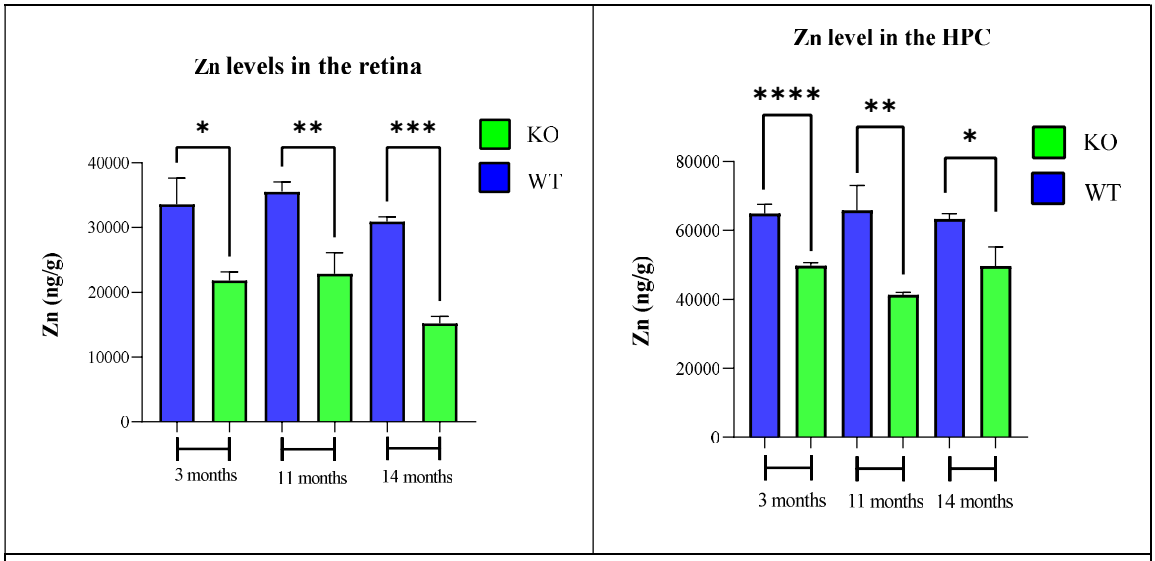

Fig.4.8. Zinc levels in the brain and retina of 3, 11, and 14- month old knockout and WT mice. *left)* Zn levels in the retina, *right)* Zn levels in the HPC. n=10 mice in each group. Error bars represent Standard Error of the Mean (SEM) (*p < 0.05, **p < 0.01, ***p < 0.001, ****p < 0.0001, Student's t-test, unpaired). HPC, hippocampus.

Gender differences in total Zn concentrations (ng/g) in the hippocampus and the retina (per dry tissue weight) of 3-, 11-, and 14-month-old ZnT3 knockout and WT mice have been investigated, as shown in Table 4.1. The overall trend of higher Zn concentrations in the WT mice compared to ZnT3 KO mice extended from 3 to 14 months of age in both males and females (retina and hippocampus).

Table 4.1- Gender differences in Zn concentrations (ng/g) in the hippocampus and the retina of ZnT3 knockout and WT mice (3, 11- and 14-month old)

Age (month)	Structure	Strain	Gender	Zn concentration (ng/g)
3	Retina	WT	Female	(36393 ± 15004)
3	Retina	KO	Female	(22143 ± 4122)
3	Retina	WT	Male	(30848 ± 10901)
3	Retina	KO	Male	(21469 ± 4355)
11	Retina	WT	Female	(32316 ± 1849)
11	Retina	KO	Female	(24459 ± 14252)
11	Retina	WT	Male	(38767 ± 4776)
11	Retina	KO	Male	(21209 ± 5766)
14	Retina	WT	Female	(30525 ± 1081)
14	Retina	KO	Female	(15202 ± 2893)
14	Retina	WT	Male	(31468 ± 3338)
14	Retina	KO	Male	(15232 ± 3713)
3	Hippocampus	WT	Female	(64228 ± 8462)
3	Hippocampus	KO	Female	(48572 ± 1329)
3	Hippocampus	WT	Male	(65759 ± 8770)
3	Hippocampus	KO	Male	(50742 ± 3514)
11	Hippocampus	WT	Female	(60116 ± 30898)
11	Hippocampus	KO	Female	(41186 ± 1740)
11	Hippocampus	WT	Male	(71495 ± 11637)
11	Hippocampus	KO	Male	(4142 ± 3003)
14	Hippocampus	WT	Female	(61280 ± 4348)
14	Hippocampus	KO	Female	(58486 ± 17732)
14	Hippocampus	WT	Male	(65508 ± 4375)
14	Hippocampus	KO	Male	(38694 ± 5802)

4.3 Discussion

In this chapter, we investigated the anatomical distribution and expression levels of zinc transporters; membrane transport proteins that regulate the concentration of zinc. In particular we focused on ZnT3 and ZIP3, as the sole mechanism responsible for efflux/influx and subsequent concentration of zinc ions in synaptic vessels. The results

showed that transgenic APP/PS1 mice express lower ZnT3/ZIP3 levels compared to WT mice and that there is a significant decline with aging. Analysis of zinc concentration in ZnT3 KO mice showed significantly lower zinc concentration levels in ZnT3 KO mice compared with WT mice.

ZnT3 and ZIP3 proteins regulate synaptic vesicular Zn^{2+} levels, and play an important role in normal cognitive function.[58] Dysfunctional ZnT3, and the subsequent dyshomeostasis of synaptic zinc, have been shown to impact the cognitive decline associated with ageing and AD directly. Characterising these proteins' anatomical distribution and expression levels aims to determine whether changes in neocortical ZnT3 and ZIP3 levels are also mirrored in the retinal tissue. The data shows that both in the retina and hippocampus, ZnT3 and ZIP3 levels are lower in APP/PS1 mice compared with WT mice. While an age-associated decline was observed in both proteins, the trend was similar for both structures, suggesting changes in hippocampal ZnT3 and ZIP3 levels are also reflected in the retina.

These findings are in accordance with previous studies, showing an age-associated decrease in the zinc transporter volume.[58, 300] The likely explanation for this phenomenon is the energy requirement for maintaining Zn volume in the brain and normal ageing of the brain.[58, 301, 302] In other words, mitochondrial damage decreases the brain energy level and, consequently, causes the loss of brain metals. Alterations in ZnT3 expression may not only be due to the ongoing neuronal cell death in AD,[303] but may also depend on the estrogen concentration. Estrogen causes a decreasing expression of adaptor proteins, resulting in low-level expression of cortical vesicular ZnT3 and Zn^{2+}.[232, 304] Increased levels of ZnT3, due to low estrogen levels, have been linked to an increased risk for AD.[303, 305, 306] Whilst we did not evaluate estrogen expression in our animal cohorts, we did have a mixed cohort of male

and female mice. This mixed-gender cohort is another likely cause for observing low ZnT3 content in the APP/PS1 mice.

Evidence from current literature suggests that genetic ablation of ZnT3 represents a phenotype surrogate for synaptic and memory deficits observed in AD.[58] Additionally, an dependent loss of trans-synaptic Zn^{2+} has been observed in the hippocampus of mice that lack the ZnT3 KO.[58] Consistent with these findings, our results not only showed that Zn levels are significantly lower in the hippocampus of ZnT3 KO mice compared with WT mice, but also a similar effect is also present in the retina of these mice.

Notwithstanding our study is the first to visualise and measure zinc transporters levels (ZnT3 and ZIP3) in the eye and brain of APP/PS1 of WT mice and also quantify zinc content in the retina of ZnT3 KO mice, our study has several limitations.

One of the Western blot limitations is sample loading volume. It is almost impossible to run a Western blot for samples with low protein concentration or low expression of the protein of interest. Non-specific bands and high background in Western blot, which are due to many factors such as poor quality of antibodies, high concentration of primary or secondary antibodies, inadequate blocking, etc., could be a major source of frustration.[307] We faced tissue folding and falling off the tissue during sectioning and numerous washing steps in the staining process, which significantly impacted image processing. By optimizing Western blot precursor concentrations, such as antibodies and blocking agents and improving the tissue sectioning skills, we will be able to minimize the errors from the abovementioned limitations.

4.4 Conclusion

In this chapter we investigated age-related changes in the zinc transporter proteins levels (ZnT3 and ZIP3) of the brain and eye mouse model (WT and APP/PS1, 9-18-months) through the immunofluorescence. The eye and brain cross-sectional images of mouse model (WT and APP/PS1, 9-18-months) obtained from immunofluorescence provided us with an anatomical distribution of zinc transporter proteins. Image-based intensity analysis was applied to examine the ZnT3 and ZIP3 abundance levels in each of these organs. Additionally, Western blot was used to assess further the abundance of ZnT3 and ZIP3 proteins in the brain of APP/PS1 and WT mice (9 to 18 months). As this is the first study investigating the role of ZnT3 as the zinc transporter in the eye, SN-ICP-MS was used to measure the Zn concentration in the eye and brain of mice model (knock-out and WT, 3, 11, and 14 months) to assess the role of ZnT3 as the zinc transporter.

Our findings demonstrate that WT samples possess higher ZnT3 and ZIP3 proteins than APP/PS1 mice over the same time period (i.e., 9 to 18 months). Moreover, an age-associated decrease was demonstrated in ZnT3 and ZIP3 abundance over the same time period (i.e., 9 to 18 months). SN-ICP-MS results confirm the role of ZnT3 as the zinc transporter in the eye and brain.

To further assess our findings about the zinc transporter proteins (ZnT3 and ZIP3), the potential role of ZnT3 and ZIP3 in the eye and brain of human AD and healthy control samples was investigated.

Chapter 5: Transition metals and Zinc transporter proteins in human

5: Distribution of transition metals and zinc transporter proteins in the eye and brain of AD and age-matched healthy human samples

5.1 Introduction

Biometals are essential for neurobiological function.[308] For instance, Zn can act as a neurotransmitter that needs to be accumulated in presynaptic terminals, followed by realising into the synaptic cleft, where it binds receptors to adjust their function.[309] Hence, their dyshomeostasis, mislocalisation, and toxic accumulation have been used as the diagnostic marker for central nervous system (CNS) diseases such as Parkinson's disease, dementia with Lewy bodies, and Alzheimer's disease. Metal neurotoxicity reduces enzymatic activities, boosts protein aggregation (Aβ and tau protein), and creates oxidative stress in the CNS, resulting in cell death and neurodegeneration disorders.[310] The monomer form of Aβ has been known as an antioxidant; however, the oligomers form of Aβ (amyloid plaques), which is the result of Aβ aggregation due to the metal dyshomeostasis,[30] generates ROS. Metal dyshomeostasis (Zn, Fe, and Cu) has participated in the pathogenesis of retinal diseases such as age-related macular degeneration (AMD).[311] AMD has similar clinical and pathological characteristics to AD, such as oxidative stress and inflammation.[312] Since the retina/choroid complex of the eye has a higher Zn concentration than other parts[91] and the retina and RPE cells are susceptible to generating ROS,[312] retinal tissue can be a perfect subject for AD diagnosis.

Due to its stability, unlike copper or iron, the divalent cationic form of zinc (Zn^{2+}) does not need a redox reaction for membrane transport.[313] Therefore, zinc transporters (ZnT3 and ZIP3) have been known for zinc influx and efflux between extracellular and intracellular

compartments.[309] ZnT3 and ZIP3 transporters are expressed in the human RPE cells[289] and mossy fiber (hippocampus).[314] [160]

Here, LA-ICP-MS (see section 2.2.3 for details) and immunofluorescence (see section 2.3.2 for details) were applied to study the transition metals concentrations (Cu, Fe, and Zn) and zinc transporters (ZnT3-ZIP3) anatomical distribution and abundance in cross-sectional slices in the human brain and eye (9 cases with AD and 6 controls). This study appears to be the first to assess transition metal concentrations and distributions (Cu, Fe, and Zn) and zinc transporters abundances (ZnT3-ZIP3) in the retina of patients with Alzheimer's disease.

5.2 Results

Similar experiments on the cross-sectional human brain and eye samples obtained from AD and age-matched healthy donors were undertaken to evaluate further if the data in animal models are also mirrored in humans (results in Chapters 3 and 4). The mean age of AD and age-matched healthy donors were 75 ± 10 (6/3 F/M) and 85 ± 10 (1/5 F/M), respectively (Table 5.1).

Table 5.1- Demographics of human samples

	AD	Healthy control
Age	75 ± 10	85 ± 10
Gender (F/M)	6/3	1/5
Hippocampus weight (grams)	1100 ± 100	1200 ± 100
Post-mortem delay (PMD-hrs)	5.5 ± 3	7 ± 2
pH	6.5 ± 0.5	6.5 ± 0.5

As we only had access to formalin-fixed paraffin-embedded (FFPE) samples, the LA-ICP-MS analysis was used (see section 2.2.3 for details) to produce a calibrated representative image of each metal distribution (Cu, Fe, and Zn). In our study, we measure the levels of metals (Cu, Zn, and Fe) across the entire human retina structure, which has a 10

μm diameter. This means that the metal levels of each retina represent the average metal content throughout the entire retina. This approach helps minimize the impact of the spatial structure or shape of the retina on the measured metal levels. However, the different eccentricities could be a co-founder and needs to be mentioned as a potential limitation. The distribution of ZnT3 and ZIP3 proteins was also investigated using immunofluorescence. An image-based analysis was then performed to measure Cu, Fe, and Zn concentrations and ZnT3 and ZIP3 abundance in the hippocampus and retina of AD and healthy human samples.

5.2.1 Anatomical distribution and quantitative levels of transition metals

- ***Copper (Cu)***

The distribution of Cu in the human hippocampus and the retina of healthy control and AD samples are shown in Figs. 5.1 A and B. The visual assessment shows that the hippocampus and retina of AD samples display higher levels of Cu compared with the healthy control samples. Results from the image analysis (Fig.5.2) confirmed the visual assessment. The hippocampus and retina of the AD samples showed significantly higher Cu levels compared with healthy controls (288.3 ± 92.4 vs 173 ± 66.8, $p<0.05$ for hippocampus, 291.6 ± 29 vs 183 ± 9.4, $p<0.05$ for retina).

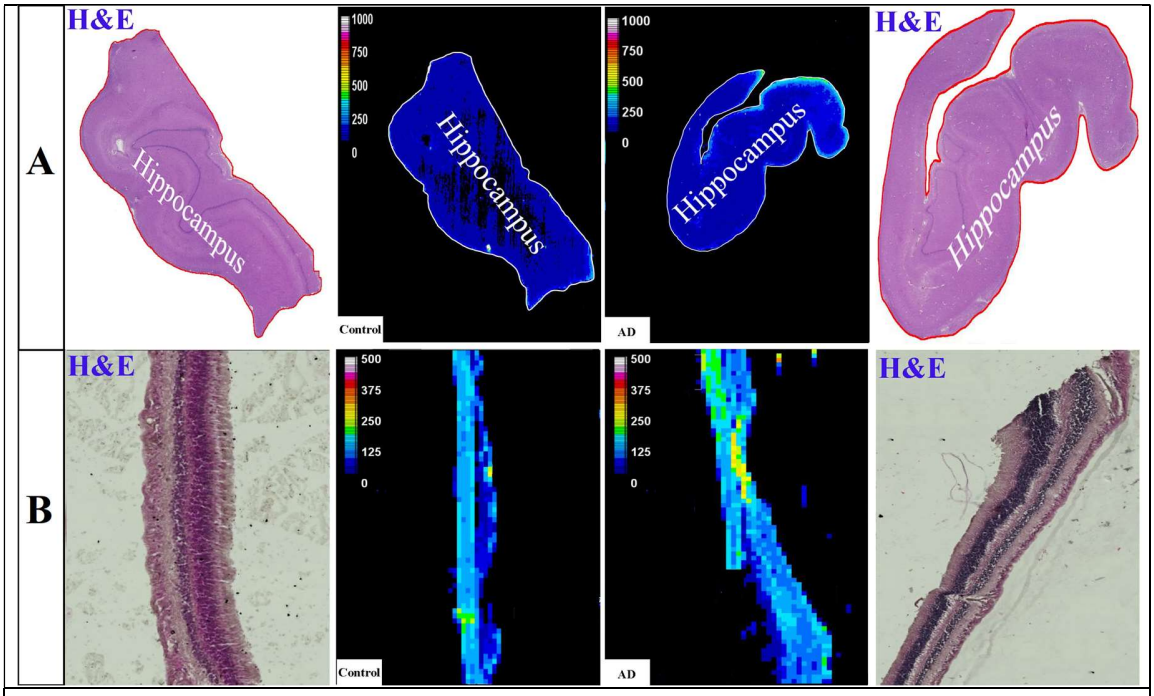

Fig.5.1. Distribution of Cu in the hippocampus (A) and eye (B). In each panel: In each panel: *Left and right image*s are representative Hematoxylin and Eosin (H&E) image demonstrating tissue architecture. *Middle*- sample map of 63Cu in a human hippocampus section of healthy control and AD (*upper row*) and human eye section of healthy control and AD (*lower row*). The scale represents calibrated Cu in ppm.

* *	Fig.5.2. Metal quantification analysis. Cu levels in the retina and HPC of AD and healthy control human samples, 9 cases with AD and 6 healthy control. Error bars represent Standard Error of the Mean (SEM) (*p < 0.05, Student's t-test, unpaired). HPC, hippocampus.

- ***Iron (Fe)***

Figs.5.3 A and B shows the Fe distribution in the human hippocampus and the eye's retina, respectively. Similar to copper, higher Fe levels were evident in the hippocampus and retina of AD human samples than in the healthy controls (Figs.5.3 A and B). Fig.5.4 represents intensity-based analysis results of Fe, which were in accordance with its calibrated quantitative image results; Fe concentration in the hippocampus and retina of AD samples are significantly higher than in healthy counterparts (217.4 ± 26.9 vs 183.4 ± 2.9, $p<0.05$ for hippocampus, 85.86 ± 12.86 vs 42.9 ± 1.3, $p<0.01$ for retina).

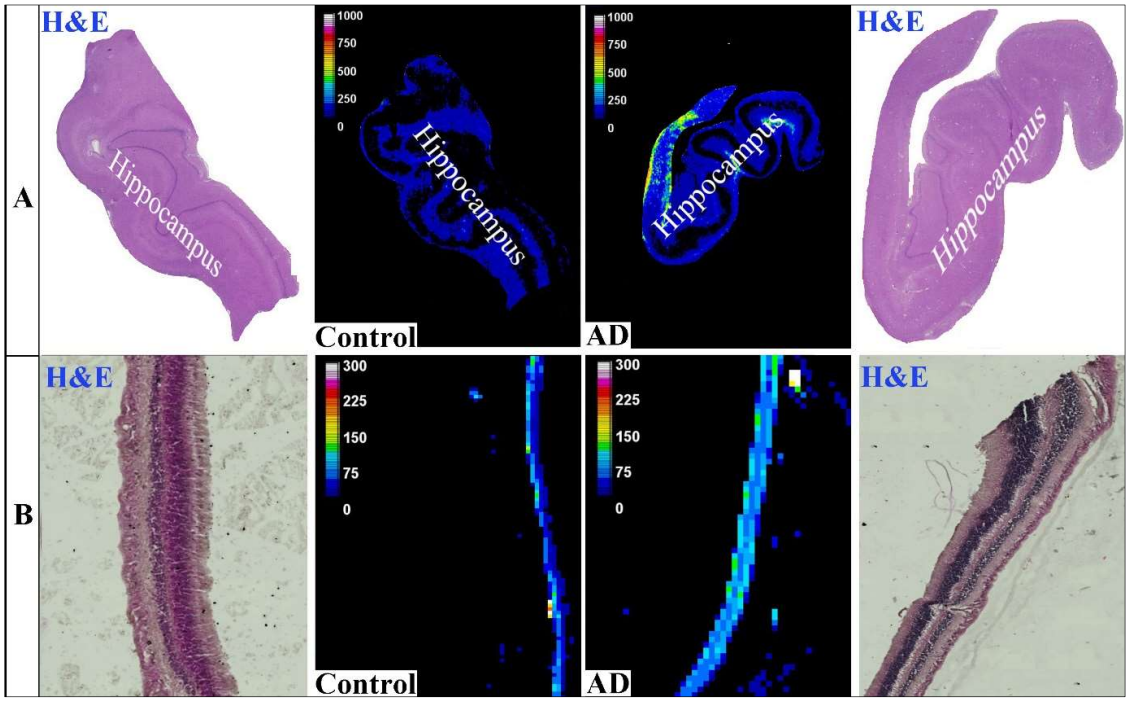

Fig.5.3. Distribution of Fe in the hippocampus (A) and eye (B). In each panel: *Left and right image*s are representative Hematoxylin and Eosin (H&E) image demonstrating tissue architecture. *Middle*- sample map of 56Fe in a human hippocampus section of healthy control and AD (*upper row*) and human eye section of healthy control and AD (*lower row*). The scale represents calibrated Fe in ppm.

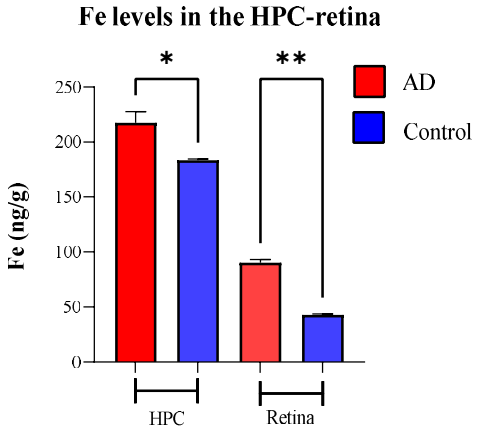

Fig.5.4. Metal quantification analysis. Fe concentrations in the retina and HPC of AD and healthy control human samples, 9 cases with AD and 6 healthy control. Error bars represent Standard Error of the Mean (SEM) (*p < 0.05, **p < 0.01, Student's t-test, unpaired). HPC, hippocampus.

- ***Zinc (Zn)***

Figs.5.5 A and B shows the anatomical distribution of Zn in the human hippocampus and the retina, respectively. Zinc calibrated quantitative image (Fig.5.5 A) of the AD hippocampus sample shows higher Zn concentration than the healthy control samples. Similarly, the retina of the AD human sample illustrates higher Zn concentration compared with healthy control sample (Fig.5.5 B). The images-based intensity analysis for Zn (Fig.5.6) matches the visual assessment of Zn-calibrated quantitative images. A significantly higher concentration of Zn was observed in the hippocampus and retina of AD samples compared with healthy controls (99.7 ± 17.6 vs 74 ± 17.4, $p<0.05$ for the hippocampus, 88 ± 6.1 vs 48.3 ± 6.5, $p<0.001$ for retina).

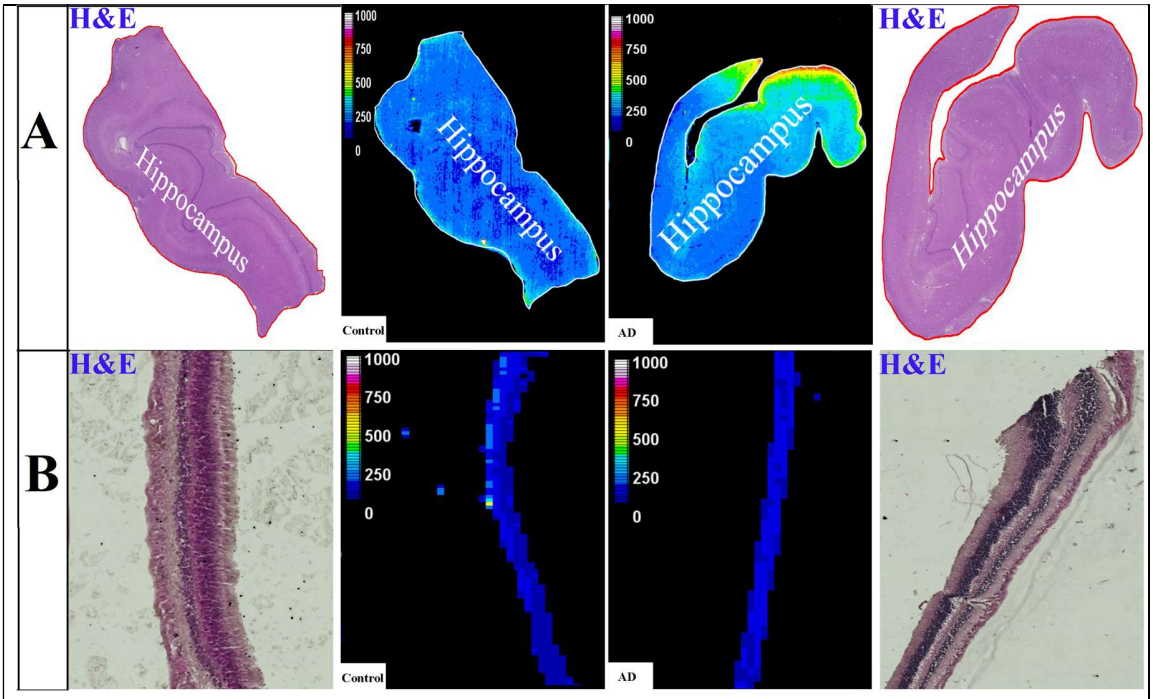

Fig.5.5. Distribution of Zn in the hippocampus (A) and eye (B). In each panel: *Left and right* images are representative Hematoxylin and Eosin (H&E) image demonstrating tissue architecture. *Middle*- intensity map of 66Zn in a human hippocampus section of healthy control and AD (*upper row*) and human eye section of healthy control and AD (*lower row*). The scale represents calibrated Zn in ppm.

* ***	Fig. 5.6. Metal quantification analysis. Zn levels in the retina and HPC of AD and healthy control human samples, 9 cases with AD and 6 healthy control. Error bars represent Standard Error of the Mean (SEM) (*p < 0.05, ***p < 0.001, Student's t-test, unpaired). HPC, hippocampus.

5.2.2. Zinc transporters (ZnT3-ZIP3) in the brain and eye of AD and healthy control human.

- ***ZnT3***

Immunofluorescence images of the ZnT3 transporter in the hippocampus and retina samples (healthy control and AD human) are illustrated in Figs. 5.7 A and B. Visual assessment of the ZnT3 transporter image demonstrates higher abundance of ZnT3 in the hippocampus of the healthy control sample compared with the AD human sample (Fig.5.7 A). The retina of the healthy control human sample shows a similar pattern, with higher levels of ZnT3 than the AD human sample (Fig.5.7 B). Results from the image-based intensity analysis (Fig.5.8) were in accordance with the visual assessment (Fig.5.7). ZnT3 levels in the retina and hippocampus of healthy control samples were significantly higher than in the AD samples (0.9 ± 0.08 vs 0.7 ± 0.1 $p<0.05$ for the hippocampus, 0.8 ± 0.05 vs 0.6 ± 0.1, $p<0.001$ for retina).

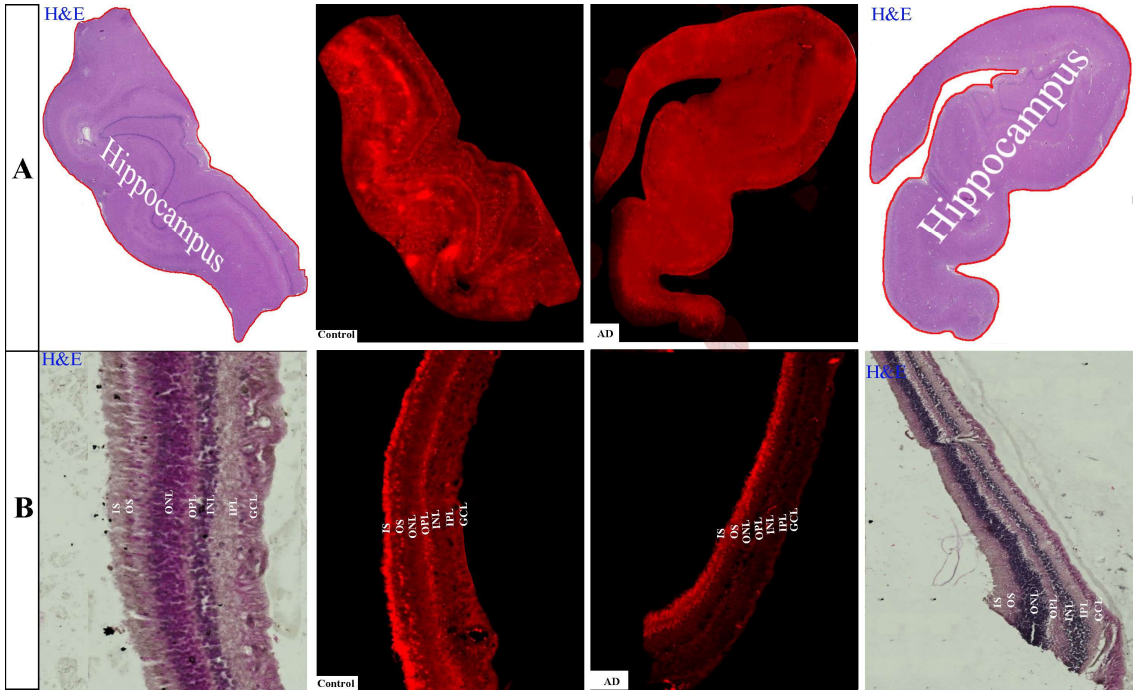

Fig.5.7. Representative immunofluorescence images for ZnT3 in the hippocampus (A) and eye (B). In each panel: *Left and right* images are representative Hematoxylin and Eosin (H&E) image demonstrating tissue architecture. *Middle*- abundance of ZnT3 transporter in a human hippocampus section of healthy control and AD (*upper row*) and human eye section of healthy control and AD (*lower row*).

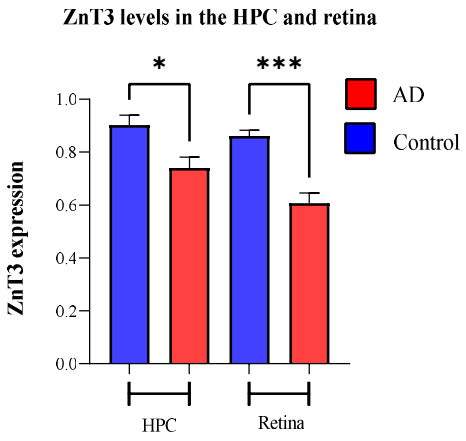

Fig. 5.8. ZnT3 levels in the human HPC and retina of AD and healthy control. 9 cases with AD and 6 healthy control. Error bars represent Standard Error of the Mean (SEM) (*p < 0.05, ***p < 0.001, Student's t-test, unpaired). HPC, hippocampus.

- ***ZIP3***

The immunofluorescence images of the ZIP3 transporter protein in the hippocampus and retina samples (healthy control and AD human) are shown in Figs. 5.9 A and B, respectively. The survey of the ZIP3 transporter images shows that the retina and hippocampus of healthy control human sample possess a higher abundance of ZIP3 compared with AD human sample (Figs.5.9 A and B). Image-based analysis results (Fig.5.10) are consistent with the visual assessment, with significantly higher ZIP3 levels observed in the retina and hippocampus of healthy control samples compared with AD samples (0.9 ± 0.09 vs 0.7 ± 0.1 $p<0.05$ for hippocampus, 1.1 ± 0.1 vs 0.7 ± 0.1, $p<0.001$ for retina).

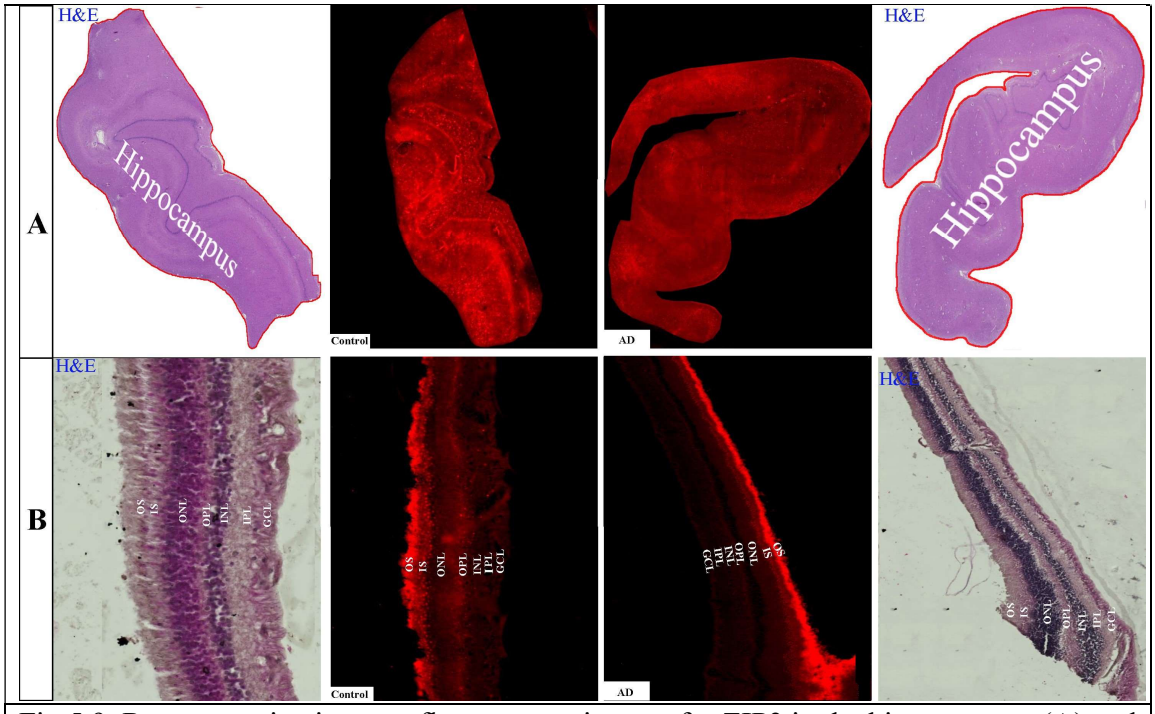

Fig.5.9. Representative immunofluorescence images for ZIP3 in the hippocampus (A) and eye (B). In each panel: Left and right images are representative Hematoxylin and Eosin (H&E) image demonstrating tissue architecture. Middle- abundance of ZIP3 transporter in a human hippocampus section of healthy control and AD (upper row) and human eye section of healthy control and AD (lower row).

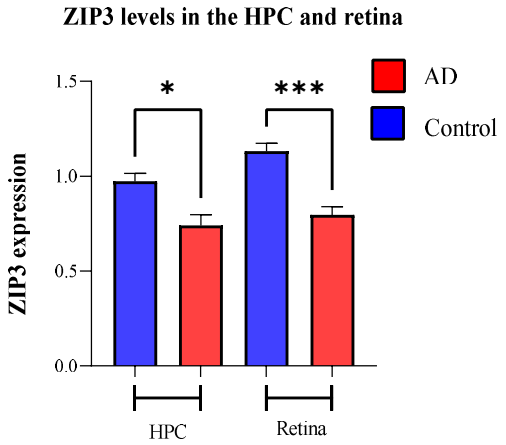

Fig.5.10. ZIP3 levels in the human HPC and retina of AD and healthy control. 9 cases with AD and 6 healthy control. Error bars represent Standard Error of the Mean (SEM) (*p < 0.05, ***p < 0.001, Student's t-test, unpaired). HPC, hippocampus.

5.3 Discussion

Continuing our investigation of transition metal distribution in the brain and the retina, in this chapter, we focused on whether the observations we made in the animal models (Chapters 3 and 4) can also be established in samples obtained from donor AD patients and healthy controls. The human study results show that healthy control samples possess lower Cu, Fe, and Zn concentrations compared with AD patients whilst expressing higher zinc transporters (ZnT3-ZIP3) in both the retina and hippocampus.

Results from our animal studies showed lower Cu levels in the hippocampus and retina of APP/PS1 mice compared with controls, an observation also reported in studies performed on human samples.[11, 52] Surprisingly, our results from donor samples contradict these reports: Cu concentration was higher in the hippocampus and retinal samples obtained from AD patients compared with healthy controls.

While our APP/PS1 mice possess lower Zn concentration in their hippocampus and retina compared with WT mice, our human study revealed that the hippocampus and retina of AD patients have higher zinc concentrations than healthy control samples. In consistent with our human results, higher zinc concentration has been reported in human AD than in healthy

control samples in studies investigating metal concentration in neurodegenerative disease.[11, 51, 315, 316]

The higher Zn concentrations in the human AD tissue could be due to the high level of zinc-enriched neuron terminals[317] in the AD brain, which results in an increase in the Zn concentration[315] and the low concentration of ZnT3 transporter in the AD human, resulting in the high Zn levels.[318]

Our Fe results in mice conflict with our human results. The hippocampus and retina of APP/PS1 mice have lower Fe concentration than WT mice, whilst the hippocampus and retina of human AD samples possess higher Fe concentration than healthy samples. Similar to our results, higher Fe concentrations in human AD samples than in healthy control have been reported.[11, 316, 319]

Dysregulating iron uptake caused by furin and iron-regulating elements and the Fe elimination process could be the possible reason for the higher Fe concentrations in human AD patients.[320, 321] Besides, it has been reported that ferritin isolated from the AD brain contains more Fe than the healthy control brain ferritin.[322]

Mice and humans share 92 % of their DNA; however, mice are only the ideal model for some human diseases.[323] To exactly reproduce complex diseases such as Alzheimer's in mice, which are involved in multiple genomic variants, researchers need to replicate exact human mutated genes in the mouse's genome.[323] However, due to insufficient enough knowledge, researchers only mutate a small genes portion to replicate the symptoms of a disease. As a result, mice do not have exactly the same disease as humans.

Furthermore, while the human and mouse brain has almost the same cells, including neurons, there are substantial differences in the expression of individual genes within the

same cell. The most significant difference is found in neurons, where genes responsible for making serotonin receptors are turned on in mice while turned off in humans. Serotonin levels have been reported to be effective for AD prevention and therapy.[324]

Finally, mice can produce their own vitamin C, while humans can not. There is significant evidence that vitamin C can protect the brain against age-related cognitive decline and Alzheimer's disease.[325, 326]

For the reasons mentioned above, it is likely that our APP/PS1 and WT mice models do not represent identical metals distributions and variations as in human brain tissues.

Unlike metal transitions which represented two different patterns in the human and mice model, zinc transporter protein level (ZnT3 and ZIP3) results show the same trend in the human and mice model, with lower zinc transporter proteins in the AD samples compared to healthy control samples.

Lower concentrations of zinc transporters (ZnT3-ZIP3) in our human AD samples than in healthy control samples are consistent with previous reports of downregulation of ZnT3 in AD patients.[58, 303, 318]

Patients with preclinical AD show a high level of Zn in their hippocampal synaptic vesicles as the AD patients, while their ZnT3 levels are the same as age-matched controls.[327] Therefore, decreasing the ZnT3 concentration in AD could be due to increased zinc concentrations.[49]

Even though our study is the first to visualise and measure transition metals concentration and zinc transporters (ZnT3 and ZIP3) level in the eye and brain of human AD and healthy control samples, several limitations need to be acknowledged.

Protein imaging in paraffin-embedded tissue requires paraffin removal and antigen retrieval before imaging, which can negatively impact proteins' composition and spatial distribution.[328] Despite the reproducibility of immunofluorescence, it suffers from non-specific binding of the antibody to target the antigen.[329] There is substantial leaching of trace elements from the tissue in the formalin fixation process, which needs to be considered.[330] Another issue with paraffin-embedded tissues is losing their antigenicity or epitope instability.[331] The errors arising from the mentioned limitations can be minimalised by optimising tissue processing and staining and dewaxing paraffin steps.

5.4 Conclusion

In this Chapter, transition metal concentrations (Cu, Fe, and Zn) and zinc transporter proteins levels (ZnT3 and ZIP3) in the human brain and eye (9 cases with AD and 6 controls) were investigated using LA-ICP-MS and immunofluorescence. Our results indicate that while the AD human brain and eye possess higher Zn, Fe, and Cu concentrations than healthy control samples, they have lower ZnT3 and ZIP3 levels than healthy control samples. One of the main goals of the current study is to assess the possibility of detecting AD through the eyes as the brain mirror. Surprisingly, our results suggest that the human eye can be used to diagnose early-onset Alzheimer's disease.

There has been growing evidence that high metal concentrations in Alzheimer's disease lead to amyloid plaque formation. A visual evaluation of the amyloid plaque levels in mice and human AD and healthy control samples via Quantum-Dot nanoprobes will be undertaken to assess this hypothesis further.

Chapter 6: Assessing the use of quantum dots as a multimodal imaging tag to identify and quantify amyloid plaques in mouse and human samples

6: Identification of amyloid plaques in mouse and human samples (AD and control)

6.1 Introduction

Assessing the concentration of amyloid-beta peptide (Aβ) is vital to diagnose amyloidogenesis. Amyloidogenesis is the general term for a group of diseases, including Alzheimer's disease (AD), Parkinson's disease (PD), type II diabetes, and spongiform encephalopathies that are based on the abnormal formation of amyloid (Aβ plaques).[332] Fibrillation of β amyloid (Aβ) peptides has been considered an important clinical hallmark in the diagnosis of AD. Several different techniques have been applied to monitor amyloid β concentration, including near-infrared spectroscopy,[333] Raman active nanofluidic device,[334] electrochemical methods,[335, 336] and localised surface plasmon resonance.[337, 338] In addition, Thioflavin and Congo red, [339-341] as the fluorescent probes, and curcumin, a safe plaque-labelling fluorochrome,[204] have also been used for studying Aβ. These methods suffer in that they require a second analysis to obtain either quantitative data or a high-resolution image. A probe that allowed both high resolution imaging and provided quantitative information would reduce the complexity of the analysis, and increase the capacity of research into Aβ. Quantum dots (QDs) have potential to be such a multimodal probe. QDs (Fig. 6.1) consist of an inorganic core semiconductor, such as CdTe or CdSe, encased in an inorganic shell made of a distinct semiconductor material with a different band gap, like ZnS.[342] The core-shell structure is further coated by an aqueous organic layer to which biomolecules can be conjugated. Quantum dots can conjugate with monoclonal antibodies (mAbs) through direct or indirect cross-linking. QDs with carboxylic or amino groups on their surface are directly

cross-linked to mAbs. Indirect cross-linking occurs when quantum dots have a streptavidin-coated surface that can be conjugated with biotinylated mAbs. Streptavidin shows a strong binding affinity towards biotin. Conjugating streptavidin and biotin is a standard approach for visualization of IHC through binding a biotinylated primary antibody to a protein target that can then be detected with a fluorescently labelled streptavidin. QDs are a generally used as an immunofluorescent probe, and are known for their high brightness,[343] resistance to photobleaching,[344] multiplexing capacity,[345] and high surface-to-volume ratio.[346] These properties could enhance the sensitivity of biological detection and imaging by at least 10- to 100-fold which [347] make them excellent fluorescent choices for in vitro and in vivo biomedical applications such as intracellular tracking,[348] diagnostics,[349] in vivo imaging,[350] and therapeutic delivery.[351] QDs have considerable advantages over organic dyes for IF, including large stokes shift, small energy loss, high fluorescence efficiency, higher stability, constant excitation wavelength, and a narrower emission spectrum,[352-354] making them a promising candidate for the applications mentioned above. Additionally, they contain metal atoms that are detectable by LA-ICP-MS. Therefore, it is possible that high resolution Immunofluorescence (IF) images can be obtained before quantitative LA-ICP-MS analysis on a single histological section.

In this chapter, we applied QD-labelled amyloid-beta (QDs-Aβ) to identify and quantify Aβ plaques associated with Alzheimer's disease in the mice (9 month) and human samples (control and AD, eye and brain). We utilized the Qdot™ 705 streptavidin conjugate, comprising a biotin-binding protein (streptavidin) covalently linked to a fluorescent label (Qdot™ nanocrystal). The Qdot binds to the Goat F(ab) Anti-Rabbit IgG H&L (Biotin) (ab7055), which in turn attaches to the β-Amyloid (D54D2) XP® Rabbit mAb, a specific

antibody targeting Aβ plaques. Additionally, Thioflavin S, a fluorescent reagent that binds directly to the plaques without needing an antibody, was used to collect comparison images to confirm the suitability of the QD probes.

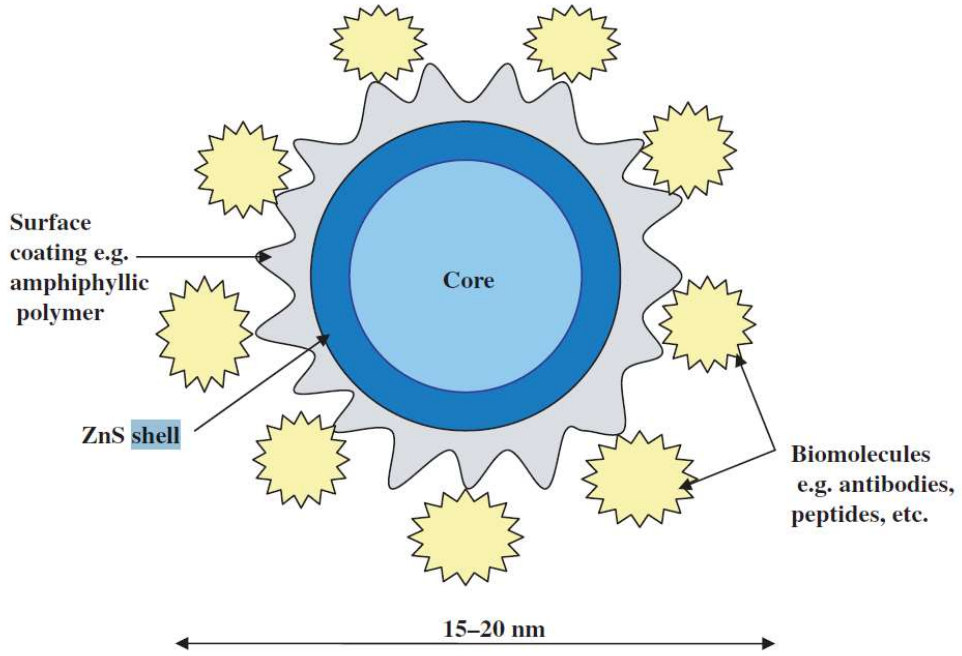

Fig. 6.1. QDs semiconductor structure.[342]

6.2 Experimental

6.2.1 Preparation of tissue

Mice frozen tissues (eye and brain) and FFPE human tissue (eye and brain) were used for this study. Human FFPE tissues were dewaxed prior to staining with antibody using the following slide wash/incubation sequences: xylene (2 x 2 minutes), 100 % ethanol (2 x 2 minutes), 90 % ethanol (2 x 2 minutes), 70 % ethanol (2 x 2 minutes), ddH_2O (1 x 2 minutes). The slides were washed with PBST (0.5 % triton) for permeabilisation (3 x 5 minutes), antigen retrieval was performed by boiling the slides in an antigen retrieval buffer in a

microwave using a microwave-safe container for 10 minutes, followed by cooling at room temperature. The final steps prior to immunolabelling were washing with PBST (0.5 % triton) (3 x 5 min), peroxidase blocking for 10 min at room temperature, and washing with PBST (0.5 % triton) (3 x 5 min).

6.2.2 Immunostaining with streptavidin conjugated Qdots

Mice and human (eye and brain) slides were incubated with MAXblock™ Blocking Medium (active motif) for 1 hour. They were then washed with TBS (3 x 5 min), before incubation with β-Amyloid (D54D2) XP® Rabbit mAb and MAXbind™ Staining Medium (active motif) (1:1000) overnight at room temperature in a humidified chamber. The slides were then washed with TBS (3 x 5 min), incubated with biotin blocking buffer (ABCAM ab64212) for 15 minutes, washed with TBS (3 x 5 min), and incubated with the mixture of Goat F(ab) Anti-Rabbit IgG H&L (Biotin) (ab7055) and MAXbind™ Staining Medium (1:250) for 2 hours at room temperature in a humidified chamber. Next, slides were washed with TBS (3 x 5 min) and incubated with the mixture of Qdot™ 705 Streptavidin Conjugate Qdot (Thermo Fisher Scientific, Q10163MP) and MAXbind™ Staining Medium (1:500) for 1 hour at room temperature in a dark humidified chamber. Slides were then counterstained with DAPI readymade solution (Sigma Aldrich, 1 μg/mL) for 10 minutes in a dark, humidified chamber, incubated with Thioflavin S (brain, 1 %) or (Eye, 2 %) for 1 min, washed with 80 % ethanol twice, 95 % ethanol, and Milli-Q water thrice, respectively. Finally, the slides were dehydrated with increasing concentration ethanol solutions (50, 75, and 90 %), coverslipped with DPX mountant (Sigma Aldrich), covered with a coverslip, air-dried (at 4 °C for 12-24 h), and imaged by fluorescence microscopy (Zeiss Axioscan slide-scanning microscope).

6.2.3 Laser Ablation-Inductively Coupled Plasma-Mass Spectrometry Imaging

Quantitative imaging of Quantum dot-labelled amyloid-beta (QDs-Aβ) eye and brain samples was conducted by LA-ICP-MS using a New Wave Research NWR-193 excimer laser (Kenelec Scientific) hyphenated to an Agilent Technologies 7900 series ICP-MS. Laser ablation was conducted by rastered lines covering the entire sections of the sample using a 193 nm laser with a 25 μm spot scanning at 100 μm/s and pulsed at 40 Hz. Quantification was performed via external, matrix-matched six-point calibration standards containing differing concentrations of Te in gelatine as per the method by Westerhausen et al.[228]

10 % gelatine solutions were prepared by dissolving 100 mg of bovine gelatine (Sigma Aldrich, Australia) in 900 μl of diluent consisting of 10 mM EDTA (Sigma Aldrich, Australia), 100 mM TRIS (Sigma Aldrich, Australia), and 1 % w/w PEG400 (Sigma Aldrich, Australia) at 54°C for 10 minutes. A high concentration solution containing tellurium were used to spike the diluent with desired concentrations of metals before being mixed with the solid gelatine. Once a homogenous gelatine solution was achieved, the mixture was pipetted onto microscope slides with the use of commercial moulds (Sigma Aldrich, Australia). The slides were placed into the freezer for at least 30 minutes until the aliquots of gelatine transformed from transparent to opaque. At this stage, the mould was peeled off, and the solid gelatine was left to air-dry and stored at room temperature. Each gelatine mixture was digested using high purity nitric acid (67-70 % w/w) diluted 100 times in triplicate and analysed using SN-ICP-MS to determine the exact concentrations of the elements in the produced gel standards.[228]

6.3 Results

6.3.1 Immunofluorescence detection of Aβ plaques in retina and brain of human and mouse models (AD and healthy control)

- **Mice retina and brain**

Retinal and brain cross-sections from APP/PS1 and WT mice were co-stained with Thio S and QDs-Aβ to determine the location of Aβ plaques, as shown in Figs. 6.2 and 6.3, respectively. According to Figs. 6.2 and 6.3, there is no sign of Aβ plaques in the retina and brain of WT samples, whereas they were clearly detected in the retina and brain of APP/PS1 samples. Additionally, the fluorescence of Thio S showed excellent colocalisation with the immunofluorescence of QDs-Aβ.

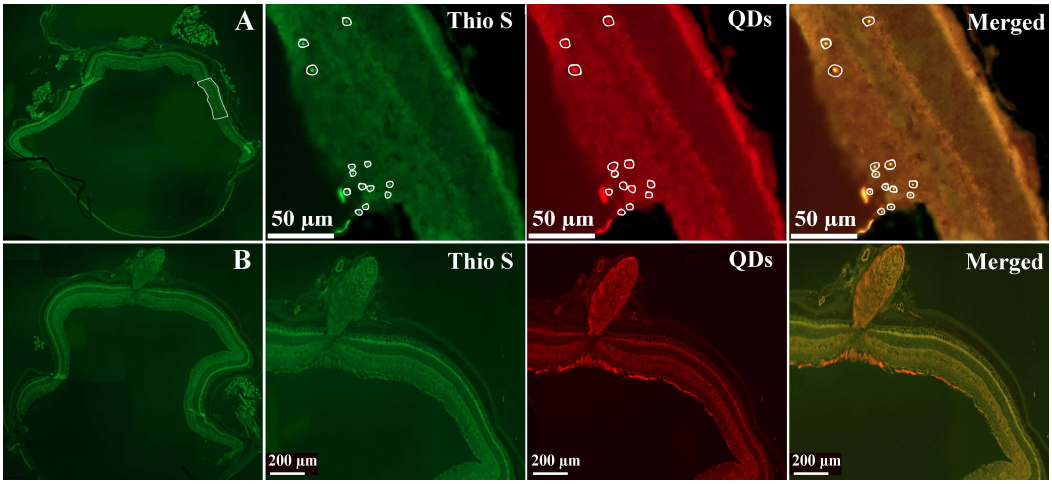

Fig.6.2. In vitro colocalisation of mice retinal Aβ plaques by Thio S and QDs-Aβ labelling in the 9-month old APP/PS1, Scale bar: 50 µm (A) and 9-month old WT mice model, Scale bar: 200 µm (B). The plaques are circled.

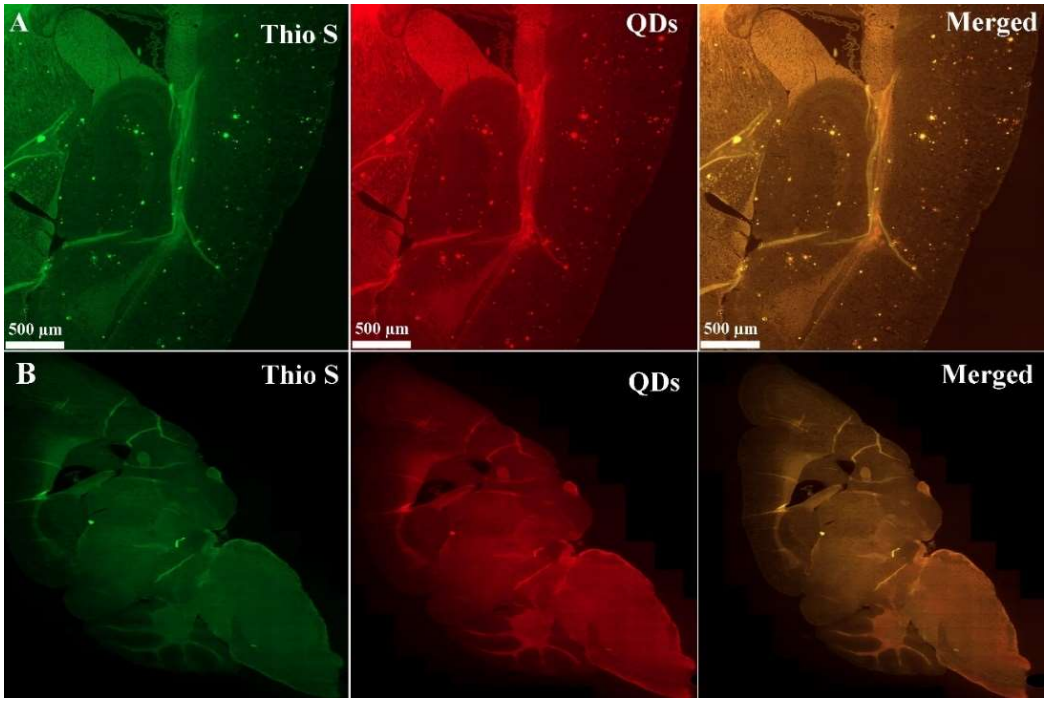

Fig.6.3. In vitro colocalisation of mice brain Aβ plaques by Thio S and QDs-Aβ labelling in the 9-month old APP/PS1, Scale bar: 500 µm (A) and 9-month old WT mice model (B).

- **Human retina and brain**

Immunofluorescence was used to measure the Aβ plaques contents in the retinal and brain cross-sections from AD and healthy control human samples, which were costained with Thio S and QDs-Aβ. Figs. 6.4-6.6 show the visualisation of Aβ plaques in the human eye and brain (AD and healthy control), respectively.

Plaques were visible in both the healthy and AD human retina co-stained with Thio S and QDs-Aβ, with a higher number of Aβ plaques in the retina of the AD samples compared with healthy human sample, as shown in Fig. 6.4.

Similar to the human retina, plaques were observed in both healthy and AD human brain (Fig. 6.5), with more Aβ plaques in the AD brain compared with healthy human brain (Fig. 6.6).

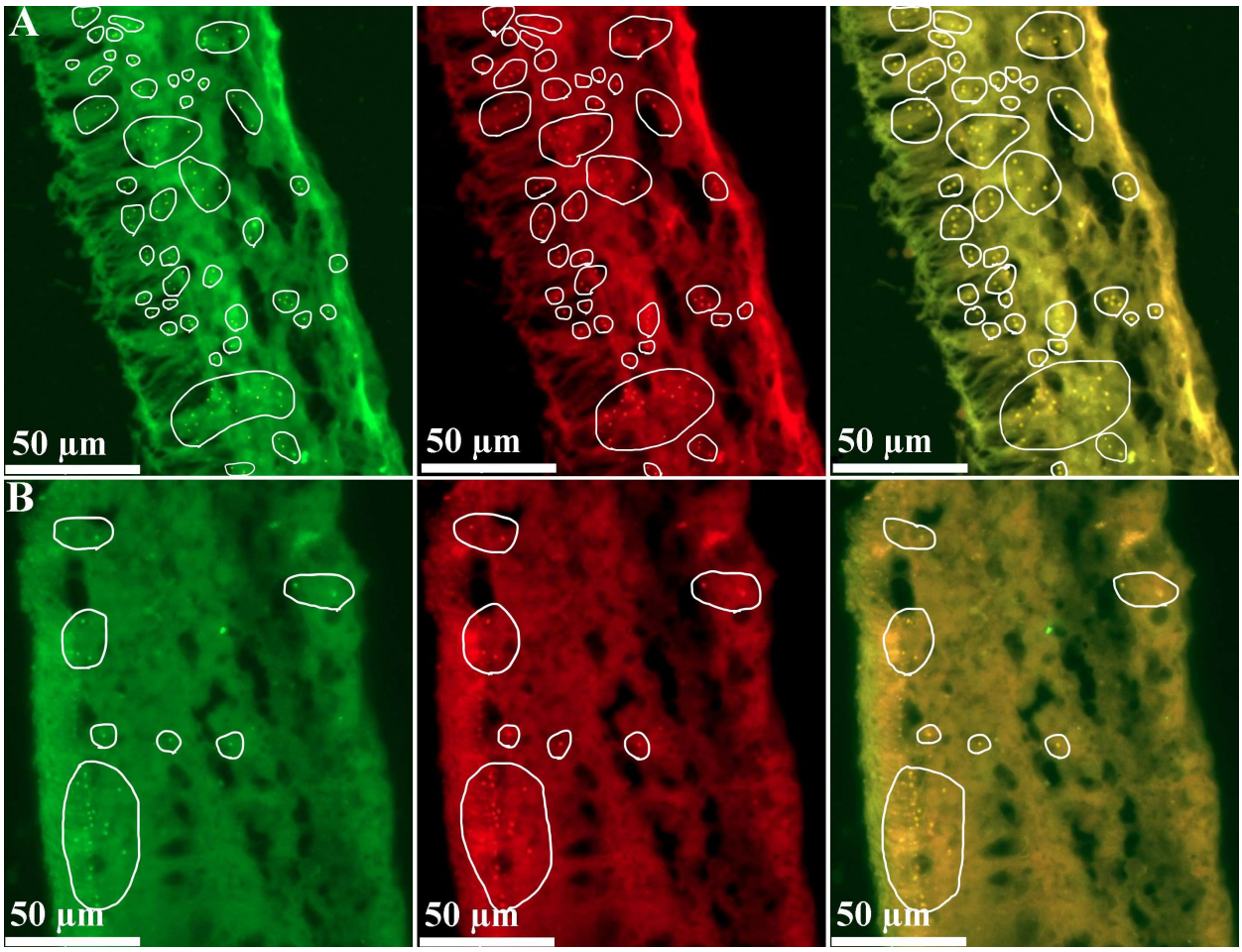

Fig.6.4. In vitro colocalisation of human eye Aβ plaques by Thio S and QDs-Aβ labelling in the APP/PS1 (A) and WT mice model, Scale bar: 50 µm (B).

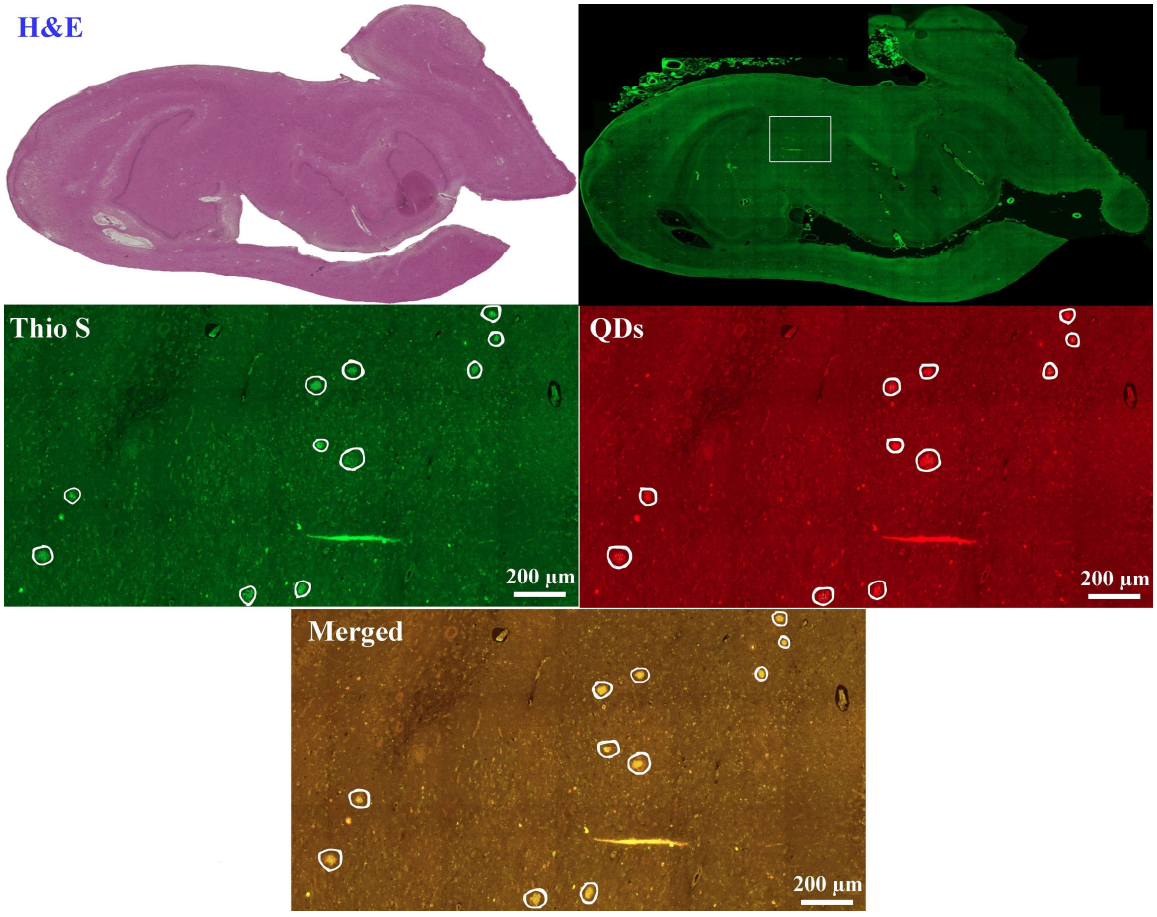

Fig.6.5. In vitro colocalisation of AD human hippocampus Aβ plaques (white bordered circles) by Thio S and QDs-Aβ labelling, Scale bar: 200 µm.

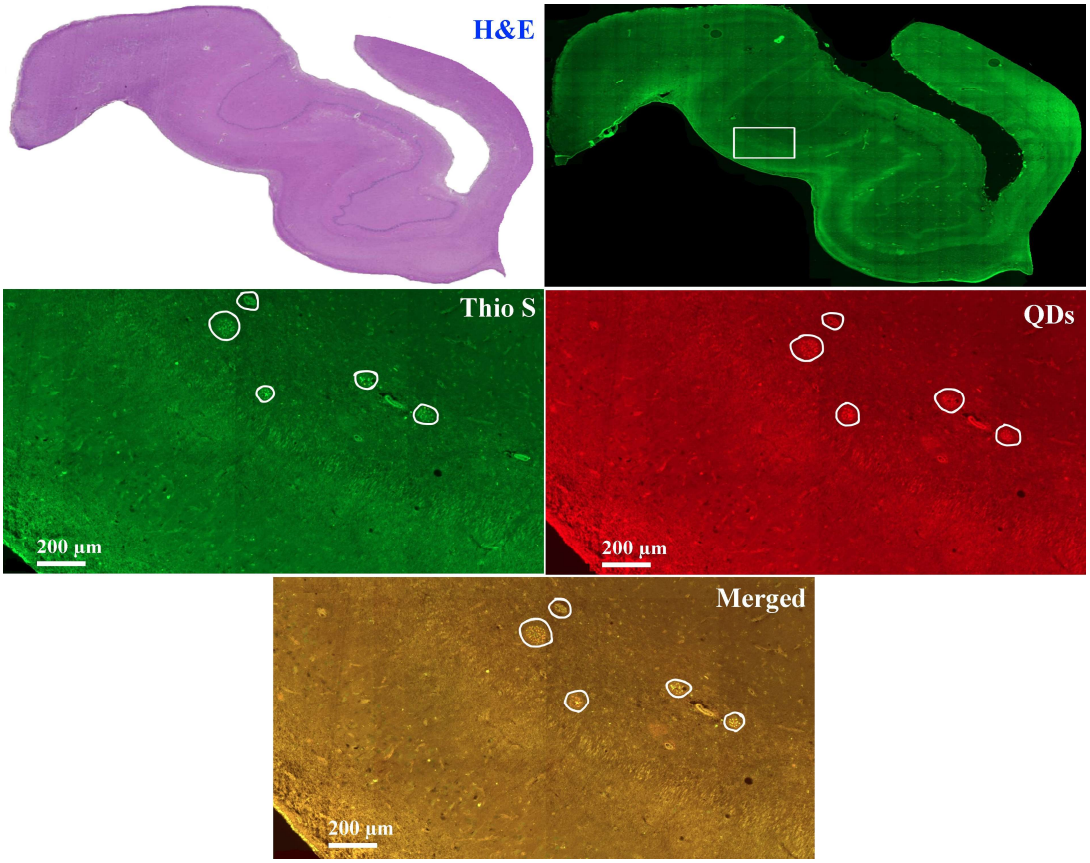

Fig.6.6. In vitro colocalisation of healthy human hippocampus Aβ plaques by Thio S and QDs-Aβ labelling, Scale bar: 200 µm.

6.3.2 LA-ICP-MS detection of Aβ plaques in retina and brain of human and mouse models (AD and healthy control)

The same sections used for Immunofluorescence imaging were used for LA-ICP-MS after removal of the coverslips in xylene.

- **Mice retina and brain**

Fig.6.7 shows the quantitative 2D images obtained for Te distribution in the mice's brain and retina (APP/PS1 and WT), respectively. The brain of the APP/PS1 mice appears to have much more widespread Te distribution at higher concentrations than the WT mice. Like the brain, the retina of APP/PS1 mice also express higher concentrations of Te than WT mice. It

should be noted that the LA-ICP-MS images do not appear to correlate with the plaque locations of the IF images, therefore the quantum dot probe may not be appropriate to co-localise high resolution IF images and quantify protein expression by LA-ICP-MS.

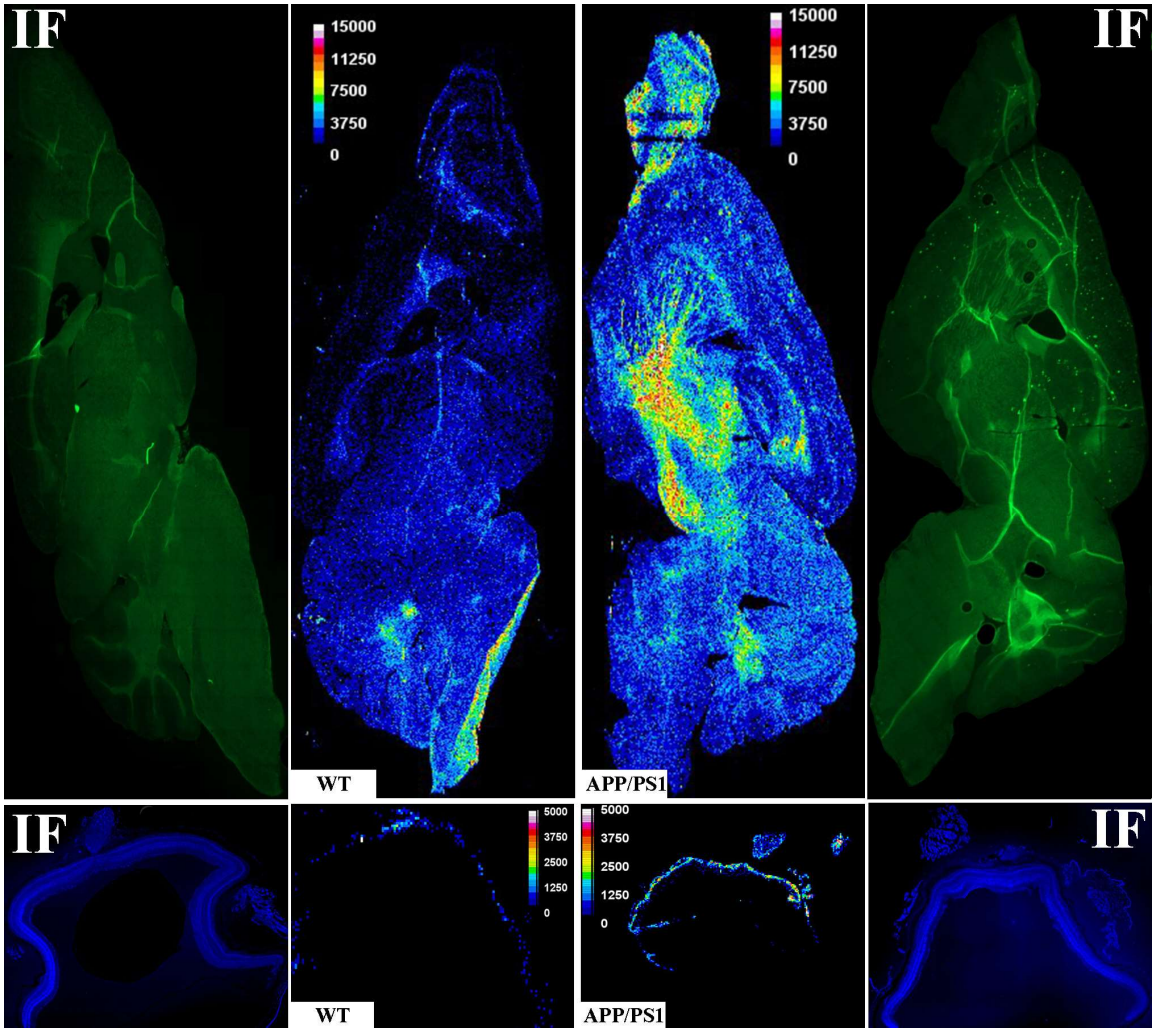

Fig.6.7 Quantitative images of Te in the mice brain and eye. Left and right images are representative immunofluorescence images demonstrating anatomical landmarks. Sample map of 125Te in mice brain sections of 9-month old WT and APP/PS1 (upper row) and mice eye sections of 9-month old WT and APP/PS1 (lower row).

- **Human's retinal and brain**

The spatial distributions of Te in QDs-Aβ -labelled brain and retinal cross-sections from AD and healthy control humans are shown in Fig.6.8.

The images of the human brain illustrate that the healthy control sample has high levels of Te than the AD human brain. Similarly, the healthy human retina also possesses higher levels of Te than the AD human brain. Again, these images do not correlate with the IF images of the QDs-Aβ.

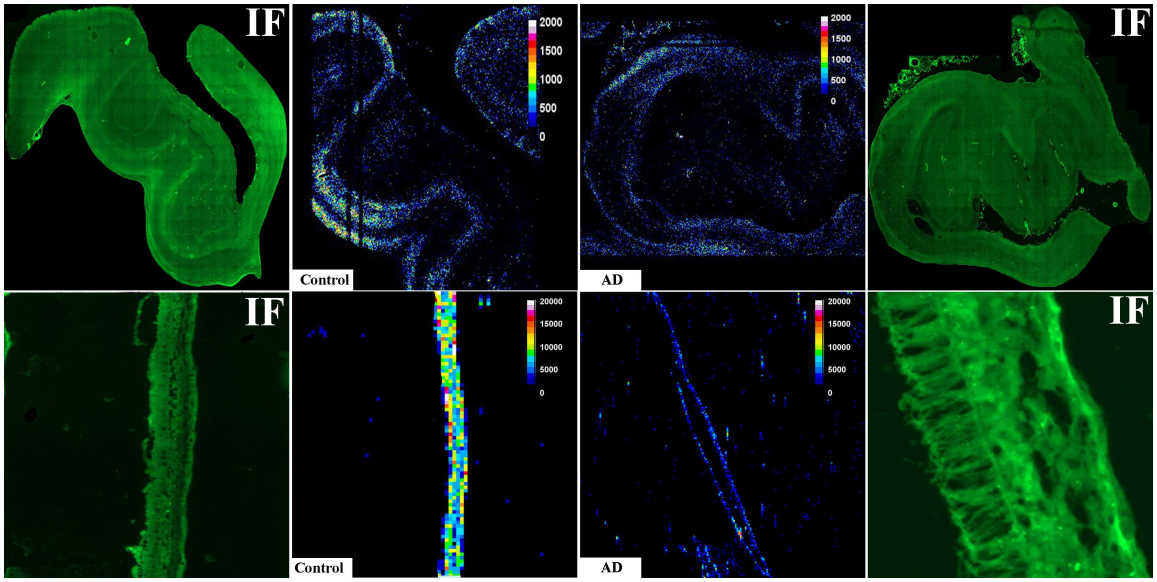

Fig.6.8 Quantitative images of Te in the human brain and eye. In each panel: Left and right images are representative Hematoxylin and Eosin (H&E) image demonstrating tissue architecture. Sample map of 125Te in human hippocampus sections of healthy control and AD (upper row) and human eye sections of healthy control and AD (lower row).

6.4 Discussion

In this chapter, we focused on the anatomical distribution and level of Aβ plaques, the hallmark pathology of AD. Our immunofluorescence results demonstrated that the retina and brain of AD humans and mice have higher Aβ plaques levels compared to healthy control

humans and mice. However, whilst the LA-ICP-MS results demonstrated that the brain and retina of APP/PS1 mice have higher Te concentrations than WT, the concentration of Te in the brain and retina of AD human samples are lower than healthy samples.

Our immunofluorescence findings are consistent with previous studies which demonstrated the existence of amyloid plaques in the retina and brain of AD samples.[204, 206, 355, 356] A possible explanation for this phenomenon is transition metal (Cu, Fe, and Zn) dyshomeostasis, which results in the aggregation of amyloid beta proteins to amyloid beta plaque.[357-360]

It is worth mentioning that the immunofluorescence results of healthy human samples (brain and retina) show a low volume of amyloid plaques. Our findings are in accordance with previous studies, which have demonstrated an age-associated presence of amyloid plaques in healthy-aged humans.[361-363]

Higher Te concentrations were obtained in the retina and brain of APP/PS1 mice using quantitative LA-ICP-MS, which corresponds to the amyloid plaques, is in accordance with previous reports with both retina and brain of AD model mice exhibiting higher numbers of amyloid plaques than WT.[204, 364, 365] Surprisingly, human retina and brain results contradict the mice results: human healthy eye and brain have higher Te concentrations than AD human samples. This was similar to the observations from Chs 3-5 which also showed differences in Zn between the human and mice. Additionally, the LA-ICP-MS images did not appear to colocalise with the IF images.

The presence of tellurium in plants and foods such as nuts, fish, and dairy products has been reported, which could be the possible reason for the high background concentration of Te in the human eye and brain samples.[366, 367] It was previously shown that the human

retina takes up toxic metals such as Hg, Pb, and Cd,[368] and this may be a contributing factor to the high levels observed here.

In this chapter, we showed feasibility for the use of QDs as a multimodal probe to investigate Aβ plaques. However, the Te background in the LA-ICP-MS images was the major limitation. It prevented the co-localisation of high resolution IF images with the quantitative LA-ICP-MS data that could give a greater insight into disease progression. Therefore, more alternative multimodal probes should be examined. Other metal-nanoparticle probes such as Au, Ag, Eu, and Cd have been employed in LA-ICP-MS imaging, however the corresponding IF images were not collected.[369-371] Novel probes such as that developed by van Acker et al which contain a metal ion and a fluorescent probe is another alternative pathway that could be explored.[372] Immuno-mass spectrometry imaging approaches are powerful tools for systematically and quantitatively measuring the protein expression using metal-labelled antibodies, but aren't able to examine sub-cellular location and therefore still require a second IF image.[373]

6.4 Conclusion

In this chapter, we utilised IF and LA-ICP-MS to determine the viability of QDs as a multimodal probe to visualise and quantify amyloid plaques in the retina and brain of humans and mice (AD and healthy). Our IF findings demonstrated that the brain and eye of mice and human AD samples contain greater numbers of amyloid plaques than healthy controls. However, whilst we noticed higher Te concentrations in the AD mice (eye and brain), the eye and brain of human AD samples showed lower amounts of Te than healthy human samples, and the images did not colocalise with the IF.

Chapter 7: Conclusions and Future Perspectives

7.1 Conclusions

Alzheimer's disease (AD) is a chronic progressive disease associated with age. Changes to the brain may start as long as 20 years prior to clinical symptoms are apparent-this is known as the asymptomatic (or preclinical) stage. While there is currently no treatment for AD, there is a consensus amongst clinicians and researchers that for any therapeutic treatment to work, we first need to determine the asymptomatic stage of the disease. Visualising amyloid beta (Aβ) plaques, a significant hall mark of the disease, may appear as the best tactic to stage asymptomatic AD, however, there are few limitations in taking this approach. Firstly, by the time Aβ plaques are formed in the brain, their neurotoxic effect would result in cognitive dysfunction, advancing the disease well past the asymptomatic stage. Secondly, current methods to visualise cerebral Aβ plaques, such as positron emission tomography (PET) are expensive, require sophisticated equipment and not widely available. This limits scaling of such methodology globally. Finally, recent evidence suggests that many cognitively-normal elderly people also show Aβ plaques in their PET scans. This further casts a shadow on the specificity of visualising Aβ plaques for determining the early stages of AD. Taken together, it appears that visualising Aβ plaques alone would not assist in identifying the asymptomatic stage of AD and an alternative approach is urgently needed.

Delving into the “amyloid cascade” theory, there is now evidence that a series of events takes place prior to soluble Aβ are transformed into toxic Aβ aggregates or plaques. Ideally, any approach that can identify this stage, has the potential to reveal the asymptomatic phase of AD. Amongst many possibilities, current advances in metal-ion metabolism research has identified a miss-metabolism in transition metals (i.e. Fe, Cu and Zn) as the core mediator of

Aβ plaque assembly. For instance, in synapses regulation of Zn^{2+} is achieved by the Zinc transporter3 (ZnT3) protein, which is primarily localised on glutamatergic synapses, especially in regions of the brain that mediate higher cognitive functions. Dysfunction of ZnT3, and the subsequent dyshomeostasis of synaptic zinc, has a direct effect on the cognitive decline associated with ageing and AD. Findings such as these reports undoubtedly demonstrates that transition metal homeostasis becomes corrupted with age and in neuropathological conditions, such as AD.

The main challenge with pursuing the idea of visualising transition metals to uncover the asymptomatic stages of AD lies in the very fact that in-vivo imaging of transition metals in the brain is extremely challenging. Whilst a diverse array of techniques is available to measure transition metal levels down to sub-micron resolution, including LA-ICP-MS, synchrotron -based X-ray fluorescence microprobe and particle-induced X-ray emission, however, they are all in-vitro and cannot be utilised in-vivo. In contrast, the eye and specifically the retina, offer a natural window to the brain, and unlike the challenges associated with imaging the brain, a range of techniques are available to image and visualise metal ion specific probes in the retina in vivo. Nevertheless, in order to develop this concept further, we first need to establish whether changes observed in cerebral transition metals are also mirrored in the retina. This gap in the literature led us to investigate whether changes in cerebral Iron, Copper, and Zinc are also observed in the retina of transgenic AD mice as well as post-mortem tissue samples obtained from human donors. Our working hypothesis was that an imbalance in retinal transition metal levels occurs in parallel to the brain in AD.

In **chapter 1** (the literature review) we covered in details the basics of transition metal involvement in AD pathophysiology and how miss-metabolism in transition metals can

initiate and exacerbate AD progression. The role of zinc transporters in AD, in particular zinc transporter 3, was also covered. In addition, we discussed the eye-brain connection and how it may be utilised to evaluate brain-related changes. We concluded that based on a growing body of evidence that demonstrated dyshomeostasis of transition metals in AD, and given the striking underlying physiological and pathological connections between the eye and the brain, a similar cascade of events may occur in the retina that may ultimately lead to evaluating retinal transition metal or specific protein levels (e.g., ZnT3, ZIP3) as a surrogate marker for staging asymptomatic AD.

To address our hypothesis, we employed laser ablation-inductively coupled plasma-mass spectrometry (LA-ICP-MS), and solution nebulization-inductively coupled plasma-mass spectrometry (SN-ICP-MS), to visualise and quantify the transitional metal concentrations of Cu, Fe, and Zn, as well as zinc transporter proteins 3 (i.e., ZnT3 and ZIP3) in the eye and brain of APP/PS1 mice and post-mortem samples obtained from human donors diagnosed with AD. The APP/PS1 mouse model was chosen as human Aβ42 is preferentially generated over Aβ40 in these animals, though levels of both proteins increase with age. Furthermore, there has been a number of studies that have demonstrated AD-specific retinal changes in these mice that are in-line with neocortical changes.

Results from our first set of experiments (**Chapter 3**) focused on investigating age-associated changes in the transition metal concentrations of the brain and retina of 9-and-18-month old APP/PS1 and WT mice. Our results demonstrated that Cu, Fe, and Zn concentrations in the WT samples are higher than in APP/PS1 mice (except the cortex) at 9-and-18 month of age. Furthermore, except for Cu, there is an age-associated decrease in Fe and Zn over the same time period (i.e., 9 to 18 months of age). Moreover, a significant

difference between the metal concentrations in the WT and APP/PS1 mice model (higher Cu, Fe, and Zn in the WT than APP/PS1) was observed, suggesting the potential of quantifying transition metals as a biomarker for AD.

We then investigated (**Chapter 4**) whether we can identify age-related changes in the zinc transporter proteins abundance (ZnT3 and ZIP3) in both the brain and retina of the same mouse models. The obtained results demonstrated the high level of ZnT3 and ZIP3 in the WT compared with APP/PS1. Furthermore, the ZnT3 and ZIP3 levels appear to decline with aging. Additionally, Western blot results further confirmed immunofluorescence outcomes with the high level of ZnT3 and ZIP3 in the WT compared with APP/PS1. In addition, similar to the immunofluorescence results, Western blot results also displayed a decline in zinc transporter proteins abundances from 9 to 18 (APP/PS1 and WT mice).

To examine the impact of ZnT3 on the histochemical reactive zinc or total elemental zinc in both the brain and retina, the total Zn concentrations (ng/g) in the hippocampus and the retina of ZnT3 knockout and WT mice (3, 11- and 14-month old) were also measured by SN-ICP-MS. Zn concentrations in the retina and hippocampus of WT samples (3, 11- and 14-month old) possess significantly higher Zn concentrations than ZnT3 KO mice, which confirmed the metal-transporting role of the ZnT3 protein in the retina and brain.

Comparing zinc transporters levels of the brain and retina (both WT and APP/PS1, 9-18 months) with their corresponding Zn concentrations, suggests that the higher zinc concentration in the WT samples may be due to the higher abundance of zinc transporters. This also provides further evidence on the potential role of zinc transporters in governing Zn content.

Continuing our investigation, we then aimed to study if the findings in the animal models are also reproduced in humans (**Chapter 5**). To achieve this, we obtained human brain and eye samples (9 cases with AD and 6 healthy controls) from the Netherlands Brain Bank. Our results demonstrated that the hippocampus and retina of human AD samples have higher levels of Cu, Fe, and Zn compared with the healthy control samples. Zinc transporter proteins abundance (ZnT3 and ZIP3) of the human brain and retina samples were also measured to assess if we can observe the same pattern as mice. Immunofluorescence results illustrated that the hippocampus and retina of human AD samples have lower levels of ZnT3 and ZIP3 compared with the healthy control samples. Similar to the animal mouse model, zinc transporters appear to govern the zinc level in the human retina and hippocampus samples, with lower concentration of zinc transporters in the human AD samples associated with higher Zn content.

Finally, we utilised quantum dot-labelled amyloid-β (QDAβ) nanoprobe (**Chapter 6**) for monitoring of Aβ plaques in the mouse and human samples (control and AD, eye and brain) by LA-ICP-MS and immunofluorescence. In this application the chosen quantum dots were not a suitable multimodal probe as the location and concentration of Aβ plaques in the AD samples derived from LA-ICP-MS images did not overlap with the immunofluorescence outcomes.

In summary, our results demonstrate, for the first time, that transition metals in the retina mirrors that of the brain (i.e., hippocampus) and that in AD, there is a significant alteration in transition metals both in the retina and hippocampus. There also seems to be an age dependent change in transition metals. Collectively, these results establish that the retina can be used as a window to assess metal dyshomeostais in the early stages of AD and has the

potential to be used as a surrogate marker for cerebral changes, paving the way for detecting AD in its asymptomatic phase.

7.2 Future perspectives

Utilising a rodent model of AD and post mortem human samples, we dissected the potential transition metal dysfunction in the retina and brain in AD. We acknowledge that this study was based on a familial rodent model of AD and that the majority of the experiments were completed ex-vivo and thus, further studies, particularly in-vivo, should be completed prior to extrapolating findings to a clinical tool. Propelled by compelling findings from this study, it appears that the retina, as a window to the brain, can provide a sound platform in assessing transition metal dysfunction in AD and uncovering the very early stages of the disease. Nevertheless, a combination of studies is required not only to fully establish the role of transition metals in AD, but also to detect any changes in the retina through a non-invasive accessible tool. These include:

I. A study to monitor transition metals and proteins changes over the entire AD pathogenesis continuum. In our study we only used mice that were 9 and 18 months old. As aging is the most significant risk factor for AD,[374] results from age-related transition metals and protein studies can supply conspicuous evidence for understanding the pathogenesis molecular mechanism related to metal dysfunction of AD in the brain and retina.

II. A study to investigate if alterations in the ZIP3 abundance also impact the histochemical reactive zinc or total elemental zinc and other metals (Fe, Mn, and Cu) in the brain and the retina. It has been reported that by specifically adjusting the expression level of zinc transporters, it is possible to alter the progression of AD.[286] In this research by measuring

the Zn content in the ZnT3 knockout mice, we found that ZnT3 governs the histochemical reactive zinc and total elemental zinc concentration. On the other hand, measuring the abundance of ZnT3 and ZIP3 in the APP/PS1 and WT mice model samples represented their implication on the Zn content. Therefore, to understand the impact of each zinc transporter on the Zn content in the AD, we suggest to measure the Zn volume in the ZIP3 knockout mice as well.

III. In the current research, we exclusively investigated zinc and its related transporter proteins (ZnT3 and ZIP3), while transporter proteins relevant to Cu and Fe metals were not assessed. It is well known that metal transporter proteins significantly impact AD progress; therefore, to establish a holistic overview of the eye and brain correlation in AD;[375, 376] we also need to investigate transporter proteins related to other transition metals in the eye and brain.

IV. In humans, 14 and 9 members of the ZIP and ZnT family, respectively, have been shown to be involved in zinc adjustment. Each demonstrate a tissue-specific, developmental, stimulus-responsive expression pattern and specific cellular and subcellular localisation.[145, 153, 377] In addition, the ZIP family are also involved in the modulation of Fe, Mn, and Cu.[378-380] The roles of five ZnT transporter protein family members (ZnT1-4 and ZnT6) on protein aggregation, amyloid plaque formation, and AD progression have been reported before.[229, 381] In this research, we just focused on the abundance of ZnT3 and ZIP3 and their impact on the eye and brain AD. To take benefit from screening the retina for staging AD, we may also need to assess the role of other ZnT and ZIP family members.

V. A study to monitor zinc transporters changes over the retinal layers. Optic nerve degeneration, neuronal loss, and reduced thickness in retinal layers manifest in Alzheimer's disease.[193] Our human eye zinc transporters (ZnT3 and ZIP3) images exhibit varying intensities across distinct retinal layers. To better understand the pathological features of AD in the diverse retinal layers, we propose mapping of retinal biomarkers across them.

References

1. Zhang, Y.; Gladyshev, V. N., Comparative genomics of trace elements: emerging dynamic view of trace element utilization and function. *Chem Rev* **2009,** *109* (10), 4828-61.
2. Bleackley, M. R.; Macgillivray, R. T., Transition metal homeostasis: from yeast to human disease. *Biometals* **2011,** *24* (5), 785-809.
3. Maret, W., The Metals in the Biological Periodic System of the Elements: Concepts and Conjectures. *Int J Mol Sci* **2016,** *17* (1).
4. Wu, E. W.; Schaumberg, D. A.; Park, S. K., Environmental cadmium and lead exposures and age-related macular degeneration in U.S. adults: the National Health and Nutrition Examination Survey 2005 to 2008. *Environ Res* **2014,** *133*, 178-84.
5. Bhattacharya, P. T.; Misra, S. R.; Hussain, M., Nutritional Aspects of Essential Trace Elements in Oral Health and Disease: An Extensive Review. *Scientifica (Cairo)* **2016,** *2016*, 5464373.
6. Billman, G. E., Homeostasis: The Underappreciated and Far Too Often Ignored Central Organizing Principle of Physiology. *Front Physiol* **2020,** *11*, 200.
7. Tardy, A. L.; Pouteau, E.; Marquez, D.; Yilmaz, C.; Scholey, A., Vitamins and Minerals for Energy, Fatigue and Cognition: A Narrative Review of the Biochemical and Clinical Evidence. *Nutrients* **2020,** *12* (1).
8. Bonda, D. J.; Lee, H. G.; Blair, J. A.; Zhu, X.; Perry, G.; Smith, M. A., Role of metal dyshomeostasis in Alzheimer's disease. *Metallomics* **2011,** *3* (3), 267-70.
9. Strozyk, D.; Launer, L. J.; Adlard, P. A.; Cherny, R. A.; Tsatsanis, A.; Volitakis, I.; Blennow, K.; Petrovitch, H.; White, L. R.; Bush, A. I., Zinc and copper modulate Alzheimer Abeta levels in human cerebrospinal fluid. *Neurobiol Aging* **2009,** *30* (7), 1069-77.
10. Plantin, L. O.; Lying-Tunell, U.; Kristensson, K., Trace elements in the human central nervous system studied with neutron activation analysis. *Biol Trace Elem Res* **1987,** *13* (1), 69-75.
11. Deibel, M. A.; Ehmann, W. D.; Markesbery, W. R., Copper, iron, and zinc imbalances in severely degenerated brain regions in Alzheimer's disease: possible relation to oxidative stress. *Journal of the neurological sciences* **1996,** *143* (1-2), 137-42.
12. James, S. A.; Volitakis, I.; Adlard, P. A.; Duce, J. A.; Masters, C. L.; Cherny, R. A.; Bush, A. I., Elevated labile Cu is associated with oxidative pathology in Alzheimer disease. *Free Radic Biol Med* **2012,** *52* (2), 298-302.
13. Capo, C. R.; Arciello, M.; Squitti, R.; Cassetta, E.; Rossini, P. M.; Calabrese, L.; Rossi, L., Features of ceruloplasmin in the cerebrospinal fluid of Alzheimer's disease patients. *Biometals* **2008,** *21* (3), 367-72.
14. Bucossi, S.; Ventriglia, M.; Panetta, V.; Salustri, C.; Pasqualetti, P.; Mariani, S.; Siotto, M.; Rossini, P. M.; Squitti, R., Copper in Alzheimer's disease: a meta-analysis of serum,plasma, and cerebrospinal fluid studies. *Journal of Alzheimer's disease : JAD* **2011,** *24* (1), 175-85.
15. Squitti, R.; Lupoi, D.; Pasqualetti, P.; Dal Forno, G.; Vernieri, F.; Chiovenda, P.; Rossi, L.; Cortesi, M.; Cassetta, E.; Rossini, P. M., Elevation of serum copper levels in Alzheimer's disease. *Neurology* **2002,** *59* (8), 1153-61.
16. Brewer, G. J.; Kanzer, S. H.; Zimmerman, E. A.; Celmins, D. F.; Heckman, S. M.; Dick, R., Copper and ceruloplasmin abnormalities in Alzheimer's disease. *Am J Alzheimers Dis Other Demen* **2010,** *25* (6), 490-7.
17. Vural, H.; Demirin, H.; Kara, Y.; Eren, I.; Delibas, N., Alterations of plasma magnesium, copper, zinc, iron and selenium concentrations and some related erythrocyte antioxidant enzyme activities in patients with Alzheimer's disease. *J Trace Elem Med Biol* **2010,** *24* (3), 169-73.
18. Molina, J. A.; Jiménez-Jiménez, F. J.; Aguilar, M. V.; Meseguer, I.; Mateos-Vega, C. J.; González-Muñoz, M. J.; de Bustos, F.; Porta, J.; Ortí-Pareja, M.; Zurdo, M.; Barrios, E.; Martínez-Para, M. C., Cerebrospinal fluid levels of transition metals in patients with Alzheimer's disease. *J Neural Transm (Vienna)* **1998,** *105* (4-5), 479-88.
19. Ozcankaya, R.; Delibas, N., Malondialdehyde, superoxide dismutase, melatonin, iron, copper, and zinc blood concentrations in patients with Alzheimer disease: cross-sectional study. *Croat Med J* **2002,** *43* (1), 28-32.
20. Squitti, R.; Ghidoni, R.; Scrascia, F.; Benussi, L.; Panetta, V.; Pasqualetti, P.; Moffa, F.; Bernardini, S.; Ventriglia, M.; Binetti, G.; Rossini, P. M., Free copper distinguishes mild cognitive impairment subjects from healthy elderly individuals. *J Alzheimers Dis* **2011,** *23* (2), 239-48.
21. Squitti, R.; Pasqualetti, P.; Cassetta, E.; Dal Forno, G.; Cesaretti, S.; Pedace, F.; Finazzi-Agrò, A.; Rossini, P. M., Elevation of serum copper levels discriminates Alzheimer's disease from vascular dementia. *Neurology* **2003,** *60* (12), 2013-4.
22. Squitti, R.; Cassetta, E.; Dal Forno, G.; Lupoi, D.; Lippolis, G.; Pauri, F.; Vernieri, F.; Cappa, A.; Rossini, P. M., Copper perturbation in 2 monozygotic twins discordant for degree of cognitive impairment. *Arch Neurol* **2004,** *61* (5), 738-43.
23. Squitti, R.; Pasqualetti, P.; Dal Forno, G.; Moffa, F.; Cassetta, E.; Lupoi, D.; Vernieri, F.; Rossi, L.; Baldassini, M.; Rossini, P. M., Excess of serum copper not related to ceruloplasmin in Alzheimer disease. *Neurology* **2005,** *64* (6), 1040-6.

24. Squitti, R.; Barbati, G.; Rossi, L.; Ventriglia, M.; Dal Forno, G.; Cesaretti, S.; Moffa, F.; Caridi, I.; Cassetta, E.; Pasqualetti, P.; Calabrese, L.; Lupoi, D.; Rossini, P. M., Excess of nonceruloplasmin serum copper in AD correlates with MMSE, CSF [beta]-amyloid, and h-tau. *Neurology* **2006,** *67* (1), 76-82.
25. Squitti, R.; Bressi, F.; Pasqualetti, P.; Bonomini, C.; Ghidoni, R.; Binetti, G.; Cassetta, E.; Moffa, F.; Ventriglia, M.; Vernieri, F.; Rossini, P. M., Longitudinal prognostic value of serum "free" copper in patients with Alzheimer disease. *Neurology* **2009,** *72* (1), 50-5.
26. Salustri, C.; Squitti, R.; Zappasodi, F.; Ventriglia, M.; Bevacqua, M. G.; Fontana, M.; Tecchio, F., Oxidative stress and brain glutamate-mediated excitability in depressed patients. *J Affect Disord* **2010,** *127* (1-3), 321-5.
27. James, S. A.; Churches, Q. I.; de Jonge, M. D.; Birchall, I. E.; Streltsov, V.; McColl, G.; Adlard, P. A.; Hare, D. J., Iron, Copper, and Zinc Concentration in Aβ Plaques in the APP/PS1 Mouse Model of Alzheimer's Disease Correlates with Metal Levels in the Surrounding Neuropil. *ACS chemical neuroscience* **2017,** *8* (3), 629-637.
28. Bagheri, S.; Squitti, R.; Haertlé, T.; Siotto, M.; Saboury, A. A., Role of Copper in the Onset of Alzheimer's Disease Compared to Other Metals. *Frontiers in Aging Neuroscience* **2018,** *9*.
29. Multhaup, G.; Schlicksupp, A.; Hesse, L.; Beher, D.; Ruppert, T.; Masters, C. L.; Beyreuther, K., The amyloid precursor protein of Alzheimer's disease in the reduction of copper(II) to copper(I). *Science* **1996,** *271* (5254), 1406-9.
30. Kim, A. C.; Lim, S.; Kim, Y. K., Metal Ion Effects on Aβ and Tau Aggregation. *International journal of molecular sciences* **2018,** *19* (1).
31. Minicozzi, V.; Stellato, F.; Comai, M.; Dalla Serra, M.; Potrich, C.; Meyer-Klaucke, W.; Morante, S., Identifying the minimal copper- and zinc-binding site sequence in amyloid-beta peptides. *J Biol Chem* **2008,** *283* (16), 10784-92.
32. Huang, X.; Cuajungco, M. P.; Atwood, C. S.; Hartshorn, M. A.; Tyndall, J. D.; Hanson, G. R.; Stokes, K. C.; Leopold, M.; Multhaup, G.; Goldstein, L. E.; Scarpa, R. C.; Saunders, A. J.; Lim, J.; Moir, R. D.; Glabe, C.; Bowden, E. F.; Masters, C. L.; Fairlie, D. P.; Tanzi, R. E.; Bush, A. I., Cu(II) potentiation of alzheimer abeta neurotoxicity. Correlation with cell-free hydrogen peroxide production and metal reduction. *J Biol Chem* **1999,** *274* (52), 37111-6.
33. Maynard, C. J.; Cappai, R.; Volitakis, I.; Cherny, R. A.; White, A. R.; Beyreuther, K.; Masters, C. L.; Bush, A. I.; Li, Q. X., Overexpression of Alzheimer's disease amyloid-beta opposes the age-dependent elevations of brain copper and iron. *J Biol Chem* **2002,** *277* (47), 44670-6.
34. Mills, E.; Dong, X. P.; Wang, F.; Xu, H., Mechanisms of brain iron transport: insight into neurodegeneration and CNS disorders. *Future Med Chem* **2010,** *2* (1), 51-64.
35. Liu, J. L.; Fan, Y. G.; Yang, Z. S.; Wang, Z. Y.; Guo, C., Iron and Alzheimer's Disease: From Pathogenesis to Therapeutic Implications. *Front Neurosci* **2018,** *12*, 632.
36. Bartzokis, G.; Sultzer, D.; Mintz, J.; Holt, L. E.; Marx, P.; Phelan, C. K.; Marder, S. R., In vivo evaluation of brain iron in Alzheimer's disease and normal subjects using MRI. *Biol Psychiatry* **1994,** *35* (7), 480-7.
37. LeVine, S. M., Iron deposits in multiple sclerosis and Alzheimer's disease brains. *Brain Res* **1997,** *760* (1-2), 298-303.
38. Wang, D.; Li, Y. Y.; Luo, J. H.; Li, Y. H., Age-related iron deposition in the basal ganglia of controls and Alzheimer disease patients quantified using susceptibility weighted imaging. *Arch Gerontol Geriatr* **2014,** *59* (2), 439-49.
39. Moon, Y.; Han, S. H.; Moon, W. J., Patterns of Brain Iron Accumulation in Vascular Dementia and Alzheimer's Dementia Using Quantitative Susceptibility Mapping Imaging. *J Alzheimers Dis* **2016,** *51* (3), 737-45.
40. Wang, Z. X.; Tan, L.; Wang, H. F.; Ma, J.; Liu, J.; Tan, M. S.; Sun, J. H.; Zhu, X. C.; Jiang, T.; Yu, J. T., Serum Iron, Zinc, and Copper Levels in Patients with Alzheimer's Disease: A Replication Study and Meta-Analyses. *Journal of Alzheimer's disease : JAD* **2015,** *47* (3), 565-81.
41. Tao, Y.; Wang, Y.; Rogers, J. T.; Wang, F., Perturbed iron distribution in Alzheimer's disease serum, cerebrospinal fluid, and selected brain regions: a systematic review and meta-analysis. *J Alzheimers Dis* **2014,** *42* (2), 679-90.
42. Rogers, J. T.; Bush, A. I.; Cho, H. H.; Smith, D. H.; Thomson, A. M.; Friedlich, A. L.; Lahiri, D. K.; Leedman, P. J.; Huang, X.; Cahill, C. M., Iron and the translation of the amyloid precursor protein (APP) and ferritin mRNAs: riboregulation against neural oxidative damage in Alzheimer's disease. *Biochem Soc Trans* **2008,** *36* (Pt 6), 1282-7.
43. Duce, J. A.; Tsatsanis, A.; Cater, M. A.; James, S. A.; Robb, E.; Wikhe, K.; Leong, S. L.; Perez, K.; Johanssen, T.; Greenough, M. A.; Cho, H. H.; Galatis, D.; Moir, R. D.; Masters, C. L.; McLean, C.; Tanzi, R. E.; Cappai, R.; Barnham, K. J.; Ciccotosto, G. D.; Rogers, J. T.; Bush, A. I., Iron-export ferroxidase activity of β-amyloid precursor protein is inhibited by zinc in Alzheimer's disease. *Cell* **2010,** *142* (6), 857-67.
44. Smith, M. A.; Harris, P. L.; Sayre, L. M.; Perry, G., Iron accumulation in Alzheimer disease is a source of redox-generated free radicals. *Proceedings of the National Academy of Sciences of the United States of America* **1997,** *94* (18), 9866-8.
45. Zhang, L.; Zhao, B.; Yew, D. T.; Kusiak, J. W.; Roth, G. S., Processing of Alzheimer's amyloid precursor protein during H2O2-induced apoptosis in human neuronal cells. *Biochem Biophys Res Commun* **1997,** *235* (3), 845-8.
46. Ayton, S.; Fazlollahi, A.; Bourgeat, P.; Raniga, P.; Ng, A.; Lim, Y. Y.; Diouf, I.; Farquharson, S.; Fripp, J.; Ames, D.; Doecke, J.; Desmond, P.; Ordidge, R.; Masters, C. L.; Rowe, C. C.; Maruff, P.; Villemagne, V. L.; Salvado, O.; Bush,

A. I., Cerebral quantitative susceptibility mapping predicts amyloid-β-related cognitive decline. *Brain* **2017,** *140* (8), 2112-2119.
47. Gamblin, T. C.; King, M. E.; Kuret, J.; Berry, R. W.; Binder, L. I., Oxidative regulation of fatty acid-induced tau polymerization. *Biochemistry* **2000,** *39* (46), 14203-10.
48. Cuajungco, M. P.; Lees, G. J., Zinc and Alzheimer's disease: is there a direct link? *Brain research. Brain research reviews* **1997,** *23* (3), 219-36.
49. Nuttall, J. R.; Oteiza, P. I., Zinc and the aging brain. *Genes Nutr* **2014,** *9* (1), 379.
50. Lovell, M. A.; Robertson, J. D.; Teesdale, W. J.; Campbell, J. L.; Markesbery, W. R., Copper, iron and zinc in Alzheimer's disease senile plaques. *Journal of the neurological sciences* **1998,** *158* (1), 47-52.
51. Religa, D.; Strozyk, D.; Cherny, R. A.; Volitakis, I.; Haroutunian, V.; Winblad, B.; Naslund, J.; Bush, A. I., Elevated cortical zinc in Alzheimer disease. *Neurology* **2006,** *67* (1), 69-75.
52. Schrag, M.; Mueller, C.; Oyoyo, U.; Smith, M. A.; Kirsch, W. M., Iron, zinc and copper in the Alzheimer's disease brain: a quantitative meta-analysis. Some insight on the influence of citation bias on scientific opinion. *Progress in neurobiology* **2011,** *94* (3), 296-306.
53. Ventriglia, M.; Brewer, G. J.; Simonelli, I.; Mariani, S.; Siotto, M.; Bucossi, S.; Squitti, R., Zinc in Alzheimer's Disease: A Meta-Analysis of Serum, Plasma, and Cerebrospinal Fluid Studies. *J Alzheimers Dis* **2015,** *46* (1), 75-87.
54. Li, D. D.; Zhang, W.; Wang, Z. Y.; Zhao, P., Serum Copper, Zinc, and Iron Levels in Patients with Alzheimer's Disease: A Meta-Analysis of Case-Control Studies. *Front Aging Neurosci* **2017,** *9*, 300.
55. Barnham, K. J.; Bush, A. I., Metals in Alzheimer's and Parkinson's diseases. *Curr Opin Chem Biol* **2008,** *12* (2), 222-8.
56. Halliwell, B., The wanderings of a free radical. *Free Radic Biol Med* **2009,** *46* (5), 531-42.
57. Halliwell, B., Role of free radicals in the neurodegenerative diseases: therapeutic implications for antioxidant treatment. *Drugs Aging* **2001,** *18* (9), 685-716.
58. Adlard, P. A.; Parncutt, J. M.; Finkelstein, D. I.; Bush, A. I., Cognitive loss in zinc transporter-3 knock-out mice: a phenocopy for the synaptic and memory deficits of Alzheimer's disease? *The Journal of neuroscience : the official journal of the Society for Neuroscience* **2010,** *30* (5), 1631-6.
59. Lovell, M. A.; Xie, C.; Markesbery, W. R., Protection against amyloid beta peptide toxicity by zinc. *Brain research* **1999,** *823* (1-2), 88-95.
60. Cardoso, S. M.; Rego, A. C.; Pereira, C.; Oliveira, C. R., Protective effect of zinc on amyloid-beta 25-35 and 1-40 mediated toxicity. *Neurotox Res* **2005,** *7* (4), 273-81.
61. Fasae, K. D.; Abolaji, A. O.; Faloye, T. R.; Odunsi, A. Y.; Oyetayo, B. O.; Enya, J. I.; Rotimi, J. A.; Akinyemi, R. O.; Whitworth, A. J.; Aschner, M., Metallobiology and therapeutic chelation of biometals (copper, zinc and iron) in Alzheimer's disease: Limitations, and current and future perspectives. *Journal of Trace Elements in Medicine and Biology* **2021,** *67*, 126779.
62. Cuajungco, M. P.; Lees, G. J., Zinc metabolism in the brain: relevance to human neurodegenerative disorders. *Neurobiology of disease* **1997,** *4* (3-4), 137-69.
63. Smidt, K.; Rungby, J., ZnT3: a zinc transporter active in several organs. *Biometals : an international journal on the role of metal ions in biology, biochemistry, and medicine* **2012,** *25* (1), 1-8.
64. Karcioglu, Z. A., Zinc in the eye. *Survey of ophthalmology* **1982,** *27* (2), 114-22.
65. Galin, M. A.; Nano, H. D.; Hall, T., Ocular zinc concentration. *Investigative ophthalmology* **1962,** *1*, 142-8.
66. Wensink, J.; Lenglet, W. J.; Vis, R. D.; Van den Hamer, C. J., The effect of dietary zinc deficiency on the mossy fiber zinc content of the rat hippocampus. A microbeam PIXE study. Particle Induced X-Ray Emission. *Histochemistry* **1987,** *87* (1), 65-9.
67. Maares, M.; Haase, H., A Guide to Human Zinc Absorption: General Overview and Recent Advances of In Vitro Intestinal Models. *Nutrients* **2020,** *12* (3).
68. Costello, L. C.; Fenselau, C. C.; Franklin, R. B., Evidence for operation of the direct zinc ligand exchange mechanism for trafficking, transport, and reactivity of zinc in mammalian cells. *J Inorg Biochem* **2011,** *105* (5), 589-99.
69. Takeda, A., Zinc signaling in the hippocampus and its relation to pathogenesis of depression. *Mol Neurobiol* **2011,** *44* (2), 166-74.
70. Nakashima, A. S.; Dyck, R. H., Dynamic, experience-dependent modulation of synaptic zinc within the excitatory synapses of the mouse barrel cortex. *Neuroscience* **2010,** *170* (4), 1015-9.
71. McCall, K. A.; Huang, C.-c.; Fierke, C. A., Function and Mechanism of Zinc Metalloenzymes. *The Journal of Nutrition* **2000,** *130* (5), 1437S-1446S.
72. Andreini, C.; Banci, L.; Bertini, I.; Rosato, A., Counting the zinc-proteins encoded in the human genome. *J Proteome Res* **2006,** *5* (1), 196-201.
73. Wintergerst, E. S.; Maggini, S.; Hornig, D. H., Immune-enhancing role of vitamin C and zinc and effect on clinical conditions. *Ann Nutr Metab* **2006,** *50* (2), 85-94.
74. Prasad, A. S., Zinc in human health: effect of zinc on immune cells. *Mol Med* **2008,** *14* (5-6), 353-7.

75. Shankar, A. H.; Prasad, A. S., Zinc and immune function: the biological basis of altered resistance to infection. *Am J Clin Nutr* **1998,** *68* (2 Suppl), 447s-463s.
76. Sandstead, H. H., Understanding zinc: recent observations and interpretations. *J Lab Clin Med* **1994,** *124* (3), 322-7.
77. Mccarthy, T. J.; Zeelie, J. J.; Krause, D. J. J. J. o. C. P.; Therapeutics, The antimicrobial action of zinc ion/antioxidant combinations. **1992,** *17*.
78. Solomons, N. W., Mild human zinc deficiency produces an imbalance between cell-mediated and humoral immunity. *Nutr Rev* **1998,** *56* (1 Pt 1), 27-8.
79. Prasad, A. S., Zinc: an overview. *Nutrition* **1995,** *11* (1 Suppl), 93-9.
80. Heyneman, C. A., Zinc deficiency and taste disorders. *Ann Pharmacother* **1996,** *30* (2), 186-7.
81. Prasad, A. S.; Beck, F. W.; Grabowski, S. M.; Kaplan, J.; Mathog, R. H., Zinc deficiency: changes in cytokine production and T-cell subpopulations in patients with head and neck cancer and in noncancer subjects. *Proc Assoc Am Physicians* **1997,** *109* (1), 68-77.
82. Simmer, K.; Thompson, R. P., Zinc in the fetus and newborn. *Acta Paediatr Scand Suppl* **1985,** *319*, 158-63.
83. Fabris, N.; Mocchegiani, E., Zinc, human diseases and aging. *Aging (Milan, Italy)* **1995,** *7* (2), 77-93.
84. Maret, W.; Sandstead, H. H., Zinc requirements and the risks and benefits of zinc supplementation. *J Trace Elem Med Biol* **2006,** *20* (1), 3-18.
85. Institute of Medicine Panel on, M., In *Dietary Reference Intakes for Vitamin A, Vitamin K, Arsenic, Boron, Chromium, Copper, Iodine, Iron, Manganese, Molybdenum, Nickel, Silicon, Vanadium, and Zinc*, National Academies Press (US)

Copyright 2001 by the National Academy of Sciences. All rights reserved.: Washington (DC), 2001.
86. Jurowski, K.; Szewczyk, B.; Nowak, G.; Piekoszewski, W., Biological consequences of zinc deficiency in the pathomechanisms of selected diseases. *J Biol Inorg Chem* **2014,** *19* (7), 1069-79.
87. Grahn, B. H.; Paterson, P. G.; Gottschall-Pass, K. T.; Zhang, Z., Zinc and the eye. *Journal of the American College of Nutrition* **2001,** *20* (2 Suppl), 106-18.
88. Sajovic, J.; Meglič, A.; Glavač, D.; Markelj, Š.; Hawlina, M.; Fakin, A., The Role of Vitamin A in Retinal Diseases. *Int J Mol Sci* **2022,** *23* (3).
89. Smith, J. C., Jr., The vitamin A-zinc connection: a review. *Ann N Y Acad Sci* **1980,** *355*, 62-75.
90. Smith, J. E.; Brown, E. D.; Smith, J. C., Jr., The effect of zinc deficiency on the metabolism of retinol-binding protein in the rat. *J Lab Clin Med* **1974,** *84* (5), 692-7.
91. Gilbert, R.; Peto, T.; Lengyel, I.; Emri, E., Zinc Nutrition and Inflammation in the Aging Retina. *Mol Nutr Food Res* **2019,** *63* (15), e1801049.
92. Ugarte, M.; Osborne, N. N., Zinc in the retina. *Prog Neurobiol* **2001,** *64* (3), 219-49.
93. Akagi, T.; Kaneda, M.; Ishii, K.; Hashikawa, T., Differential subcellular localization of zinc in the rat retina. *The journal of histochemistry and cytochemistry : official journal of the Histochemistry Society* **2001,** *49* (1), 87-96.
94. Ripps, H.; Chappell, R. L., Review: Zinc's functional significance in the vertebrate retina. *Mol Vis* **2014,** *20*, 1067-74.
95. Iqbal, S.; Ali, I., Effect of maternal zinc supplementation or zinc status on pregnancy complications and perinatal outcomes: An umbrella review of meta-analyses. *Heliyon* **2021,** *7* (7), e07540.
96. Evans, J. R.; Lawrenson, J. G., Antioxidant vitamin and mineral supplements for slowing the progression of age-related macular degeneration. *Cochrane Database Syst Rev* **2012,** *11*, Cd000254.
97. McCarthy, T. J.; Zeelie, J. J.; Krause, D. J., The antimicrobial action of zinc ion/antioxidant combinations. *J Clin Pharm Ther* **1992,** *17* (1), 51-4.
98. Valberg, L. S.; Flanagan, P. R.; Kertesz, A.; Bondy, D. C., Zinc absorption in inflammatory bowel disease. *Dig Dis Sci* **1986,** *31* (7), 724-31.
99. Rink, L.; Gabriel, P., Zinc and the immune system. *Proc Nutr Soc* **2000,** *59* (4), 541-52.
100. Hershfinkel, M.; Silverman, W. F.; Sekler, I., The zinc sensing receptor, a link between zinc and cell signaling. *Mol Med* **2007,** *13* (7-8), 331-6.
101. Bitanihirwe, B. K.; Cunningham, M. G., Zinc: the brain's dark horse. *Synapse* **2009,** *63* (11), 1029-49.
102. Hambidge, K. M.; Krebs, N. F., Zinc deficiency: a special challenge. *J Nutr* **2007,** *137* (4), 1101-5.
103. Nakashima, A. S.; Dyck, R. H., Zinc and cortical plasticity. *Brain Res Rev* **2009,** *59* (2), 347-73.
104. Lindskog, S., Structure and mechanism of carbonic anhydrase. *Pharmacol Ther* **1997,** *74* (1), 1-20.
105. Yolton, D. P., Nutritional effects of zinc on ocular and systemic physiology. *J Am Optom Assoc* **1981,** *52* (5), 409-14.
106. Fischer, P. W.; Giroux, A.; L'Abbé, M. R., The effect of dietary zinc on intestinal copper absorption. *Am J Clin Nutr* **1981,** *34* (9), 1670-5.

107. Plum, L. M.; Rink, L.; Haase, H., The essential toxin: impact of zinc on human health. *International journal of environmental research and public health* **2010,** *7* (4), 1342-65.
108. Fosmire, G. J., Zinc toxicity. *The American journal of clinical nutrition* **1990,** *51* (2), 225-227.
109. Porea, T. J.; Belmont, J. W.; Mahoney, D. H., Jr., Zinc-induced anemia and neutropenia in an adolescent. *J Pediatr* **2000,** *136* (5), 688-90.
110. Ryu, M.-S.; Aydemir, T. B., Chapter 23 - Zinc. In *Present Knowledge in Nutrition (Eleventh Edition)*, Marriott, B. P.; Birt, D. F.; Stallings, V. A.; Yates, A. A., Eds. Academic Press: 2020; pp 393-408.
111. Samman, S.; Roberts, D. C. K., Zinc and cholesterol metabolism. *Nutrition Research* **1988,** *8* (5), 559-570.
112. Duncan, A.; Yacoubian, C.; Watson, N.; Morrison, I., The risk of copper deficiency in patients prescribed zinc supplements. *J Clin Pathol* **2015,** *68* (9), 723-5.
113. Tran, C. D.; Cool, J.; Xian, C. J., Dietary zinc and metallothionein on small intestinal disaccharidases activity in mice. *World J Gastroenterol* **2011,** *17* (3), 354-60.
114. Durnam, D. M.; Palmiter, R. D., Transcriptional regulation of the mouse metallothionein-I gene by heavy metals. *J Biol Chem* **1981,** *256* (11), 5712-6.
115. Giedroc, D. P.; Chen, X.; Apuy, J. L., Metal response element (MRE)-binding transcription factor-1 (MTF-1): structure, function, and regulation. *Antioxid Redox Signal* **2001,** *3* (4), 577-96.
116. Miura, N.; Koizumi, S., [Heavy metal responses of the human metallothionein isoform genes]. *Yakugaku Zasshi* **2007,** *127* (4), 665-73.
117. Yokoyama, M.; Koh, J.; Choi, D. W., Brief exposure to zinc is toxic to cortical neurons. *Neurosci Lett* **1986,** *71* (3), 351-5.
118. Frederickson, C. J.; Klitenick, M. A.; Manton, W. I.; Kirkpatrick, J. B., Cytoarchitectonic distribution of zinc in the hippocampus of man and the rat. *Brain Res* **1983,** *273* (2), 335-9.
119. Assaf, S. Y.; Chung, S. H., Release of endogenous Zn2+ from brain tissue during activity. *Nature* **1984,** *308* (5961), 734-6.
120. Sloviter, R. S., A selective loss of hippocampal mossy fiber Timm stain accompanies granule cell seizure activity induced by perforant path stimulation. *Brain Res* **1985,** *330* (1), 150-3.
121. Siesjö, B. K., Basic mechanisms of traumatic brain damage. *Ann Emerg Med* **1993,** *22* (6), 959-69.
122. Frederickson, C. J.; Koh, J. Y.; Bush, A. I., The neurobiology of zinc in health and disease. *Nature reviews. Neuroscience* **2005,** *6* (6), 449-62.
123. Choi, D. W.; Koh, J. Y., Zinc and brain injury. *Annu Rev Neurosci* **1998,** *21*, 347-75.
124. Weiss, J. H.; Sensi, S. L.; Koh, J. Y., Zn(2+): a novel ionic mediator of neural injury in brain disease. *Trends Pharmacol Sci* **2000,** *21* (10), 395-401.
125. Tønder, N.; Johansen, F. F.; Frederickson, C. J.; Zimmer, J.; Diemer, N. H., Possible role of zinc in the selective degeneration of dentate hilar neurons after cerebral ischemia in the adult rat. *Neurosci Lett* **1990,** *109* (3), 247-52.
126. Koh, J. Y.; Suh, S. W.; Gwag, B. J.; He, Y. Y.; Hsu, C. Y.; Choi, D. W., The role of zinc in selective neuronal death after transient global cerebral ischemia. *Science* **1996,** *272* (5264), 1013-6.
127. Pierrel, F.; Cobine, P. A.; Winge, D. R., Metal Ion availability in mitochondria. *Biometals* **2007,** *20* (3-4), 675-82.
128. Capasso, M.; Jeng, J. M.; Malavolta, M.; Mocchegiani, E.; Sensi, S. L., Zinc dyshomeostasis: a key modulator of neuronal injury. *J Alzheimers Dis* **2005,** *8* (2), 93-108; discussion 209-15.
129. Beyersmann, D.; Haase, H., Functions of zinc in signaling, proliferation and differentiation of mammalian cells. *Biometals* **2001,** *14* (3-4), 331-41.
130. Lee, S. R.; Noh, S. J.; Pronto, J. R.; Jeong, Y. J.; Kim, H. K.; Song, I. S.; Xu, Z.; Kwon, H. Y.; Kang, S. C.; Sohn, E. H.; Ko, K. S.; Rhee, B. D.; Kim, N.; Han, J., The Critical Roles of Zinc: Beyond Impact on Myocardial Signaling. *Korean J Physiol Pharmacol* **2015,** *19* (5), 389-99.
131. Ebadi, M.; Iversen, P. L.; Hao, R.; Cerutis, D. R.; Rojas, P.; Happe, H. K.; Murrin, L. C.; Pfeiffer, R. F., Expression and regulation of brain metallothionein. *Neurochemistry international* **1995,** *27* (1), 1-22.
132. Vallee, B. L., The function of metallothionein. *Neurochem Int* **1995,** *27* (1), 23-33.
133. Choi, S.; Bird, A. J., Zinc'ing sensibly: controlling zinc homeostasis at the transcriptional level. *Metallomics* **2014,** *6* (7), 1198-215.
134. Krężel, A.; Maret, W., The Functions of Metamorphic Metallothioneins in Zinc and Copper Metabolism. *Int J Mol Sci* **2017,** *18* (6).
135. Palmiter, R. D.; Findley, S. D.; Whitmore, T. E.; Durnam, D. M., MT-III, a brain-specific member of the metallothionein gene family. *Proceedings of the National Academy of Sciences of the United States of America* **1992,** *89* (14), 6333-7.
136. Masters, B. A.; Quaife, C. J.; Erickson, J. C.; Kelly, E. J.; Froelick, G. J.; Zambrowicz, B. P.; Brinster, R. L.; Palmiter, R. D., Metallothionein III is expressed in neurons that sequester zinc in synaptic vesicles. *J Neurosci* **1994,** *14* (10), 5844-57.

137. Erickson, J. C.; Hollopeter, G.; Thomas, S. A.; Froelick, G. J.; Palmiter, R. D., Disruption of the metallothionein-III gene in mice: analysis of brain zinc, behavior, and neuron vulnerability to metals, aging, and seizures. *J Neurosci* **1997,** *17* (4), 1271-81.
138. Uchida, Y.; Takio, K.; Titani, K.; Ihara, Y.; Tomonaga, M., The growth inhibitory factor that is deficient in the Alzheimer's disease brain is a 68 amino acid metallothionein-like protein. *Neuron* **1991,** *7* (2), 337-47.
139. Tsuji, S.; Kobayashi, H.; Uchida, Y.; Ihara, Y.; Miyatake, T., Molecular cloning of human growth inhibitory factor cDNA and its down-regulation in Alzheimer's disease. *Embo j* **1992,** *11* (13), 4843-50.
140. Erickson, J. C.; Sewell, A. K.; Jensen, L. T.; Winge, D. R.; Palmiter, R. D., Enhanced neurotrophic activity in Alzheimer's disease cortex is not associated with down-regulation of metallothionein-III (GIF). *Brain Res* **1994,** *649* (1-2), 297-304.
141. Amoureux, M. C.; Van Gool, D.; Herrero, M. T.; Dom, R.; Colpaert, F. C.; Pauwels, P. J., Regulation of metallothionein-III (GIF) mRNA in the brain of patients with Alzheimer disease is not impaired. *Mol Chem Neuropathol* **1997,** *32* (1-3), 101-21.
142. Stuart, G. W.; Searle, P. F.; Palmiter, R. D., Identification of multiple metal regulatory elements in mouse metallothionein-I promoter by assaying synthetic sequences. *Nature* **1985,** *317* (6040), 828-31.
143. Sekler, I.; Sensi, S. L.; Hershfinkel, M.; Silverman, W. F., Mechanism and regulation of cellular zinc transport. *Mol Med* **2007,** *13* (7-8), 337-43.
144. Baltaci, A. K.; Yuce, K., Zinc Transporter Proteins. *Neurochem Res* **2018,** *43* (3), 517-530.
145. Eide, D. J., Zinc transporters and the cellular trafficking of zinc. *Biochim Biophys Acta* **2006,** *1763* (7), 711-22.
146. Hantke, K., Bacterial zinc transporters and regulators. *Biometals* **2001,** *14* (3-4), 239-49.
147. Wang, K.; Sitsel, O.; Meloni, G.; Autzen, H. E.; Andersson, M.; Klymchuk, T.; Nielsen, A. M.; Rees, D. C.; Nissen, P.; Gourdon, P., Structure and mechanism of Zn2+-transporting P-type ATPases. *Nature* **2014,** *514* (7523), 518-22.
148. Liuzzi, J. P.; Cousins, R. J., Mammalian zinc transporters. *Annu Rev Nutr* **2004,** *24*, 151-72.
149. Taylor, K. M.; Nicholson, R. I., The LZT proteins; the LIV-1 subfamily of zinc transporters. *Biochim Biophys Acta* **2003,** *1611* (1-2), 16-30.
150. Guerinot, M. L., The ZIP family of metal transporters. *Biochimica et biophysica acta* **2000,** *1465* (1-2), 190-8.
151. Eide, D. J., The SLC39 family of metal ion transporters. *Pflugers Arch* **2004,** *447* (5), 796-800.
152. Palmiter, R. D.; Huang, L., Efflux and compartmentalization of zinc by members of the SLC30 family of solute carriers. *Pflugers Arch* **2004,** *447* (5), 744-51.
153. Kambe, T.; Tsuji, T.; Hashimoto, A.; Itsumura, N., The Physiological, Biochemical, and Molecular Roles of Zinc Transporters in Zinc Homeostasis and Metabolism. *Physiol Rev* **2015,** *95* (3), 749-84.
154. Chen, Y. H.; Kim, J. H.; Stallcup, M. R., GAC63, a GRIP1-dependent nuclear receptor coactivator. *Mol Cell Biol* **2005,** *25* (14), 5965-72.
155. Thingholm, T. E.; Rönnstrand, L.; Rosenberg, P. A., Why and how to investigate the role of protein phosphorylation in ZIP and ZnT zinc transporter activity and regulation. *Cell Mol Life Sci* **2020,** *77* (16), 3085-3102.
156. Cole, T. B.; Wenzel, H. J.; Kafer, K. E.; Schwartzkroin, P. A.; Palmiter, R. D., Elimination of zinc from synaptic vesicles in the intact mouse brain by disruption of the ZnT3 gene. **1999,** *96* (4), 1716-1721.
157. MacDiarmid, C. W.; Milanick, M. A.; Eide, D. J., Biochemical properties of vacuolar zinc transport systems of Saccharomyces cerevisiae. *J Biol Chem* **2002,** *277* (42), 39187-94.
158. Kambe, T.; Yamaguchi-Iwai, Y.; Sasaki, R.; Nagao, M., Overview of mammalian zinc transporters. *Cell Mol Life Sci* **2004,** *61* (1), 49-68.
159. Cole, T. B.; Wenzel, H. J.; Kafer, K. E.; Schwartzkroin, P. A.; Palmiter, R. D., Elimination of zinc from synaptic vesicles in the intact mouse brain by disruption of the ZnT3 gene. *Proceedings of the National Academy of Sciences of the United States of America* **1999,** *96* (4), 1716-21.
160. Wenzel, H. J.; Cole, T. B.; Born, D. E.; Schwartzkroin, P. A.; Palmiter, R. D., Ultrastructural localization of zinc transporter-3 (ZnT-3) to synaptic vesicle membranes within mossy fiber boutons in the hippocampus of mouse and monkey. *Proc Natl Acad Sci U S A* **1997,** *94* (23), 12676-81.
161. Wang, Z. Y.; Danscher, G.; Dahlström, A.; Li, J. Y., Zinc transporter 3 and zinc ions in the rodent superior cervical ganglion neurons. *Neuroscience* **2003,** *120* (3), 605-16.
162. Wang, Z. Y.; Stoltenberg, M.; Huang, L.; Danscher, G.; Dahlström, A.; Shi, Y.; Li, J. Y., Abundant expression of zinc transporters in Bergman glia of mouse cerebellum. *Brain Res Bull* **2005,** *64* (5), 441-8.
163. Wang, Z. Y.; Stoltenberg, M.; Jo, S. M.; Huang, L.; Larsen, A.; Dahlström, A.; Danscher, G., Dynamic zinc pools in mouse choroid plexus. *Neuroreport* **2004,** *15* (11), 1801-4.
164. Whitfield, D. R.; Vallortigara, J.; Alghamdi, A.; Howlett, D.; Hortobágyi, T.; Johnson, M.; Attems, J.; Newhouse, S.; Ballard, C.; Thomas, A. J.; O'Brien, J. T.; Aarsland, D.; Francis, P. T., Assessment of ZnT3 and PSD95 protein levels in Lewy body dementias and Alzheimer's disease: association with cognitive impairment. *Neurobiology of aging* **2014,** *35* (12), 2836-2844.

165. Martel, G.; Hevi, C.; Friebely, O.; Baybutt, T.; Shumyatsky, G. P., Zinc transporter 3 is involved in learned fear and extinction, but not in innate fear. *Learn Mem* **2010,** *17* (11), 582-90.
166. Sindreu, C.; Palmiter, R. D.; Storm, D. R., Zinc transporter ZnT-3 regulates presynaptic Erk1/2 signaling and hippocampus-dependent memory. **2011,** *108* (8), 3366-3370.
167. Suphioglu, C.; De Mel, D.; Kumar, L.; Sadli, N.; Freestone, D.; Michalczyk, A.; Sinclair, A.; Ackland, M. L., The omega-3 fatty acid, DHA, decreases neuronal cell death in association with altered zinc transport. *FEBS Lett* **2010,** *584* (3), 612-8.
168. Dufner-Beattie, J.; Huang, Z. L.; Geiser, J.; Xu, W.; Andrews, G. K., Generation and characterization of mice lacking the zinc uptake transporter ZIP3. *Molecular and cellular biology* **2005,** *25* (13), 5607-15.
169. Kelleher, S. L.; Lönnerdal, B., Zip3 plays a major role in zinc uptake into mammary epithelial cells and is regulated by prolactin. *American journal of physiology. Cell physiology* **2005,** *288* (5), C1042-7.
170. Wang, F.; Dufner-Beattie, J.; Kim, B. E.; Petris, M. J.; Andrews, G.; Eide, D. J., Zinc-stimulated endocytosis controls activity of the mouse ZIP1 and ZIP3 zinc uptake transporters. *J Biol Chem* **2004,** *279* (23), 24631-9.
171. Zhao, H.; Eide, D., The yeast ZRT1 gene encodes the zinc transporter protein of a high-affinity uptake system induced by zinc limitation. **1996,** *93* (6), 2454-2458.
172. Zhao, H.; Eide, D., The ZRT2 gene encodes the low affinity zinc transporter in Saccharomyces cerevisiae. *J Biol Chem* **1996,** *271* (38), 23203-10.
173. Kelleher, S. L.; Lopez, V.; Lönnerdal, B.; Dufner-Beattie, J.; Andrews, G. K., Zip3 (Slc39a3) functions in zinc reuptake from the alveolar lumen in lactating mammary gland. *Am J Physiol Regul Integr Comp Physiol* **2009,** *297* (1), R194-201.
174. Dufner-Beattie, J.; Langmade, S. J.; Wang, F.; Eide, D.; Andrews, G. K., Structure, function, and regulation of a subfamily of mouse zinc transporter genes. *The Journal of biological chemistry* **2003,** *278* (50), 50142-50.
175. Redenti, S.; Chappell, R. L., Neuroimaging of zinc released by depolarization of rat retinal cells. *Vision research* **2005,** *45* (28), 3520-3525.
176. Kaneda, M.; Ishii, K.; Akagi, T.; Tatsukawa, T.; Hashikawa, T., Endogenous zinc can be a modulator of glycinergic signaling pathway in the rat retina. *Journal of molecular histology* **2005,** *36* (3), 179-85.
177. Lengyel, I.; Flinn, J. M.; Peto, T.; Linkous, D. H.; Cano, K.; Bird, A. C.; Lanzirotti, A.; Frederickson, C. J.; van Kuijk, F. J., High concentration of zinc in sub-retinal pigment epithelial deposits. *Exp Eye Res* **2007,** *84* (4), 772-80.
178. Maret, W., Metallothionein redox biology in the cytoprotective and cytotoxic functions of zinc. *Exp Gerontol* **2008,** *43* (5), 363-9.
179. Colvin, R. A.; Holmes, W. R.; Fontaine, C. P.; Maret, W., Cytosolic zinc buffering and muffling: their role in intracellular zinc homeostasis. *Metallomics* **2010,** *2* (5), 306-17.
180. Wang, X.; Wang, Z. Y.; Gao, H. L.; Danscher, G.; Huang, L., Localization of ZnT7 and zinc ions in mouse retina--immunohistochemistry and selenium autometallography. *Brain Res Bull* **2006,** *71* (1-3), 91-6.
181. Wu, S. M.; Qiao, X.; Noebels, J. L.; Yang, X. L., Localization and modulatory actions of zinc in vertebrate retina. *Vision Res* **1993,** *33* (18), 2611-6.
182. Bowness, J. M.; Morton, R. A.; Shakir, M. H.; Stubbs, A. L., Distribution of copper and zinc in mammalian eyes. Occurrence of metals in melanin fractions from eye tissues. *The Biochemical journal* **1952,** *51* (4), 521-30.
183. Erie, J. C.; Good, J. A.; Butz, J. A.; Pulido, J. S., Reduced zinc and copper in the retinal pigment epithelium and choroid in age-related macular degeneration. *American journal of ophthalmology* **2009,** *147* (2), 276-282.e1.
184. Wills, N. K.; Ramanujam, V. M.; Kalariya, N.; Lewis, J. R.; van Kuijk, F. J., Copper and zinc distribution in the human retina: relationship to cadmium accumulation, age, and gender. *Exp Eye Res* **2008,** *87* (2), 80-8.
185. Fabe, J. S.; Grahn, B. H.; Paterson, P. G., Zinc concentration of selected ocular tissues in zinc-deficient rats. *Biological trace element research* **2000,** *75* (1-3), 43-52.
186. Vishwanathan, R.; Chung, M.; Johnson, E. J., A systematic review on zinc for the prevention and treatment of age-related macular degeneration. *Invest Ophthalmol Vis Sci* **2013,** *54* (6), 3985-98.
187. Bowes Rickman, C.; Farsiu, S.; Toth, C. A.; Klingeborn, M., Dry age-related macular degeneration: mechanisms, therapeutic targets, and imaging. *Invest Ophthalmol Vis Sci* **2013,** *54* (14), Orsf68-80.
188. Ugarte, M.; Osborne, N. N., The localization of endogenous zinc and the in vitro effect of exogenous zinc on the GABA immunoreactivity and formation of reactive oxygen species in the retina. *Gen Pharmacol* **1998,** *30* (3), 297-303.
189. Wyszynski, R. E.; Bruner, W. E.; Cano, D. B.; Morgan, K. M.; Davis, C. B.; Sternberg, P., A donor-age-dependent change in the activity of alpha-mannosidase in human cultured RPE cells. *Invest Ophthalmol Vis Sci* **1989,** *30* (11), 2341-7.
190. Javaid, F. Z.; Brenton, J.; Guo, L.; Cordeiro, M. F., Visual and Ocular Manifestations of Alzheimer's Disease and Their Use as Biomarkers for Diagnosis and Progression. *Front Neurol* **2016,** *7*, 55.
191. Lim, J. K.; Li, Q. X.; He, Z.; Vingrys, A. J.; Wong, V. H.; Currier, N.; Mullen, J.; Bui, B. V.; Nguyen, C. T., The Eye As a Biomarker for Alzheimer's Disease. *Frontiers in neuroscience* **2016,** *10*, 536.
192. Laha, B.; Stafford, B. K.; Huberman, A. D., Regenerating optic pathways from the eye to the brain. *Science* **2017,** *356* (6342), 1031-1034.

193. Liao, C.; Xu, J.; Chen, Y.; Ip, N. Y., Retinal Dysfunction in Alzheimer's Disease and Implications for Biomarkers. *Biomolecules* **2021,** *11* (8).
194. Slijkerman, R. W.; Song, F.; Astuti, G. D.; Huynen, M. A.; van Wijk, E.; Stieger, K.; Collin, R. W., The pros and cons of vertebrate animal models for functional and therapeutic research on inherited retinal dystrophies. *Prog Retin Eye Res* **2015,** *48*, 137-59.
195. Mirzaei, N.; Shi, H.; Oviatt, M.; Doustar, J.; Rentsendorj, A.; Fuchs, D. T.; Sheyn, J.; Black, K. L.; Koronyo, Y.; Koronyo-Hamaoui, M., Alzheimer's Retinopathy: Seeing Disease in the Eyes. *Frontiers in neuroscience* **2020,** *14*, 921.
196. Morin, P. J.; Abraham, C. R.; Amaratunga, A.; Johnson, R. J.; Huber, G.; Sandell, J. H.; Fine, R. E., Amyloid precursor protein is synthesized by retinal ganglion cells, rapidly transported to the optic nerve plasma membrane and nerve terminals, and metabolized. *Journal of neurochemistry* **1993,** *61* (2), 464-73.
197. Johnson, L. V.; Leitner, W. P.; Rivest, A. J.; Staples, M. K.; Radeke, M. J.; Anderson, D. H., The Alzheimer's A beta -peptide is deposited at sites of complement activation in pathologic deposits associated with aging and age-related macular degeneration. *Proc Natl Acad Sci U S A* **2002,** *99* (18), 11830-5.
198. Byerly, M. S.; Blackshaw, S., Vertebrate retina and hypothalamus development. *Wiley Interdiscip Rev Syst Biol Med* **2009,** *1* (3), 380-389.
199. Maude, R. J.; Dondorp, A. M.; Abu Sayeed, A.; Day, N. P.; White, N. J.; Beare, N. A., The eye in cerebral malaria: what can it teach us? *Trans R Soc Trop Med Hyg* **2009,** *103* (7), 661-4.
200. Cai, J.; Qi, X.; Kociok, N.; Skosyrski, S.; Emilio, A.; Ruan, Q.; Han, S.; Liu, L.; Chen, Z.; Bowes Rickman, C.; Golde, T.; Grant, M. B.; Saftig, P.; Serneels, L.; de Strooper, B.; Joussen, A. M.; Boulton, M. E., β-Secretase (BACE1) inhibition causes retinal pathology by vascular dysregulation and accumulation of age pigment. *EMBO Mol Med* **2012,** *4* (9), 980-91.
201. Li, L.; Luo, J.; Chen, D.; Tong, J. B.; Zeng, L. P.; Cao, Y. Q.; Xiang, J.; Luo, X. G.; Shi, J. M.; Wang, H.; Huang, J. F., BACE1 in the retina: a sensitive biomarker for monitoring early pathological changes in Alzheimer's disease. *Neural Regen Res* **2016,** *11* (3), 447-53.
202. Trost, A.; Lange, S.; Schroedl, F.; Bruckner, D.; Motloch, K. A.; Bogner, B.; Kaser-Eichberger, A.; Strohmaier, C.; Runge, C.; Aigner, L.; Rivera, F. J.; Reitsamer, H. A., Brain and Retinal Pericytes: Origin, Function and Role. *Front Cell Neurosci* **2016,** *10*, 20.
203. Vecino, E.; Rodriguez, F. D.; Ruzafa, N.; Pereiro, X.; Sharma, S. C., Glia-neuron interactions in the mammalian retina. *Prog Retin Eye Res* **2016,** *51*, 1-40.
204. Koronyo-Hamaoui, M.; Koronyo, Y.; Ljubimov, A. V.; Miller, C. A.; Ko, M. K.; Black, K. L.; Schwartz, M.; Farkas, D. L., Identification of amyloid plaques in retinas from Alzheimer's patients and noninvasive in vivo optical imaging of retinal plaques in a mouse model. *Neuroimage* **2011,** *54 Suppl 1*, S204-17.
205. Patton, N.; Aslam, T.; Macgillivray, T.; Pattie, A.; Deary, I. J.; Dhillon, B., Retinal vascular image analysis as a potential screening tool for cerebrovascular disease: a rationale based on homology between cerebral and retinal microvasculatures. *J Anat* **2005,** *206* (4), 319-48.
206. Koronyo, Y.; Salumbides, B. C.; Black, K. L.; Koronyo-Hamaoui, M., Alzheimer's disease in the retina: imaging retinal aβ plaques for early diagnosis and therapy assessment. *Neurodegener Dis* **2012,** *10* (1-4), 285-93.
207. Koronyo, Y.; Biggs, D.; Barron, E.; Boyer, D. S.; Pearlman, J. A.; Au, W. J.; Kile, S. J.; Blanco, A.; Fuchs, D. T.; Ashfaq, A.; Frautschy, S.; Cole, G. M.; Miller, C. A.; Hinton, D. R.; Verdooner, S. R.; Black, K. L.; Koronyo-Hamaoui, M., Retinal amyloid pathology and proof-of-concept imaging trial in Alzheimer's disease. *JCI insight* **2017,** *2* (16).
208. Shi, Z.; Wu, Y.; Wang, M.; Cao, J.; Feng, W.; Cheng, Y.; Li, C.; Shen, Y., Greater attenuation of retinal nerve fiber layer thickness in Alzheimer's disease patients. *J Alzheimers Dis* **2014,** *40* (2), 277-83.
209. Hart, N. J.; Koronyo, Y.; Black, K. L.; Koronyo-Hamaoui, M., Ocular indicators of Alzheimer's: exploring disease in the retina. *Acta Neuropathol* **2016,** *132* (6), 767-787.
210. Doustar, J.; Torbati, T.; Black, K. L.; Koronyo, Y.; Koronyo-Hamaoui, M., Optical Coherence Tomography in Alzheimer's Disease and Other Neurodegenerative Diseases. *Front Neurol* **2017,** *8*, 701.
211. Cheung, C. Y.; Ikram, M. K.; Chen, C.; Wong, T. Y., Imaging retina to study dementia and stroke. *Prog Retin Eye Res* **2017,** *57*, 89-107.
212. van Wijngaarden, P.; Hadoux, X.; Alwan, M.; Keel, S.; Dirani, M., Emerging ocular biomarkers of Alzheimer disease. *Clin Exp Ophthalmol* **2017,** *45* (1), 54-61.
213. Dehghani, C.; Frost, S.; Jayasena, R.; Masters, C. L.; Kanagasingam, Y., Ocular Biomarkers of Alzheimer's Disease: The Role of Anterior Eye and Potential Future Directions. *Invest Ophthalmol Vis Sci* **2018,** *59* (8), 3554-3563.
214. Hirayama, Y., Histochemical localization of zinc and copper in rat ocular tissues. *Acta Histochem* **1990,** *89* (1), 107-11.
215. Jabbour-Zahab, R.; Chagot, D.; Blanc, F.; Grizel, H., Mantle histology, histochemistry and ultrastructure of the pearl oyster Pinctada margaritifera (L.). *Aquatic Living Resources* **1992,** *5*, 287-298.
216. Lobinski, R.; Moulin, C.; Ortega, R., Imaging and speciation of trace elements in biological environment. *Biochimie* **2006,** *88* (11), 1591-604.

217. Cheon, J.; Lee, J. H., Synergistically integrated nanoparticles as multimodal probes for nanobiotechnology. *Acc Chem Res* **2008,** *41* (12), 1630-40.
218. McRae, R.; Bagchi, P.; Sumalekshmy, S.; Fahrni, C. J., In situ imaging of metals in cells and tissues. *Chem Rev* **2009,** *109* (10), 4780-827.
219. Beach, T. G.; Monsell, S. E.; Phillips, L. E.; Kukull, W., Accuracy of the clinical diagnosis of Alzheimer disease at National Institute on Aging Alzheimer Disease Centers, 2005-2010. *J Neuropathol Exp Neurol* **2012,** *71* (4), 266-73.
220. Robson, A.-L.; Dastoor, P. C.; Flynn, J.; Palmer, W.; Martin, A.; Smith, D. W.; Woldu, A.; Hua, S., Advantages and Limitations of Current Imaging Techniques for Characterizing Liposome Morphology. *Frontiers in Pharmacology* **2018,** *9*.
221. Brown, R. J. C.; Milton, M. J. T., Analytical techniques for trace element analysis: an overview. *TrAC Trends in Analytical Chemistry* **2005,** *24* (3), 266-274.
222. Paul, B.; Hare, D. J.; Bishop, D. P.; Paton, C.; Nguyen, V. T.; Cole, N.; Niedwiecki, M. M.; Andreozzi, E.; Vais, A.; Billings, J. L.; Bray, L.; Bush, A. I.; McColl, G.; Roberts, B. R.; Adlard, P. A.; Finkelstein, D. I.; Hellstrom, J.; Hergt, J. M.; Woodhead, J. D.; Doble, P. A., Visualising mouse neuroanatomy and function by metal distribution using laser ablation-inductively coupled plasma-mass spectrometry imaging. *Chem Sci* **2015,** *6* (10), 5383-5393.
223. Georgevsky, D.; Retsas, S.; Raoufi, N.; Shimoni, O.; Golzan, S. M., A longitudinal assessment of retinal function and structure in the APP/PS1 transgenic mouse model of Alzheimer's disease. *Translational Neurodegeneration* **2019,** *8* (1), 30.
224. Zhanmu, O.; Yang, X.; Gong, H.; Li, X., Paraffin-embedding for large volume bio-tissue. *Sci Rep* **2020,** *10* (1), 12639.
225. Kakuda, N.; Miyasaka, T.; Iwasaki, N.; Nirasawa, T.; Wada-Kakuda, S.; Takahashi-Fujigasaki, J.; Murayama, S.; Ihara, Y.; Ikegawa, M., Distinct deposition of amyloid-β species in brains with Alzheimer's disease pathology visualized with MALDI imaging mass spectrometry. *Acta Neuropathol Commun* **2017,** *5* (1), 73.
226. Eisele, Y. S.; Fritschi, S. K.; Hamaguchi, T.; Obermüller, U.; Füger, P.; Skodras, A.; Schäfer, C.; Odenthal, J.; Heikenwalder, M.; Staufenbiel, M.; Jucker, M., Multiple factors contribute to the peripheral induction of cerebral β-amyloidosis. *J Neurosci* **2014,** *34* (31), 10264-73.
227. Hare, D. J.; Kysenius, K.; Paul, B.; Knauer, B.; Hutchinson, R. W.; O'Connor, C.; Fryer, F.; Hennessey, T. P.; Bush, A. I.; Crouch, P. J.; Doble, P. A., Imaging Metals in Brain Tissue by Laser Ablation - Inductively Coupled Plasma - Mass Spectrometry (LA-ICP-MS). *J Vis Exp* **2017,** (119).
228. Westerhausen, M. T.; Lockwood, T. E.; Gonzalez de Vega, R.; Röhnelt, A.; Bishop, D. P.; Cole, N.; Doble, P. A.; Clases, D., Low background mould-prepared gelatine standards for reproducible quantification in elemental bio-imaging. *Analyst* **2019,** *144* (23), 6881-6888.
229. Zhang, L. H.; Wang, X.; Zheng, Z. H.; Ren, H.; Stoltenberg, M.; Danscher, G.; Huang, L.; Rong, M.; Wang, Z. Y., Altered expression and distribution of zinc transporters in APP/PS1 transgenic mouse brain. *Neurobiol Aging* **2010,** *31* (1), 74-87.
230. Zaqout, S.; Becker, L. L.; Kaindl, A. M., Immunofluorescence Staining of Paraffin Sections Step by Step. *Front Neuroanat* **2020,** *14*, 582218.
231. Ulian-Benitez, S.; Hjelmstad, A. S.; Barbosa, G. O.; Haghighi, P., Eosin whole-brain mount staining to analyze neurodegeneration in a fly model of Alzheimer's disease. *STAR Protoc* **2022,** *3* (2), 101377.
232. Lee, J. Y.; Kim, J. H.; Hong, S. H.; Lee, J. Y.; Cherny, R. A.; Bush, A. I.; Palmiter, R. D.; Koh, J. Y., Estrogen decreases zinc transporter 3 expression and synaptic vesicle zinc levels in mouse brain. *J Biol Chem* **2004,** *279* (10), 8602-7.
233. The Allen Mouse Brain Atlas. https://mouse.brain-map.org/static/atlas.
234. Park, S. W.; Kim, J. H.; Park, W. J.; Kim, J. H., Limbal Approach-Subretinal Injection of Viral Vectors for Gene Therapy in Mice Retinal Pigment Epithelium. *J Vis Exp* **2015,** (102), e53030.
235. Leinonen, H.; Pham, N. C.; Boyd, T.; Santoso, J.; Palczewski, K.; Vinberg, F., Homeostatic plasticity in the retina is associated with maintenance of night vision during retinal degenerative disease. *Elife* **2020,** *9*.
236. Kim, B.; Feldman, E. L., Insulin receptor substrate (IRS)-2, not IRS-1, protects human neuroblastoma cells against apoptosis. *Apoptosis* **2009,** *14* (5), 665-73.
237. Atwood, C. S.; Huang, X.; Moir, R. D.; Tanzi, R. E.; Bush, A. I., Role of free radicals and metal ions in the pathogenesis of Alzheimer's disease. *Metal ions in biological systems* **1999,** *36*, 309-64.
238. Wegst-Uhrich, S. R.; Mullin, E. J.; Ding, D.; Manohar, S.; Salvi, R.; Aga, D. S.; Roth, J. A., Endogenous concentrations of biologically relevant metals in rat brain and cochlea determined by inductively coupled plasma mass spectrometry. *Biometals* **2015,** *28* (1), 187-96.
239. Bush, A. I.; Tanzi, R. E., Therapeutics for Alzheimer's disease based on the metal hypothesis. *Neurotherapeutics* **2008,** *5* (3), 421-32.
240. Roberts, B. R.; Ryan, T. M.; Bush, A. I.; Masters, C. L.; Duce, J. A., The role of metallobiology and amyloid-β peptides in Alzheimer's disease. *J Neurochem* **2012,** *120 Suppl 1*, 149-166.

241. Bush, A. I.; Pettingell, W. H.; Multhaup, G.; d Paradis, M.; Vonsattel, J. P.; Gusella, J. F.; Beyreuther, K.; Masters, C. L.; Tanzi, R. E., Rapid induction of Alzheimer A beta amyloid formation by zinc. *Science (New York, N.Y.)* **1994,** *265* (5177), 1464-7.
242. Atwood, C. S.; Moir, R. D.; Huang, X.; Scarpa, R. C.; Bacarra, N. M.; Romano, D. M.; Hartshorn, M. A.; Tanzi, R. E.; Bush, A. I., Dramatic aggregation of Alzheimer abeta by Cu(II) is induced by conditions representing physiological acidosis. *The Journal of biological chemistry* **1998,** *273* (21), 12817-26.
243. Markesbery, W. R., The role of oxidative stress in Alzheimer disease. *Arch Neurol* **1999,** *56* (12), 1449-52.
244. Rottkamp, C. A.; Raina, A. K.; Zhu, X.; Gaier, E.; Bush, A. I.; Atwood, C. S.; Chevion, M.; Perry, G.; Smith, M. A., Redox-active iron mediates amyloid-beta toxicity. *Free radical biology & medicine* **2001,** *30* (4), 447-50.
245. Schubert, D.; Chevion, M., The role of iron in beta amyloid toxicity. *Biochem Biophys Res Commun* **1995,** *216* (2), 702-7.
246. Pham, T. Q.; Kifley, A.; Mitchell, P.; Wang, J. J., Relation of age-related macular degeneration and cognitive impairment in an older population. *Gerontology* **2006,** *52* (6), 353-8.
247. Wong, T. Y.; Klein, R.; Nieto, F. J.; Moraes, S. A.; Mosley, T. H.; Couper, D. J.; Klein, B. E.; Boland, L. L.; Hubbard, L. D.; Sharrett, A. R., Is early age-related maculopathy related to cognitive function? The Atherosclerosis Risk in Communities Study. *Am J Ophthalmol* **2002,** *134* (6), 828-35.
248. Klaver, C. C.; Ott, A.; Hofman, A.; Assink, J. J.; Breteler, M. M.; de Jong, P. T., Is age-related maculopathy associated with Alzheimer's Disease? The Rotterdam Study. *Am J Epidemiol* **1999,** *150* (9), 963-8.
249. Woo, S. J.; Park, K. H.; Ahn, J.; Choe, J. Y.; Jeong, H.; Han, J. W.; Kim, T. H.; Kim, K. W., Cognitive impairment in age-related macular degeneration and geographic atrophy. *Ophthalmology* **2012,** *119* (10), 2094-101.
250. Hyun, H. J.; Sohn, J.; Ahn, Y. H.; Shin, H. C.; Koh, J. Y.; Yoon, Y. H., Depletion of intracellular zinc induces macromolecule synthesis- and caspase-dependent apoptosis of cultured retinal cells. *Brain Res* **2000,** *869* (1-2), 39-48.
251. Clemons, T. E.; Milton, R. C.; Klein, R.; Seddon, J. M.; Ferris, F. L., 3rd, Risk factors for the incidence of Advanced Age-Related Macular Degeneration in the Age-Related Eye Disease Study (AREDS) AREDS report no. 19. *Ophthalmology* **2005,** *112* (4), 533-9.
252. A randomized, placebo-controlled, clinical trial of high-dose supplementation with vitamins C and E, beta carotene, and zinc for age-related macular degeneration and vision loss: AREDS report no. 8. *Arch Ophthalmol* **2001,** *119* (10), 1417-36.
253. van Leeuwen, R.; Boekhoorn, S.; Vingerling, J. R.; Witteman, J. C. M.; Klaver, C. C. W.; Hofman, A.; de Jong, P. T. V. M., Dietary Intake of Antioxidants and Risk of Age-Related Macular Degeneration. *JAMA* **2005,** *294* (24), 3101-3107.
254. Gengler, S.; Hamilton, A.; Hölscher, C., Synaptic plasticity in the hippocampus of a APP/PS1 mouse model of Alzheimer's disease is impaired in old but not young mice. *PLoS One* **2010,** *5* (3), e9764.
255. Miller, L. M.; Wang, Q.; Telivala, T. P.; Smith, R. J.; Lanzirotti, A.; Miklossy, J., Synchrotron-based infrared and X-ray imaging shows focalized accumulation of Cu and Zn co-localized with beta-amyloid deposits in Alzheimer's disease. *J Struct Biol* **2006,** *155* (1), 30-7.
256. White, A. R.; Barnham, K. J.; Bush, A. I., Metal homeostasis in Alzheimer's disease. *Expert Rev Neurother* **2006,** *6* (5), 711-22.
257. Xu, J.; Church, S. J.; Patassini, S.; Begley, P.; Waldvogel, H. J.; Curtis, M. A.; Faull, R. L. M.; Unwin, R. D.; Cooper, G. J. S., Evidence for widespread, severe brain copper deficiency in Alzheimer's dementia. *Metallomics : integrated biometal science* **2017,** *9* (8), 1106-1119.
258. Graham, S. F.; Nasaruddin, M. B.; Carey, M.; Holscher, C.; McGuinness, B.; Kehoe, P. G.; Love, S.; Passmore, P.; Elliott, C. T.; Meharg, A. A.; Green, B. D., Age-associated changes of brain copper, iron, and zinc in Alzheimer's disease and dementia with Lewy bodies. *Journal of Alzheimer's disease : JAD* **2014,** *42* (4), 1407-13.
259. Akatsu, H.; Hori, A.; Yamamoto, T.; Yoshida, M.; Mimuro, M.; Hashizume, Y.; Tooyama, I.; Yezdimer, E. M., Transition metal abnormalities in progressive dementias. *Biometals* **2012,** *25* (2), 337-50.
260. Wang, H.; Wang, M.; Wang, B.; Li, M.; Chen, H.; Yu, X.; Zhao, Y.; Feng, W.; Chai, Z., The distribution profile and oxidation states of biometals in APP transgenic mouse brain: dyshomeostasis with age and as a function of the development of Alzheimer's disease. *Metallomics* **2012,** *4* (3), 289-96.
261. Deloncle, R.; Guillard, O., Is brain copper deficiency in Alzheimer's, Lewy body, and Creutzfeldt Jakob diseases the common key for a free radical mechanism and oxidative stress-induced damage? *Journal of Alzheimer's disease : JAD* **2015,** *43* (4), 1149-56.
262. Reddy, P. H.; Beal, M. F., Amyloid beta, mitochondrial dysfunction and synaptic damage: implications for cognitive decline in aging and Alzheimer's disease. *Trends Mol Med* **2008,** *14* (2), 45-53.
263. Fu, S.; Jiang, W.; Zheng, W., Age-dependent increase of brain copper levels and expressions of copper regulatory proteins in the subventricular zone and choroid plexus. *Front Mol Neurosci* **2015,** *8*, 22.
264. Ding, B.; Chen, K. M.; Ling, H. W.; Sun, F.; Li, X.; Wan, T.; Chai, W. M.; Zhang, H.; Zhan, Y.; Guan, Y. J., Correlation of iron in the hippocampus with MMSE in patients with Alzheimer's disease. *J Magn Reson Imaging* **2009,** *29* (4), 793-8.

265. Smith, M. A.; Zhu, X.; Tabaton, M.; Liu, G.; McKeel, D. W., Jr.; Cohen, M. L.; Wang, X.; Siedlak, S. L.; Dwyer, B. E.; Hayashi, T.; Nakamura, M.; Nunomura, A.; Perry, G., Increased iron and free radical generation in preclinical Alzheimer disease and mild cognitive impairment. *J Alzheimers Dis* **2010,** *19* (1), 363-72.
266. Belaidi, A. A.; Bush, A. I., Iron neurochemistry in Alzheimer's disease and Parkinson's disease: targets for therapeutics. *Journal of neurochemistry* **2016,** *139 Suppl 1*, 179-197.
267. Raha, A. A.; Vaishnav, R. A.; Friedland, R. P.; Bomford, A.; Raha-Chowdhury, R., The systemic iron-regulatory proteins hepcidin and ferroportin are reduced in the brain in Alzheimer's disease. *Acta neuropathologica communications* **2013,** *1*, 55.
268. Belaidi, A. A.; Gunn, A. P.; Wong, B. X.; Ayton, S.; Appukuttan, A. T.; Roberts, B. R.; Duce, J. A.; Bush, A. I., Marked Age-Related Changes in Brain Iron Homeostasis in Amyloid Protein Precursor Knockout Mice. *Neurotherapeutics* **2018,** *15* (4), 1055-1062.
269. Connor, J. R.; Menzies, S. L.; St Martin, S. M.; Mufson, E. J., Cellular distribution of transferrin, ferritin, and iron in normal and aged human brains. *J Neurosci Res* **1990,** *27* (4), 595-611.
270. Sato, T.; Shapiro, J. S.; Chang, H. C.; Miller, R. A.; Ardehali, H., Aging is associated with increased brain iron through cortex-derived hepcidin expression. *Elife* **2022,** *11*.
271. Panayi, A. E.; Spyrou, N. M.; Iversen, B. S.; White, M. A.; Part, P., Determination of cadmium and zinc in Alzheimer's brain tissue using inductively coupled plasma mass spectrometry. *J Neurol Sci* **2002,** *195* (1), 1-10.
272. Corrigan, F. M.; Reynolds, G. P.; Ward, N. I., Hippocampal tin, aluminum and zinc in Alzheimer's disease. *Biometals* **1993,** *6* (3), 149-54.
273. Braidy, N.; Poljak, A.; Marjo, C.; Rutlidge, H.; Rich, A.; Jugder, B. E.; Jayasena, T.; Inestrosa, N. C.; Sachdev, P. S., Identification of Cerebral Metal Ion Imbalance in the Brain of Aging Octodon degus. *Frontiers in aging neuroscience* **2017,** *9*, 66.
274. Adam, P.; Křížková, S.; Heger, Z.; Babula, P.; Pekařík, V.; Vaculovičoá, M.; Gomes, C. M.; Kizek, R.; Adam, V., Metallothioneins in Prion- and Amyloid-Related Diseases. *Journal of Alzheimer's disease : JAD* **2016,** *51* (3), 637-56.
275. Wang, B.; Wood, I. S.; Trayhurn, P., PCR arrays identify metallothionein-3 as a highly hypoxia-inducible gene in human adipocytes. *Biochemical and biophysical research communications* **2008,** *368* (1), 88-93.
276. Koh, J. Y.; Lee, S. J., Metallothionein-3 as a multifunctional player in the control of cellular processes and diseases. *Mol Brain* **2020,** *13* (1), 116.
277. Cabrera Á, J., Zinc, aging, and immunosenescence: an overview. *Pathobiol Aging Age Relat Dis* **2015,** *5*, 25592.
278. Tonge, K. In *The distribution of copper, zinc and iron in the brain and the implications for Alzheimer's disease*, 2017.
279. Perez, C. M. In *Interplay between synaptic GPCRs in Alzheimer's disease*, 2019.
280. Van Dam, D.; De Deyn, P. P., Animal models in the drug discovery pipeline for Alzheimer's disease. *British journal of pharmacology* **2011,** *164* (4), 1285-300.
281. Squitti, R.; Pal, A.; Picozza, M.; Avan, A.; Ventriglia, M.; Rongioletti, M. C.; Hoogenraad, T., Zinc Therapy in Early Alzheimer's Disease: Safety and Potential Therapeutic Efficacy. *Biomolecules* **2020,** *10* (8), 1164.
282. Squitti, R.; Pal, A.; Picozza, M.; Avan, A.; Ventriglia, M.; Rongioletti, M. C.; Hoogenraad, T., Zinc Therapy in Early Alzheimer's Disease: Safety and Potential Therapeutic Efficacy. *Biomolecules* **2020,** *10* (8).
283. Scheers, N., Regulatory effects of Cu, Zn, and Ca on Fe absorption: the intricate play between nutrient transporters. *Nutrients* **2013,** *5* (3), 957-70.
284. Barr, C. A.; Burdette, S. C., The zinc paradigm for metalloneurochemistry. *Essays Biochem* **2017,** *61* (2), 225-235.
285. Peters, M. B.; Yang, Y.; Wang, B.; Füsti-Molnár, L.; Weaver, M. N.; Merz, K. M., Jr., Structural Survey of Zinc Containing Proteins and the Development of the Zinc AMBER Force Field (ZAFF). *J Chem Theory Comput* **2010,** *6* (9), 2935-2947.
286. Xu, Y.; Xiao, G.; Liu, L.; Lang, M., Zinc transporters in Alzheimer's disease. *Mol Brain* **2019,** *12* (1), 106.
287. Cousins, R. J.; Liuzzi, J. P.; Lichten, L. A., Mammalian zinc transport, trafficking, and signals. *The Journal of biological chemistry* **2006,** *281* (34), 24085-9.
288. Qian, J.; Xu, K.; Yoo, J.; Chen, T. T.; Andrews, G.; Noebels, J. L., Knockout of Zn transporters Zip-1 and Zip-3 attenuates seizure-induced CA1 neurodegeneration. *The Journal of neuroscience : the official journal of the Society for Neuroscience* **2011,** *31* (1), 97-104.
289. Leung, K. W.; Liu, M.; Xu, X.; Seiler, M. J.; Barnstable, C. J.; Tombran-Tink, J., Expression of ZnT and ZIP zinc transporters in the human RPE and their regulation by neurotrophic factors. *Invest Ophthalmol Vis Sci* **2008,** *49* (3), 1221-31.
290. Sikora, J.; Ouagazzal, A. M., Synaptic Zinc: An Emerging Player in Parkinson's Disease. *International journal of molecular sciences* **2021,** *22* (9).
291. Kaneko, M.; Noguchi, T.; Ikegami, S.; Sakurai, T.; Kakita, A.; Toyoshima, Y.; Kambe, T.; Yamada, M.; Inden, M.; Hara, H.; Oyanagi, K.; Inuzuka, T.; Takahashi, H.; Hozumi, I., Zinc transporters ZnT3 and ZnT6 are downregulated in the spinal cords of patients with sporadic amyotrophic lateral sclerosis. *J Neurosci Res* **2015,** *93* (2), 370-9.

292. Redenti, S.; Chappell, R. L., Localization of zinc transporter-3 (ZnT-3) in mouse retina. *Vision Res* **2004,** *44* (28), 3317-21.
293. Redenti, S.; Chappell, R. L., Müller cell zinc transporter-3 labeling suggests a role in outer retina zinc homeostasis. *Mol Med* **2007,** *13* (7-8), 376-9.
294. Márquez García, A.; Salazar, V.; Lima Pérez, L., Consequences of zinc deficiency on zinc localization, taurine transport, and zinc transporters in rat retina. *Microsc Res Tech* **2022,** *85* (10), 3382-3390.
295. Palmiter, R. D.; Cole, T. B.; Quaife, C. J.; Findley, S. D., ZnT-3, a putative transporter of zinc into synaptic vesicles. *Proc Natl Acad Sci U S A* **1996,** *93* (25), 14934-9.
296. Bai, S.; Sheline, C. R.; Zhou, Y.; Sheline, C. T., A reduced zinc diet or zinc transporter 3 knockout attenuate light induced zinc accumulation and retinal degeneration. *Exp Eye Res* **2013,** *108*, 59-67.
297. Linkous, D. H.; Flinn, J. M.; Koh, J. Y.; Lanzirotti, A.; Bertsch, P. M.; Jones, B. F.; Giblin, L. J.; Frederickson, C. J., Evidence that the ZNT3 protein controls the total amount of elemental zinc in synaptic vesicles. *The journal of histochemistry and cytochemistry : official journal of the Histochemistry Society* **2008,** *56* (1), 3-6.
298. Smart, T. G.; Hosie, A. M.; Miller, P. S., Zn2+ ions: modulators of excitatory and inhibitory synaptic activity. *Neuroscientist* **2004,** *10* (5), 432-42.
299. Paoletti, P.; Vergnano, A. M.; Barbour, B.; Casado, M., Zinc at glutamatergic synapses. *Neuroscience* **2009,** *158* (1), 126-36.
300. Olesen, R. H.; Hyde, T. M.; Kleinman, J. E.; Smidt, K.; Rungby, J.; Larsen, A., Obesity and age-related alterations in the gene expression of zinc-transporter proteins in the human brain. *Translational psychiatry* **2016,** *6* (6), e838.
301. Melov, S.; Adlard, P. A.; Morten, K.; Johnson, F.; Golden, T. R.; Hinerfeld, D.; Schilling, B.; Mavros, C.; Masters, C. L.; Volitakis, I.; Li, Q. X.; Laughton, K.; Hubbard, A.; Cherny, R. A.; Gibson, B.; Bush, A. I., Mitochondrial oxidative stress causes hyperphosphorylation of tau. *PLoS One* **2007,** *2* (6), e536.
302. Beyer, N.; Coulson, D. T.; Heggarty, S.; Ravid, R.; Hellemans, J.; Irvine, G. B.; Johnston, J. A., Zinc transporter mRNA levels in Alzheimer's disease postmortem brain. *Journal of Alzheimer's disease : JAD* **2012,** *29* (4), 863-73.
303. Beyer, N.; Coulson, D. T.; Heggarty, S.; Ravid, R.; Irvine, G. B.; Hellemans, J.; Johnston, J. A., ZnT3 mRNA levels are reduced in Alzheimer's disease post-mortem brain. *Mol Neurodegener* **2009,** *4*, 53.
304. Kantheti, P.; Qiao, X.; Diaz, M. E.; Peden, A. A.; Meyer, G. E.; Carskadon, S. L.; Kapfhamer, D.; Sufalko, D.; Robinson, M. S.; Noebels, J. L.; Burmeister, M., Mutation in AP-3 delta in the mocha mouse links endosomal transport to storage deficiency in platelets, melanosomes, and synaptic vesicles. *Neuron* **1998,** *21* (1), 111-22.
305. Rahman, A.; Jackson, H.; Hristov, H.; Isaacson, R. S.; Saif, N.; Shetty, T.; Etingin, O.; Henchcliffe, C.; Brinton, R. D.; Mosconi, L., Sex and Gender Driven Modifiers of Alzheimer's: The Role for Estrogenic Control Across Age, Race, Medical, and Lifestyle Risks. *Frontiers in aging neuroscience* **2019,** *11*, 315.
306. Brinton, R. D.; Yao, J.; Yin, F.; Mack, W. J.; Cadenas, E., Perimenopause as a neurological transition state. *Nature Reviews Endocrinology* **2015,** *11* (7), 393-405.
307. Ghosh, R.; Gilda, J. E.; Gomes, A. V., The necessity of and strategies for improving confidence in the accuracy of western blots. *Expert Rev Proteomics* **2014,** *11* (5), 549-60.
308. Lavado, L. K.; Zhang, M. H.; Patel, K.; Khan, S.; Patel, U. K., Biometals as Potential Predictors of the Neurodegenerative Decline in Alzheimer's Disease. *Cureus* **2019,** *11* (9), e5573.
309. McAllister, B. B.; Dyck, R. H., Zinc transporter 3 (ZnT3) and vesicular zinc in central nervous system function. *Neurosci Biobehav Rev* **2017,** *80*, 329-350.
310. Andrade, V. M.; Aschner, M.; Marreilha Dos Santos, A. P., Neurotoxicity of Metal Mixtures. *Adv Neurobiol* **2017,** *18*, 227-265.
311. Ugarte, M.; Osborne, N. N.; Brown, L. A.; Bishop, P. N., Iron, zinc, and copper in retinal physiology and disease. *Survey of ophthalmology* **2013,** *58* (6), 585-609.
312. Kaarniranta, K.; Salminen, A.; Haapasalo, A.; Soininen, H.; Hiltunen, M., Age-related macular degeneration (AMD): Alzheimer's disease in the eye? *Journal of Alzheimer's disease : JAD* **2011,** *24* (4), 615-31.
313. Hara, T.; Takeda, T. A.; Takagishi, T.; Fukue, K.; Kambe, T.; Fukada, T., Physiological roles of zinc transporters: molecular and genetic importance in zinc homeostasis. *J Physiol Sci* **2017,** *67* (2), 283-301.
314. Bogdanovic, M.; Asraf, H.; Gottesman, N.; Sekler, I.; Aizenman, E.; Hershfinkel, M., The ZIP3 Zinc Transporter Is Localized to Mossy Fiber Terminals and Is Required for Kainate-Induced Degeneration of CA3 Neurons. *J Neurosci* **2022,** *42* (13), 2824-2834.
315. Danscher, G.; Jensen, K. B.; Frederickson, C. J.; Kemp, K.; Andreasen, A.; Juhl, S.; Stoltenberg, M.; Ravid, R., Increased amount of zinc in the hippocampus and amygdala of Alzheimer's diseased brains: a proton-induced X-ray emission spectroscopic analysis of cryostat sections from autopsy material. *J Neurosci Methods* **1997,** *76* (1), 53-9.
316. Cornett, C. R.; Markesbery, W. R.; Ehmann, W. D., Imbalances of trace elements related to oxidative damage in Alzheimer's disease brain. *Neurotoxicology* **1998,** *19* (3), 339-45.
317. Wang, Z. Y.; Li, J. Y.; Danscher, G.; Dahlström, A., Localization of zinc-enriched neurons in the mouse peripheral sympathetic system. *Brain research* **2002,** *928* (1-2), 165-74.

318. Bjorklund, N. L.; Reese, L. C.; Sadagoparamanujam, V. M.; Ghirardi, V.; Woltjer, R. L.; Taglialatela, G., Absence of amyloid β oligomers at the postsynapse and regulated synaptic Zn2+ in cognitively intact aged individuals with Alzheimer's disease neuropathology. *Molecular neurodegeneration* **2012,** *7* (1), 23.
319. van Duijn, S.; Bulk, M.; van Duinen, S. G.; Nabuurs, R. J. A.; van Buchem, M. A.; van der Weerd, L.; Natté, R., Cortical Iron Reflects Severity of Alzheimer's Disease. *J Alzheimers Dis* **2017,** *60* (4), 1533-1545.
320. Meadowcroft, M. D.; Connor, J. R.; Yang, Q. X., Cortical iron regulation and inflammatory response in Alzheimer's disease and APPSWE/PS1ΔE9 mice: a histological perspective. *Frontiers in neuroscience* **2015,** *9*, 255.
321. Ward, R. J.; Zucca, F. A.; Duyn, J. H.; Crichton, R. R.; Zecca, L., The role of iron in brain ageing and neurodegenerative disorders. *Lancet Neurol* **2014,** *13* (10), 1045-60.
322. Fleming, J.; Joshi, J. G., Ferritin: isolation of aluminum-ferritin complex from brain. *Proceedings of the National Academy of Sciences of the United States of America* **1987,** *84* (22), 7866-70.
323. Hodge, R. D.; Bakken, T. E.; Miller, J. A.; Smith, K. A.; Barkan, E. R.; Graybuck, L. T.; Close, J. L.; Long, B.; Johansen, N.; Penn, O.; Yao, Z.; Eggermont, J.; Höllt, T.; Levi, B. P.; Shehata, S. I.; Aevermann, B.; Beller, A.; Bertagnolli, D.; Brouner, K.; Casper, T.; Cobbs, C.; Dalley, R.; Dee, N.; Ding, S.-L.; Ellenbogen, R. G.; Fong, O.; Garren, E.; Goldy, J.; Gwinn, R. P.; Hirschstein, D.; Keene, C. D.; Keshk, M.; Ko, A. L.; Lathia, K.; Mahfouz, A.; Maltzer, Z.; McGraw, M.; Nguyen, T. N.; Nyhus, J.; Ojemann, J. G.; Oldre, A.; Parry, S.; Reynolds, S.; Rimorin, C.; Shapovalova, N. V.; Somasundaram, S.; Szafer, A.; Thomsen, E. R.; Tieu, M.; Quon, G.; Scheuermann, R. H.; Yuste, R.; Sunkin, S. M.; Lelieveldt, B.; Feng, D.; Ng, L.; Bernard, A.; Hawrylycz, M.; Phillips, J. W.; Tasic, B.; Zeng, H.; Jones, A. R.; Koch, C.; Lein, E. S., Conserved cell types with divergent features in human versus mouse cortex. *Nature* **2019,** *573* (7772), 61-68.
324. Wilkinson, D.; Windfeld, K.; Colding-Jørgensen, E., Safety and efficacy of idalopirdine, a 5-HT6 receptor antagonist, in patients with moderate Alzheimer's disease (LADDER): a randomised, double-blind, placebo-controlled phase 2 trial. *The Lancet. Neurology* **2014,** *13* (11), 1092-1099.
325. Harrison, F. E., A critical review of vitamin C for the prevention of age-related cognitive decline and Alzheimer's disease. *Journal of Alzheimer's disease : JAD* **2012,** *29* (4), 711-26.
326. Naidu, K. A., Vitamin C in human health and disease is still a mystery? An overview. *Nutr J* **2003,** *2*, 7.
327. Bjorklund, N. L.; Reese, L. C.; Sadagoparamanujam, V. M.; Ghirardi, V.; Woltjer, R. L.; Taglialatela, G., Absence of amyloid β oligomers at the postsynapse and regulated synaptic Zn2+ in cognitively intact aged individuals with Alzheimer's disease neuropathology. *Mol Neurodegener* **2012,** *7*, 23.
328. Judd, A. M.; Gutierrez, D. B.; Moore, J. L.; Patterson, N. H.; Yang, J.; Romer, C. E.; Norris, J. L.; Caprioli, R. M., A recommended and verified procedure for in situ tryptic digestion of formalin-fixed paraffin-embedded tissues for analysis by matrix-assisted laser desorption/ionization imaging mass spectrometry. *J Mass Spectrom* **2019,** *54* (8), 716-727.
329. Sicherre, E.; Favier, A. L.; Riccobono, D.; Nikovics, K., Non-Specific Binding, a Limitation of the Immunofluorescence Method to Study Macrophages In Situ. *Genes (Basel)* **2021,** *12* (5).
330. Gellein, K.; Flaten, T. P.; Erikson, K. M.; Aschner, M.; Syversen, T., Leaching of trace elements from biological tissue by formalin fixation. *Biol Trace Elem Res* **2008,** *121* (3), 221-5.
331. DiVito, K. A.; Charette, L. A.; Rimm, D. L.; Camp, R. L., Long-term preservation of antigenicity on tissue microarrays. *Lab Invest* **2004,** *84* (8), 1071-8.
332. Alraawi, Z.; Banerjee, N.; Mohanty, S.; Kumar, T. K. S., Amyloidogenesis: What Do We Know So Far? *Int J Mol Sci* **2022,** *23* (22).
333. Staderini, M.; Martín, M. A.; Bolognesi, M. L.; Menéndez, J. C., Imaging of β-amyloid plaques by near infrared fluorescent tracers: a new frontier for chemical neuroscience. *Chem Soc Rev* **2015,** *44* (7), 1807-19.
334. Choi, I.; Huh, Y. S.; Erickson, D., Size-selective concentration and label-free characterization of protein aggregates using a Raman active nanofluidic device. *Lab Chip* **2011,** *11* (4), 632-8.
335. Vestergaard, M.; Kerman, K.; Saito, M.; Nagatani, N.; Takamura, Y.; Tamiya, E., A rapid label-free electrochemical detection and kinetic study of Alzheimer's amyloid beta aggregation. *J Am Chem Soc* **2005,** *127* (34), 11892-3.
336. Chikae, M.; Fukuda, T.; Kerman, K.; Idegami, K.; Miura, Y.; Tamiya, E., Amyloid-beta detection with saccharide immobilized gold nanoparticle on carbon electrode. *Bioelectrochemistry* **2008,** *74* (1), 118-23.
337. Haes, A. J.; Chang, L.; Klein, W. L.; Van Duyne, R. P., Detection of a biomarker for Alzheimer's disease from synthetic and clinical samples using a nanoscale optical biosensor. *J Am Chem Soc* **2005,** *127* (7), 2264-71.
338. Kang, M. K.; Lee, J.; Nguyen, A. H.; Sim, S. J., Label-free detection of ApoE4-mediated β-amyloid aggregation on single nanoparticle uncovering Alzheimer's disease. *Biosens Bioelectron* **2015,** *72*, 197-204.
339. Krebs, M. R.; Bromley, E. H.; Donald, A. M., The binding of thioflavin-T to amyloid fibrils: localisation and implications. *Journal of structural biology* **2005,** *149* (1), 30-7.
340. Barton, S. M.; To, E.; Rogers, B. P.; Whitmore, C.; Uppal, M.; Matsubara, J. A.; Pham, W., Inhalable Thioflavin S for the Detection of Amyloid Beta Deposits in the Retina. *Molecules (Basel, Switzerland)* **2021,** *26* (4).

341. Yakupova, E. I.; Bobyleva, L. G.; Vikhlyantsev, I. M.; Bobylev, A. G., Congo Red and amyloids: history and relationship. *Biosci Rep* **2019,** *39* (1).
342. Rizvi, S. B.; Ghaderi, S.; Keshtgar, M.; Seifalian, A. M., Semiconductor quantum dots as fluorescent probes for in vitro and in vivo bio-molecular and cellular imaging. *Nano Rev* **2010,** *1*.
343. Wagner, A. M.; Knipe, J. M.; Orive, G.; Peppas, N. A., Quantum dots in biomedical applications. *Acta Biomater* **2019,** *94*, 44-63.
344. Smith, A. M.; Duan, H.; Mohs, A. M.; Nie, S., Bioconjugated quantum dots for in vivo molecular and cellular imaging. *Adv Drug Deliv Rev* **2008,** *60* (11), 1226-1240.
345. Chen, S.; Imoukhuede, P. I., Multiplexing Angiogenic Receptor Quantification via Quantum Dots. *Anal Chem* **2019,** *91* (12), 7603-7612.
346. Ho, Y. P.; Leong, K. W., Quantum dot-based theranostics. *Nanoscale* **2010,** *2* (1), 60-8.
347. Smith, A. M.; Gao, X.; Nie, S., Quantum dot nanocrystals for in vivo molecular and cellular imaging. *Photochem Photobiol* **2004,** *80* (3), 377-85.
348. Bruchez, M. P., Quantum dots find their stride in single molecule tracking. *Current opinion in chemical biology* **2011,** *15* (6), 775-80.
349. Fang, M.; Chen, M.; Liu, L.; Li, Y., Applications of Quantum Dots in Cancer Detection and Diagnosis: A Review. *J Biomed Nanotechnol* **2017,** *13* (1), 1-16.
350. Matea, C. T.; Mocan, T.; Tabaran, F.; Pop, T.; Mosteanu, O.; Puia, C.; Iancu, C.; Mocan, L., Quantum dots in imaging, drug delivery and sensor applications. *Int J Nanomedicine* **2017,** *12*, 5421-5431.
351. Stewart, F.; Cummins, G.; Turcanu, M. V.; Cox, B. F.; Prescott, A.; Clutton, E.; Newton, I. P.; Desmulliez, M. P. Y.; Thanou, M.; Mulvana, H.; Cochran, S.; Näthke, I., Ultrasound mediated delivery of quantum dots from a proof of concept capsule endoscope to the gastrointestinal wall. *Scientific reports* **2021,** *11* (1), 2584.
352. Bilan, R.; Nabiev, I.; Sukhanova, A., Quantum Dot-Based Nanotools for Bioimaging, Diagnostics, and Drug Delivery. *Chembiochem* **2016,** *17* (22), 2103-2114.
353. Ghasemi, Y.; Peymani, P.; Afifi, S., Quantum dot: magic nanoparticle for imaging, detection and targeting. *Acta Biomed* **2009,** *80* (2), 156-65.
354. Stanisavljevic, M.; Krizkova, S.; Vaculovicova, M.; Kizek, R.; Adam, V., Quantum dots-fluorescence resonance energy transfer-based nanosensors and their application. *Biosens Bioelectron* **2015,** *74*, 562-74.
355. Selkoe, D. J., Translating cell biology into therapeutic advances in Alzheimer's disease. *Nature* **1999,** *399* (6738 Suppl), A23-31.
356. Lee, J. C.; Kim, S. J.; Hong, S.; Kim, Y., Diagnosis of Alzheimer's disease utilizing amyloid and tau as fluid biomarkers. *Experimental & Molecular Medicine* **2019,** *51* (5), 1-10.
357. Peters, D. G.; Connor, J. R.; Meadowcroft, M. D., The relationship between iron dyshomeostasis and amyloidogenesis in Alzheimer's disease: Two sides of the same coin. *Neurobiol Dis* **2015,** *81*, 49-65.
358. Huang, X.; Cuajungco, M. P.; Atwood, C. S.; Moir, R. D.; Tanzi, R. E.; Bush, A. I., Alzheimer's Disease, β-Amyloid Protein and Zinc. *The Journal of Nutrition* **2000,** *130* (5), 1488S-1492S.
359. Bagheri, S.; Squitti, R.; Haertlé, T.; Siotto, M.; Saboury, A. A., Role of Copper in the Onset of Alzheimer's Disease Compared to Other Metals. *Front Aging Neurosci* **2017,** *9*, 446.
360. Li, Y.; Jiao, Q.; Xu, H.; Du, X.; Shi, L.; Jia, F.; Jiang, H., Biometal Dyshomeostasis and Toxic Metal Accumulations in the Development of Alzheimer's Disease. *Front Mol Neurosci* **2017,** *10*, 339.
361. Jack, C. R., Jr.; Wiste, H. J.; Weigand, S. D.; Rocca, W. A.; Knopman, D. S.; Mielke, M. M.; Lowe, V. J.; Senjem, M. L.; Gunter, J. L.; Preboske, G. M.; Pankratz, V. S.; Vemuri, P.; Petersen, R. C., Age-specific population frequencies of cerebral β-amyloidosis and neurodegeneration among people with normal cognitive function aged 50-89 years: a cross-sectional study. *Lancet Neurol* **2014,** *13* (10), 997-1005.
362. Mormino, E. C., The relevance of beta-amyloid on markers of Alzheimer's disease in clinically normal individuals and factors that influence these associations. *Neuropsychol Rev* **2014,** *24* (3), 300-12.
363. Rodrigue, K. M.; Kennedy, K. M.; Devous, M. D., Sr.; Rieck, J. R.; Hebrank, A. C.; Diaz-Arrastia, R.; Mathews, D.; Park, D. C., β-Amyloid burden in healthy aging: regional distribution and cognitive consequences. *Neurology* **2012,** *78* (6), 387-95.
364. Pedrero-Prieto, C. M.; Flores-Cuadrado, A.; Saiz-Sánchez, D.; Úbeda-Bañón, I.; Frontiñán-Rubio, J.; Alcaín, F. J.; Mateos-Hernández, L.; de la Fuente, J.; Durán-Prado, M.; Villar, M.; Martínez-Marcos, A.; Peinado, J. R., Human amyloid-β enriched extracts: evaluation of in vitro and in vivo internalization and molecular characterization. *Alzheimer's Research & Therapy* **2019,** *11* (1), 56.
365. Querol-Vilaseca, M.; Colom-Cadena, M.; Pegueroles, J.; Nuñez-Llaves, R.; Luque-Cabecerans, J.; Muñoz-Llahuna, L.; Andilla, J.; Belbin, O.; Spires-Jones, T. L.; Gelpi, E.; Clarimon, J.; Loza-Alvarez, P.; Fortea, J.; Lleó, A., Nanoscale structure of amyloid-β plaques in Alzheimer's disease. *Scientific Reports* **2019,** *9* (1), 5181.
366. Filippini, T.; Tancredi, S.; Malagoli, C.; Malavolti, M.; Bargellini, A.; Vescovi, L.; Nicolini, F.; Vinceti, M., Dietary Estimated Intake of Trace Elements: Risk Assessment in an Italian Population. *Exposure and Health* **2020,** *12* (4), 641-655.

367. Doulgeridou, A.; Amlund, H.; Sloth, J. J.; Hansen, M., Review of Potentially Toxic Rare Earth Elements, Thallium and Tellurium in Plant-based Foods. *Efsa j* **2020,** *18* (Suppl 1), e181101.
368. Pamphlett, R.; Cherepanoff, S.; Too, L. K.; Kum Jew, S.; Doble, P. A.; Bishop, D. P., The distribution of toxic metals in the human retina and optic nerve head: Implications for age-related macular degeneration. *PLoS One* **2020,** *15* (10), e0241054.
369. Vlcnovska, M.; Stossova, A.; Kuchynka, M.; Dillingerova, V.; Polanska, H.; Masarik, M.; Hrstka, R.; Adam, V.; Kanicky, V.; Vaculovic, T.; Vaculovicova, M., Comparison of Metal Nanoparticles (Au, Ag, Eu, Cd) Used for Immunoanalysis Using LA-ICP-MS Detection. *Molecules* **2021,** *26* (3).
370. Lores-Padín, A.; Fernández, B.; García, M.; González-Iglesias, H.; Pereiro, R., Real matrix-matched standards for quantitative bioimaging of cytosolic proteins in individual cells using metal nanoclusters as immunoprobes-label: A case study using laser ablation ICP-MS detection. *Analytica Chimica Acta* **2022,** *1221*, 340128.
371. Müller, L.; Traub, H.; Jakubowski, N., Novel Applications of Lanthanoides as Analytical or Diagnostic Tools in the Life Sciences by ICP-MS-based Techniques. *Physical Sciences Reviews* **2016,** *1* (11).
372. Stewart, T. J., Across the spectrum: integrating multidimensional metal analytics for in situ metallomic imaging. *Metallomics* **2019,** *11* (1), 29-49.
373. Bishop, D. P.; Westerhausen, M. T.; Barthelemy, F.; Lockwood, T.; Cole, N.; Gibbs, E. M.; Crosbie, R. H.; Nelson, S. F.; Miceli, M. C.; Doble, P. A.; Wanagat, J., Quantitative immuno-mass spectrometry imaging of skeletal muscle dystrophin. *Sci Rep* **2021,** *11* (1), 1128.
374. Zhang, Q.; Li, J.; Weng, L., Identification and Validation of Aging-Related Genes in Alzheimer's Disease. *Frontiers in neuroscience* **2022,** *16*.
375. Cristóvão, J. S.; Santos, R.; Gomes, C. M., Metals and Neuronal Metal Binding Proteins Implicated in Alzheimer's Disease. *Oxidative medicine and cellular longevity* **2016,** *2016*, 9812178.
376. Zheng, W.; Xin, N.; Chi, Z. H.; Zhao, B. L.; Zhang, J.; Li, J. Y.; Wang, Z. Y., Divalent metal transporter 1 is involved in amyloid precursor protein processing and Abeta generation. *FASEB journal : official publication of the Federation of American Societies for Experimental Biology* **2009,** *23* (12), 4207-17.
377. Fukada, T.; Kambe, T., Molecular and genetic features of zinc transporters in physiology and pathogenesis. *Metallomics* **2011,** *3* (7), 662-74.
378. Lin, Y. F.; Liang, H. M.; Yang, S. Y.; Boch, A.; Clemens, S.; Chen, C. C.; Wu, J. F.; Huang, J. L.; Yeh, K. C., Arabidopsis IRT3 is a zinc-regulated and plasma membrane localized zinc/iron transporter. *New Phytol* **2009,** *182* (2), 392-404.
379. Pedas, P.; Ytting, C. K.; Fuglsang, A. T.; Jahn, T. P.; Schjoerring, J. K.; Husted, S., Manganese efficiency in barley: identification and characterization of the metal ion transporter HvIRT1. *Plant Physiol* **2008,** *148* (1), 455-66.
380. Cohen, C. K.; Garvin, D. F.; Kochian, L. V., Kinetic properties of a micronutrient transporter from Pisum sativum indicate a primary function in Fe uptake from the soil. *Planta* **2004,** *218* (5), 784-92.
381. Lovell, M. A.; Smith, J. L.; Xiong, S.; Markesbery, W. R., Alterations in zinc transporter protein-1 (ZnT-1) in the brain of subjects with mild cognitive impairment, early, and late-stage Alzheimer's disease. *Neurotox Res* **2005,** *7* (4), 265-71.